DISSERTATION

CHRONIC WASTING DISEASE IN TRANSGENIC MICE AND WHITE-TAILED DEER – PRION TRAFFICKING AND PATHOGENESIS

Submitted by

Davis Martin Seelig

Department of Microbiology, Immunology and Pathology

In partial fulfillment of the requirements

For the Degree of Doctor of Philosophy

Colorado State University

Fort Collins, Colorado

Summer 2010

COLORADO STATE UNIVERSITY

June 25, 2010

WE HEREBY RECOMMEND THAT THE DISSERTATION PREPARED UNDER OUR SUPERVISION BY DAVIS MARTIN SEELIG ENTITLED CHRONIC WASTING DISEASE IN TRANSGENIC MICE AND WHITE-TAILED DEER – PRION TRAFFICKING AND PATHOGENESIS BE ACCEPTED AS FULFILLING IN PART REQUIREMENTS FOR THE DEGREE OF DOCTOR OF PHILOSOPHY.

Committee on Graduate Work

Mark Zabel

Eric Ross

Advisor: Edward A. Hoover

Co-Advisor: Gary Mason

Department Head: Edward A. Hoover

ABSTRACT OF DISSERTATION

CHRONIC WASTING DISEASE IN TRANSGENIC MICE AND WHITE-TAILED DEER – PRION TRAFFICKING AND PATHOGENESIS

Chronic wasting disease (CWD) is a naturally occurring, horizontally transmitted prion disease of cervids, including deer, elk and moose. Typical of all prion diseases, CWD is characterized by the forced conversion of the normal prion protein (PrP^{C}) into a misfolded isoform (PrP^{CWD}), which accumulates in tissues of the lymphoid, endocrine, and nervous systems. The accumulation of PrP^{CWD} in the nervous system results in a constellation of 4 microscopic brain lesions: (1) neuronal degeneration and/or loss, (2) neuronal and neuropil degenerative spongiosis, (3) reactive gliosis with absent-to-minimal inflammation, and (4), in some form, protease-resistant (amyloid) plaques of PrP^{CWD}. CWD is unique in that it is the only transmissible spongiform encephalopathy (TSE) known to infect free-ranging wildlife species and in its facile lateral transmission. This disease has been shown to be transmissible to deer fawns by oral exposure and infectious prions have been demonstrated in the saliva, blood, and muscle tissue of CWD-infected deer, although mechanisms of horizontal transmission in nature and *in vivo* prion trafficking remain uncertain. Given the limits inherent in experimental

inoculation studies in the native cervid host, characterization of an efficient murine transgenic model is crucial to advance understanding of CWD and in the elucidation of novel features inherent to CWD which may help to explain the high degree of horizontal transmission, the infectivity of blood, and the shedding of prions via the urine and saliva.

In this dissertation, the two lineages of cervid prion protein (Tg[CerPrP]) expressing mice are shown to be effective surrogates for the study of CWD through their faithful recapitulation of the clinical and pathologic features of the disease as described in native species. Using tissue-based *in situ* immunohistochemistry (IHC) protocols, systemic expression of PrP^{C} was detected in the lymphoid, nervous, hemopoietic, endocrine, and certain epithelial tissues of Tg[CerPrP] mice. In multi-route inoculation longitudinal studies of CWD-infected mice, PrP^{CWD} was identified in tissues of the nervous, lymphoid, endocrine, hemopoietic, and gastrointestinal (GI) systems.

The pathway by which CWD prions efficiently transit from the periphery to the central nervous system remains incompletely understood. In the longitudinal evaluation of CWD-inoculated Tg[CerPrP] mice, increasing amounts of PrP^{CWD} were identified in the cells and fiber tracts of the constituents of the autonomic nervous system, including the parasympathetic, sympathetic, and enteric nervous systems. Such a temporal-spatial pattern of PrP^{CWD} accumulation implicates these elements as major pathways for CWD prion neuroinvasion and GI prion invasion and shedding. These findings may explain the ease by which CWD prions are taken up from and shed into the environment, and thereby its high degree of horizontal transmission.

While the infectious nature of urine, saliva, and blood from CWD-infected cervids has been confirmed, the manner in which such infectivity is acquired is unknown. To address this uncertainty, I evaluated tissues of the urinary, salivary, and hemopoietic systems from CWD-infected deer using enhanced IHC. In these studies, PrP^{CWD} was identified in the renal tubular epithelium and in selected populations of bone marrow cells, suggesting that these populations are, in part, responsible for the previously described phenomena of “prionuria” and “prionemia.”

Davis Martin Seelig
Department of Microbiology, Immunology and Pathology
Colorado State University
Fort Collins CO, 80523
Summer 2010

ACKNOWLEDGEMENTS

Many people have generously contributed to the studies conducted in this dissertation and I am eminently grateful to all of them. First and foremost, I thank Ed Hoover, my major professor and mentor, for his unwavering enthusiasm, energy, sense of humor and, most importantly, patience. He is a scientist without parallel and a mentor without compare. His friendship, support, guidance, and motivation will never be forgotten and will always be cherished.

I am grateful to everyone in the CSU Retrovirus and Prion Research Lab, but would like to recognize Nichols Haley for his friendship and camaraderie over the past 6 years. I would also like to recognize other members of the laboratory, including Nate Denkers for help with immunohistochemistry, and Jeannette Hayes-Klug and Sheila Hayes for their expertise in laboratory animal-care. I would like to thank David Osborn and Sallie Dahmes for valuable deer-related materials, without whom the deer studies that formed the foundation for portions of this dissertation would have not been completed. I would like to extend thanks to Glenn Telling and the members of his laboratory, notably Tanya Seward and Shawn Browning, for their invaluable roles in the creation of the transgenic mice used in these studies.

I would like to acknowledge the members of my graduate committee, including Eric Ross, Mark Zabel, and my co-advisor, Gary Mason. Gary brought great insight and intellect into the design and interpretation of these studies and, often more importantly, great levity into our regular progress meetings. I thank the members of the histology

department in the CSU Diagnostic Medical Center, most notably Todd Bass, who spent many hours preparing and trimming a never-ending flow of study materials, and taught me the fine art of paraffin block tissue sectioning. I'd like to thank Eric Lee who aided me in confocal studies and Jan Langeveld for kindly donating numerous antibodies used in these studies.

I would also like to thank past and current faculty members at CSU, including Christine Olver, Randy Basaraba, E.J. Ehrhart, Dan Gould, Debra Kamstock, Karamjeet Pandher, and Robert Norrdin, who have provided unlimited encouragement during my PhD training. I am forever indebted to Paul and Anne Avery, who have been a constant source of friendship, inspiration and moral support.

Financial support for this work was provided by contract N01-A1-25491 from the National Institute of Allergy and Infectious Disease, National Institutes of Health by grant T32-RR07072 from the National Center for Research Resources, National Institutes of Health.

DEDICATION

This work is humbly dedicated to my mentor, Edward Hoover. His guidance, support, intellect, and sense of humor during the past 5 years have helped to transform an uncertain veterinarian into something resembling a scientist.

Moreover, I'd like to dedicate this work to my partner in life and love, Catherine Hageman. Her support, encouragement, and editing acumen during this time have been immeasurable.

TABLE OF CONTENTS

INTRODUCTION

The prion diseases:

The prion diseases are a unique group of uniformly fatal neurodegenerative diseases caused by an unconventional pathogen and characterized by the presence of vacuoles, or spongiform encephalopathy, in the central nervous system (CNS). Reflective of their infectious and neuropathologic capacities, they are also denoted as transmissible spongiform encephalopathies (TSEs), and have been recognized clinically in humans (e.g. Creutzfeldt-Jakob Disease [CJD], Gerstmann-Straussler-Scheinker [GSS], Fatal-Familial-Insomnia [FFI] and kuru) since the early 1900s and in animals (e.g., sheep scrapie) in excess of 250 years.(Schneider, Fangerau et al. 2008) Originally termed "slow viruses," the transmissibility of prion diseases was first demonstrated in 1936 by Cuillé and Chelle with the successful infection of sheep and goats with brain and spinal cord suspensions from infected animals which was followed by demonstration of true horizontal infection by Greig 4 years later.(Schneider, Fangerau et al. 2008) Since the initial identification of scrapie, the scope of mammalian prion diseases has broadened with identification of transmissible mink encephalopathy (TME), bovine spongiform encephalopathy (BSE), exotic ungulate encephalopathy (EUE), feline spongiform encephalopathy (FSE), and chronic wasting disease of cervids (CWD), the latter of which serves as the subject for the studies contained in this dissertation.

Perspectives on TSEs adopted in this dissertation:

The term prion, or "proteinaceous infectious protein," was first coined in 1982 by Prusiner (Prusiner 1982), built upon work by Alper (Alper, Haig et al. 1966), Gordon (Gordon 1946), and others who demonstrated that the infectious agent in scrapie was resistant to treatments, including UV radiation, formalin, and heat, known to inactivate common pathogens (i.e. viruses and bacteria). Underpinning the pathogenesis of these diseases is the characteristic formation of aggregates of a conformationally altered and post-translationally modified isoform of the normal, cellular prion protein (designated PrP^{C}).(Williams 2005) In this process, the normally α-helical rich prion protein is transformed into a β-sheet rich isoform.

The CWD studies described in this proposal are framed in the context of the most widely accepted paradigm for the etiology of TSEs: the protein-only hypothesis. In this hypothesis, it is postulated that TSEs occur as a result of infection with the misfolded, protease-resistant isoform, denoted PrP^{RES}, which propagates by enciphering its altered conformation onto native PrP^{C}.(Griffith 1967; Prusiner 1982; Soto and Castilla 2004) Confirmation of the hypothesis has been provided by Kim et al, demonstrating TSE infectivity in hamsters inoculated with prions derived by recombinant prion protein without any mammalian cofactors, including RNA and/or lipids.(Kim, Cali et al.) This misfolded isoform may be assigned one of many names, including PrP^{SC} (scrapie-associated abnormal prion protein), PrP^{RES}, or, as is the case in the studies presented here, as PrP^{CWD} (CWD-associated abnormal prion protein).

The TSEs are united by a constellation of 4 microscopic brain lesions: (1) neuronal degeneration and/or loss, (2) neuronal and neuropil degenerative spongiosis, (3) reactive gliosis with absent-to-minimal inflammation, and (4), in some form, protease-resistant (amyloid) plaques of PrP^{RES}. Additionally, the detection of PrP^{RES} has been shown to correlate strongly with infectivity and disease.(Bolton, Rudelli et al. 1991; Race, Jenny et al. 1998) Finally, the studies contained in this dissertation are founded on the understanding that PrP^{CWD}-specific immunohistochemistry (IHC) can be used to provide insights into patterns of prion trafficking, shedding, and pathogenesis in CWD-infected cervids and transgenic murine model systems.

The prion protein and prion disease:

PrP^{C} is a highly conserved, host-encoded, protease-sensitive, glycosylphosphatidylinositol (GPI)-linked, membrane-bound glycoprotein which is broadly expressed throughout the organs of the lymphoid, hematopoietic, cardiovascular, urogenital, and musculoskeletal systems, suggestive of a conserved function. (Aguzzi, Sigurdson et al. 2008) Structurally, PrP^{C} contains 3 α-helical regions and a single β-sheet, and functionally has been implicated in immunoregulation, signal transduction, copper binding, synaptic transmission, induction of apoptosis, protection against apoptotic stimuli, and hematopoiesis.(Aguzzi, Sigurdson et al. 2008) The importance of PrP^{C} in prion disease pathogenesis was originally shown by work demonstrating that, irrespective of the TSE, the expression of PrP^{C} is considered pre-requisite for the

development of prion disease as mice not expressing the cognate PrP^{C} ($PrP^{0/0}$ mice) are resistant to prion infection.(Bueler, Aguzzi et al. 1993) Moreover, expression of PrP^{C} in peripheral (non-CNS) tissues has been shown to be necessary for the spread of infection to the CNS following peripheral inoculation.(Brandner, Isenmann et al. 1996; Blattler, Brandner et al. 1997; Glatzel and Aguzzi 2000)

TSEs as current and emerging human pathogens:

Prior to 1996, it was generally accepted that the infective potential of the prion diseases was low and the sporadic reports of human TSE transmission were restricted to: (i) ingestion of infected brain (kuru) (Duffy, Wolf et al. 1974) or (ii) the use of contaminated medical instruments, neural tissue transplants (dura mater or cornea), or growth hormones (iatrogenic CJD, iCJD).(Bernoulli, Siegfried et al. 1977; Fradkin, Schonberger et al. 1991; Will 1993) This belief changed with the emergence of a variant form of CJD, termed vCJD, in the UK. vCJD is now widely believed to be the human form of bovine spongiform encephalopathy (BSE) (Will, Ironside et al. 1996), which by 2006 had infected over 180 people.(Collee, Bradley et al. 2006) The origin and interspecies transmission of BSE are believed to have occurred through consumption of scrapie-infected meat products.(Chesebro 2003) In addition to epidemiological evidence, the link between vCJD and BSE has been strengthened by experimental cross-infection studies in bovine and human PrP transgenic mice in which the bovine and human

diseases proved indistinguishable neuropathologically.(Hill, Desbruslais et al. 1997) The human health risk represented by CWD remains unknown.

Transgenic mice in prion disease studies:

A notable feature of prion diseases are their novel paradigm of transmissibility. In general, inoculation of individuals with prion-containing material derived from the same species efficiently reproduces disease in the inoculated group. In contrast, the introduction of prions from one species into a heterologous species is typically inefficient, which is a phenomenon known as the species barrier. Although a complete understanding of the determinants of the species barrier has yet to be realized, work with transgenic (Tg) mice and cell-free systems implicate the primary sequence as a key determinant in the efficiency of prion infectivity such that an identical match in the amino acid sequence between the misfolded PrP^{RES} in the inoculum and PrP^{C} in the host generally yields the most efficient propagation of disease. In CWD, the species barrier is best exemplified by the resistance of several laboratory strains of mice, including those expressing the mouse and human PrP, to infection with CWD prions.(Browning, Mason et al. 2004; Kong, Huang et al. 2005)

Abrogation of the species barrier is best facilitated by ensuring a match between prion sequence in the source inoculum and the target species by genetic manipulation. In CWD, this phenomenon is best exemplified by transgenic mice expressing cervid PrP^{C}, thus conferring enhanced susceptibility to CWD prions.(Browning, Mason et al. 2004;

Kong, Huang et al. 2005; Tamguney, Giles et al. 2006) Transgenic and conventional mouse strains have proven invaluable in the study of many of the features of prion diseases, including: (a) the fundamental role of PrP^{C} in the TSE's, (b) the anatomic sites of PrP^{RES} replication and its pathway of spread, (c) the atypical inflammatory response, (d) the transpecies origin of many prion diseases, (e) the mapping of brain lesions, (f) the nature of prion strains, and (g) the species barrier.(Griffith 1967; Prusiner 1982; Kimberlin and Walker 1989; Scott, Safar et al. 1997; Race, Oldstone et al. 2000; Baron 2002; Weissmann and Flechsig 2003) To facilitate the creation of such heterologous-species, PrP-expressing Tg mice, there have been a number of genetic constructs created to allow for the introduction of foreign PrP^{C} into $PrP^{0/0}$ mice.

The earliest Tg mice were created using a transgene vector derived from PrP gene sequences isolated from the Syrian hamster. Thus, this vector, known as the cos.Tet vector, mediates PrP gene expression directed by the hamster prion promoter.(Scott, Foster et al. 1989) This strategy was used to create the strain of mule deer PrP-expressing mice (1536 Tg[CerPrP] mice) used in the first studies in this dissertation.(Browning, Mason et al. 2004) More recently, a second expression vector system (MoPrP.Xho) has been created which utilizes the native mouse prion promoter and thus allows for a more widespread expression of heterologous species PrP in transgenic mouse models.(Borchelt, Davis et al. 1996) This construct has proven effective in the creation of Tg[CerPrP] mice and was utilized to create the strain of elk PrP-expressing mice (5037 Tg[CerPrP-E] mice) utilized in the second set of studies presented here.(Angers, Seward et al. 2009) Given the limits inherent in experimental

inoculation studies in the native cervid host, characterization of an efficient murine transgenic model is crucial to advance understanding of CWD.

Chronic wasting disease – A novel prion disease of cervids:

Chronic wasting disease (CWD) is a TSE known to affect captive and wild cervid populations, including mule deer, white tailed deer, Rocky mountain elk, and moose.(Sigurdson 2008) CWD was first identified in the late 1960's in captive mule deer in Colorado and was first confirmed as a TSE in 1978.(Williams and Young 1980) Since its original identification, CWD has been confirmed in 19 states, 2 Canadian provinces, and South Korea. CWD is unique in the highly efficient manner in which it is horizontally transmitted, resulting in local prevalence rates as high as 30%, which is likely the result of: shedding of prions in excreta, density of animals, and the prolonged persistence of environmental infectious reservoirs.(Miller, Williams et al. 2004; Williams 2005; Haley, Mathiason et al. 2009)

Natural exposure to CWD is likely via the oral route, presumably via direct or indirect exposure to CWD-infected excreta (urine, feces, blood, or saliva).(Sigurdson, Williams et al. 1999; Mathiason, Powers et al. 2006; Haley, Mathiason et al. 2009) Clinical symptoms of CWD may include ataxia, hind-limb paresis, and generalized wasting.(Williams and Young 1980; Sigurdson and Miller 2003; Williams 2005) Post-mortem analysis usually reveals the presence of PrP^{CWD} in lymphoid tissues (Fox, Jewell et al. 2006), as well as spongiform degeneration, reactive astrocytic gliosis, and

perivascular and plaque-like PrP^{CWD} deposits in the nervous system.(Williams 2005; Sigurdson 2008) Similar to other prion diseases, including scrapie and vCJD, specific polymorphisms in the primary structure of the *Prnp* gene confer variable susceptibility to CWD with reduced disease observed in white-tailed deer with G96S, mule deer heterozygous for serine and phenylalanine (S/F heterozygous) or F/F homozygous at codon 225, and elk with M132L polymorphisms.(Goldmann 2008)

Zoonotic potential of CWD infection:

The interspecies transmissibility of prion diseases is well-documented and may represent the source of TSEs affecting humans and animals. For example, the origin of BSE is suspected to be consumption by cattle of contaminated meat and bone meal from scrapie-infected sheep.(Wilesmith, Wells et al. 1988) Likewise, TME and FSE are believed to have originated from BSE or scrapie-contaminated meat products.(Marsh, Bessen et al. 1991; Collinge, Sidle et al. 1996) As noted above, considerable evidence suggests that vCJD is the human manifestation of BSE. The World Health Organization therefore currently recommends against people consuming products from any TSE-afflicted animal. While no official ban on the consumption of meat from CWD-affected animals exists, it is discouraged by health agency officials.(Salman 2003) The basis for this position is provided by recent work demonstrating the presence of infectious CWD prions in muscle, saliva, and blood of CWD-infected deer and the interspecies transmissibility of CWD to mustelid, rodent, and non-human primate species.(Bartz,

Bessen et al. 2000; Marsh, Kincaid et al. 2005; Angers, Browning et al. 2006; Mathiason, Powers et al. 2006) Given the long incubation period of prion disease in natural hosts and the valuable role transgenic mice have played in documenting the link between BSE and vCJD and examining the species barrier, the characterization of transgenic murine models for CWD is vital in determining the risk presented by this prion disease to humans and other animal species.

In vivo trafficking of prions:

In natural TSE infection, prion spread characteristically follows a sequence of steps, some of which may operate in parallel: 1) uptake of prions from the intestinal tract, 2) the accumulation and synthesis of prions in tissues of the lymphoreticular system (LRS), 3) the invasion of the peripheral nervous system (PNS), 4) the ascending spread of prions into the CNS, and 5) the centrifugal spread of prions to peripheral tissues. In CWD, although much insight has been gained into the role of the LRS, little is known of the cellular targets and pathways by which prions traffic to and from their nervous and non-nervous tissue targets.

Enteroinvasion in prion disease:

While work in natural TSEs, including scrapie, BSE and CWD, has confirmed that oral infection is the likely natural route by which prion infection occurs, the manner

by which this process, termed “enteroinvasion” in the studies in this dissertation, occurs remains uncertain.(Sigurdson, Williams et al. 1999; Beekes and McBride 2007) Based upon anatomy and cellular interactions, there are three routes by which prion breaching of an intact GI mucosal barrier might occur via: 1) M-cell transcytosis, 2) receptor-mediated endocytosis, or 3) processes of local dendritic, glial, or neuronal cell populations, which reside in the lamina propria and muscularis layers.(van Keulen, Bossers et al. 2008) Through 1 or more of these pathways, prions traffic from the lumen of the gastrointestinal tract to gain access to the dendritic, lymphoid, glial, and nervous cell populations which are sequestered beneath the overlying intestinal epithelium (Fig Int.1). While M-cell mediated transport remains the most commonly implicated pathway, one goal of the studies in this dissertation is to determine the role of the enteric nervous system (ENS) in this process.

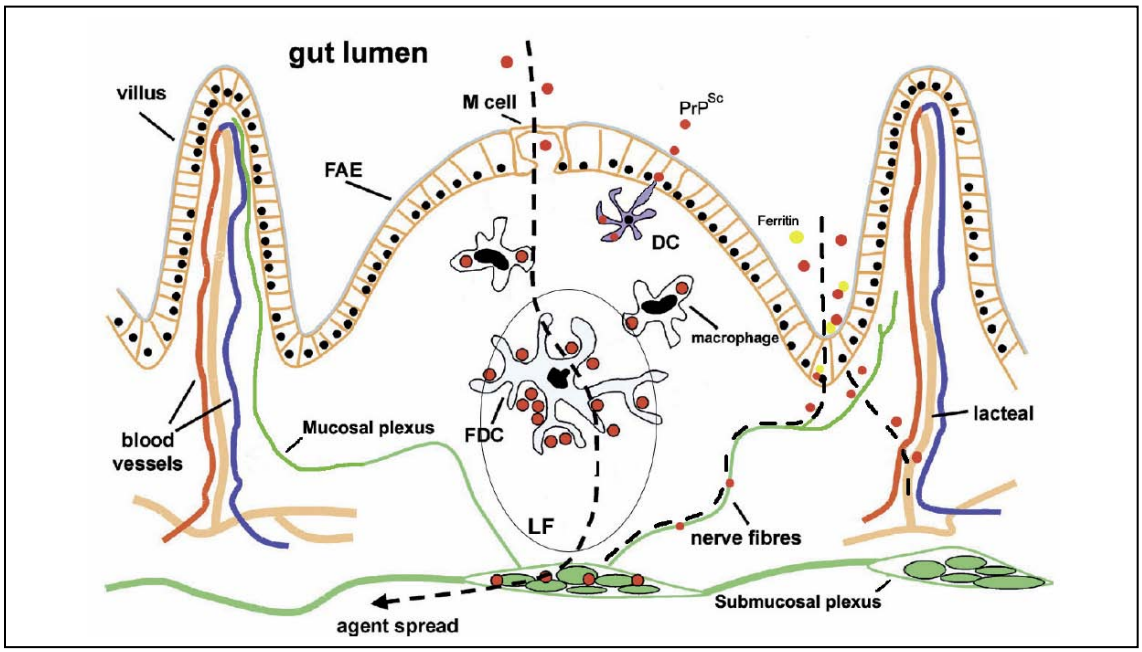

Figure INT.1 Representation of possible pathways of prion enteroinvasion. After ingestion, PrP^{RES} (red circles) can be taken up by M-cells or dendritic cells and transported to the lymphoid follicles (LF) of the Peyer's patches underlying the follicle-associated epithelium (FAE). Within lymphoid follicles, PrP^{RES} accumulates on follicular dendritic cells (FDC) and is taken up by follicular macrophages. This accumulation of PrP^{RES} could facilitate infection of adjacent plexi (green ovals) of the enteric nervous system (ENS). Alternatively, PrP^{RES} could be taken up as a complex with ferritin and transcytosed by intestinal epithelial cells through the ferritin pathway or via processes of the ENS (green lines). From ref (van Keulen, Bossers et al. 2008)

The Autonomic nervous system and prion neuroinvasion:

Peripheral inoculation studies in rodent and sheep scrapie systems indicate that the time interval between the identification of prion replication in lymphoid structures and subsequent CNS neuroinvasion is indicative of prion trafficking via the PNS. (Kimberlin, Field et al. 1983; Andreoletti, Berthon et al. 2000) Additionally, rodent scrapie and cervid CWD models demonstrate initial CNS accumulations of prions in the dorsal motor nucleus of the vagus (DMNV), the nucleus of the solitary tract (NTS), and

the intermediolateral gray matter of the thoracic spinal cord, thus implicating the two PNS components of the autonomic nervous system (ANS), namely the parasympathetic and sympathetic nervous systems, respectively as the primary conduits of neuroinvasion.(Beekes, McBride et al. 1998; Fox, Jewell et al. 2006)

The ANS is responsible for mediating interactions between internal and external environments to ensure the maintenance of homeostasis of all body systems, including the cardiovascular, respiratory, gastrointestinal, urinary, reproductive, and endocrine systems.(Robertson 2004) Anatomically, it consists of 2 branches – a component within the CNS, the central autonomic network (CAN), and a peripheral component consisting of three branches: the parasympathetic nervous system (PaNS), the sympathetic nervous system (SNS), and the ENS. The CAN is composed of several, reciprocally interconnected areas throughout the neuraxis, most notably regions of the cerebral cortex, the amygdala, the hypothalamus, periaqueductal gray matter, and several areas in the medulla.(Appenzeller 1999) Previous studies evaluating the progressive accumulation of PrP^{CWD} in the CNS of CWD-infected deer and scrapie-inoculated mice have implicated the CAN as the major route by which prions traffic within the CNS. However, a more precise understanding of the sequential pattern of PrP^{CWD} accumulation with regards to an understanding of the selective tropism of particular neuroanatomic loci is vital to developing appropriate pre-clinical diagnostic and interventional strategies.

Within the peripheral component, the PaNS and SNS are distinguished largely by their anatomic features. The PaNS originates from neurons within the brain stem and gray matter of the sacral spinal cord and sends long pre-ganglionic fibers to synapse

within terminal ganglia that lie near the target organ followed by a short, post-ganglionic fiber that contacts the target organ. In contrast, the SNS is composed of shorter pre-ganglionic neurons originating from cell bodies in the thoracolumbar region of the spinal cord (the intermediolateral column), which exit via the ventral horns as splanchnic nerves and synapse either within one of the dorsal root ganglia composing the paravertebral, sympathetic trunk or within a visceral, sympathetic ganglion (i.e., cranial cervical, celiac, cranial mesenteric, or caudal mesenteric ganglia) before a post-ganglionic fiber travels to a target organ.(Appenzeller 1999) The ENS, which is a largely independent branch of the ANS, consists of a series of plexi disseminated throughout the GI tract, which interact with fibers of both the PaNS and SNS. Its role in the prion disease pathogenesis is less certain.

The ENS and prion disease:

The ENS consists of a heterogenous population of neurons and enteric glial cells (EGCs) and support for its significance in prion disease stems from the many reports of natural and experimental TSEs, including sheep scrapie, sheep BSE, cattle BSE, and cervid CWD, in which accumulations of PrP^{RES} are seen in myenteric plexi.(Andreoletti, Berthon et al. 2000; Sigurdson, Spraker et al. 2001; Iwata, Sato et al. 2006; van Keulen, Vromans et al. 2008) Moreover, the high degree to which the ENS is innervated by the PaNS and SNS, the expression of PrP^{C} by its constituent cells, and studies demonstrating the presence of PrP^{RES} on EGCs at early time-points following oral inoculation, strongly

supports the ENS as an attractive route by which prions might traffic from the lumen of the GI tract to the CNS.(van Keulen, Schreuder et al. 2000; Marruchella, Ligios et al. 2007) In part, the goal of one of the studies in this dissertation is to provide insights into the role of the ENS in the transit of prions across the GI mucosal barrier during CWD infection.

Questions in CWD upon which this dissertation research is focused:

This thesis seeks to address several unanswered questions in CWD research, including: (1) whether CWD may be transmissible to multi-route inoculated, cervidized strains of transgenic mice, (2) what are the sequential kinetics of PrP^{CWD} accumulation in non-cervid species, and (3) how might tissue-level patterns of PrP^{CWD} accumulation provide insight into the processes of *in vivo* prion trafficking, enteroinvasion, and prion shedding? To address these questions, I evaluated the pathologic features of CWD in cervids and cervidized, transgenic mice through traditional and enhanced immunohistochemical techniques. Thereby, these studies both enhance current knowledge of CWD infection and pathogenesis, and provide novel insights in transgenic murine model systems, which have the potential to pre-empt similar, more costly *in vivo* studies in native, cervid species.

Dissertation Research:

The above background of TSE and CWD research formed the basis upon which the specific aims of this dissertation are based. The first objective was to characterize the pathogenesis of CWD in a lineage of cervid prion protein expressing transgenic mice, including the PrP^{C}-expression, PrP^{CWD}-susceptibility, and the progressive, temporal-spatial patterns of PrP^{CWD} accumulation following multi-route inoculation. I hypothesized that these mice may be susceptible to the CWD agent via multiple routes, including contact, and that the clinical signs and PrP^{CWD} distribution pattern, as characterized by histopathology and immunohistochemistry (IHC), would mimic that seen in infected cervid species. This objective was approached by exposing Tg[CerPrP] mice to CWD-infected brain homogenate via 1 of 4 routes followed by serial necropsies in order to assess for PrP^{CWD} using specific IHC.

There is limited understanding of the manner in which prions traffic in the brains of affected animals or of the pathways by which prions cross the intestinal epithelial barrier, in both experimental and natural hosts. Knowledge of such processes is vital to understanding prion dissemination pathways and to designing therapeutic or interventional strategies. Therefore, the second objective in this work was to document the progressive accumulation of PrP^{CWD} in a second lineage of Tg[CerPrP] mice, with emphasis placed on tissues of the lymphoreticular, central, and peripheral nervous systems. I hypothesized that the cells and fiber tracts of the central and peripheral components of the ANS, including the ENS, would progressively accumulate PrP^{CWD} and

facilitate the process of prion neuroinvasion as demonstrated by single and dual-label IHC using standard, fluorescent, and confocal microscopy.

Finally, while published work has confirmed the infectious nature of blood, saliva, and urine from CWD-infected cervids, the manner in which such infectivity is conferred is uncertain. Therefore, the third objective of this work was to provide tissue-level insights into the process by which such biologic fluids acquire CWD-infectivity through the use of enhanced IHC in the evaluation of the bone marrow, salivary glands, and urinary tract. The objective of this work was to determine the patterns of PrP^{CWD} accumulation in such tissues which might yield insights into the manner by which prions are efficiently shed by CWD-infected cervids and ultimately provide a basis for future, ante-mortem diagnostic strategies.

The results of this work demonstrates that such cervidized model systems faithfully mimic CWD as described in the native species and confirms that such a model provides novel insights into the process of prion enteroinvasion, neurotrafficking, and the shedding of prions via the urinary and gastrointestinal systems. In these ways, this work advances contemporary knowledge regarding CWD and prion disease research.

REFERENCES

Aguzzi, A., C. Sigurdson, et al. (2008). "Molecular mechanisms of prion pathogenesis." Annu Rev Pathol 3: 11-40.

Alper, T., D. A. Haig, et al. (1966). "The exceptionally small size of the scrapie agent." Biochem Biophys Res Commun 22(3): 278-84.

Andreoletti, O., P. Berthon, et al. (2000). "Early accumulation of PrP(Sc) in gut-associated lymphoid and nervous tissues of susceptible sheep from a Romanov flock with natural scrapie." J Gen Virol 81(Pt 12): 3115-26.

Angers, R. C., S. R. Browning, et al. (2006). "Prions in skeletal muscles of deer with chronic wasting disease." Science 311(5764): 1117.

Angers, R. C., T. S. Seward, et al. (2009). "Chronic wasting disease prions in elk antler velvet." Emerg Infect Dis 15(5): 696-703.

Appenzeller, O. (1999). The autonomic nervous system. Amsterdam ; New York, Elsevier.

Baron, T. (2002). "Mouse models of prion disease transmission." Trends Mol Med 8(10): 495-500.

Bartz, J. C., R. A. Bessen, et al. (2000). "Adaptation and selection of prion protein strain conformations following interspecies transmission of transmissible mink encephalopathy." J Virol 74(12): 5542-7.

Beekes, M. and P. A. McBride (2007). "The spread of prions through the body in naturally acquired transmissible spongiform encephalopathies." FEBS J 274(3): 588-605.

Beekes, M., P. A. McBride, et al. (1998). "Cerebral targeting indicates vagal spread of infection in hamsters fed with scrapie." J Gen Virol 79 (Pt 3): 601-7.

Bernoulli, C., J. Siegfried, et al. (1977). "Danger of accidental person-to-person transmission of Creutzfeldt-Jakob disease by surgery." Lancet 1(8009): 478-9.

Blattler, T., S. Brandner, et al. (1997). "PrP-expressing tissue required for transfer of scrapie infectivity from spleen to brain." Nature 389(6646): 69-73.

Bolton, D. C., R. D. Rudelli, et al. (1991). "Copurification of Sp33-37 and scrapie agent from hamster brain prior to detectable histopathology and clinical disease." J Gen Virol 72 (Pt 12): 2905-13.

Borchelt, D. R., J. Davis, et al. (1996). "A vector for expressing foreign genes in the brains and hearts of transgenic mice." Genet Anal 13(6): 159-63.

Brandner, S., S. Isenmann, et al. (1996). "Normal host prion protein necessary for scrapie-induced neurotoxicity." Nature 379(6563): 339-43.

Browning, S. R., G. L. Mason, et al. (2004). "Transmission of prions from mule deer and elk with chronic wasting disease to transgenic mice expressing cervid PrP." J Virol 78(23): 13345-50.

Bueler, H., A. Aguzzi, et al. (1993). "Mice devoid of PrP are resistant to scrapie." Cell 73(7): 1339-47.

Chesebro, B. (2003). "Introduction to the transmissible spongiform encephalopathies or prion diseases." Br Med Bull 66: 1-20.

Collee, J. G., R. Bradley, et al. (2006). "Variant CJD (vCJD) and bovine spongiform encephalopathy (BSE): 10 and 20 years on: part 2." Folia Neuropathol 44(2): 102-10.
Collinge, J., K. C. Sidle, et al. (1996). "Molecular analysis of prion strain variation and the aetiology of 'new variant' CJD." Nature 383(6602): 685-90.
Duffy, P., J. Wolf, et al. (1974). "Letter: Possible person-to-person transmission of Creutzfeldt-Jakob disease." N Engl J Med 290(12): 692-3.
Fox, K. A., J. E. Jewell, et al. (2006). "Patterns of PrPCWD accumulation during the course of chronic wasting disease infection in orally inoculated mule deer (Odocoileus hemionus)." J Gen Virol 87(Pt 11): 3451-61.
Fradkin, J. E., L. B. Schonberger, et al. (1991). "Creutzfeldt-Jakob disease in pituitary growth hormone recipients in the United States." Jama 265(7): 880-4.
Glatzel, M. and A. Aguzzi (2000). "PrP(C) expression in the peripheral nervous system is a determinant of prion neuroinvasion." J Gen Virol 81(Pt 11): 2813-21.
Goldmann, W. (2008). "PrP genetics in ruminant transmissible spongiform encephalopathies." Vet Res 39(4): 30.
Gordon, W. S. (1946). "Advances in veterinary research." Vet Rec 58(47): 516-25.
Griffith, J. S. (1967). "Self-replication and scrapie." Nature 215(105): 1043-4.
Haley, N. J., C. K. Mathiason, et al. (2009). "Detection of sub-clinical CWD infection in conventional test-negative deer long after oral exposure to urine and feces from CWD+ deer." PLoS One 4(11): e7990.
Hill, A. F., M. Desbruslais, et al. (1997). "The same prion strain causes vCJD and BSE." Nature 389(6650): 448-50, 526.
Iwata, N., Y. Sato, et al. (2006). "Distribution of PrP(Sc) in cattle with bovine spongiform encephalopathy slaughtered at abattoirs in Japan." Jpn J Infect Dis 59(2): 100-7.
Kim, J. I., I. Cali, et al. "Mammalian prions generated from bacterially expressed prion protein in the absence of any mammalian cofactors." J Biol Chem.
Kimberlin, R. H., H. J. Field, et al. (1983). "Pathogenesis of mouse scrapie: evidence for spread of infection from central to peripheral nervous system." J Gen Virol 64 Pt 3: 713-6.
Kimberlin, R. H. and C. A. Walker (1989). "The role of the spleen in the neuroinvasion of scrapie in mice." Virus Res 12(3): 201-11.
Kong, Q., S. Huang, et al. (2005). "Chronic wasting disease of elk: transmissibility to humans examined by transgenic mouse models." J Neurosci 25(35): 7944-9.
Marruchella, G., C. Ligios, et al. (2007). "Enteroglial and neuronal involvement without apparent neuron loss in ileal enteric nervous system plexuses from scrapie-affected sheep." J Gen Virol 88(Pt 10): 2899-904.
Marsh, R. F., R. A. Bessen, et al. (1991). "Epidemiological and experimental studies on a new incident of transmissible mink encephalopathy." J Gen Virol 72 (Pt 3): 589-94.
Marsh, R. F., A. E. Kincaid, et al. (2005). "Interspecies transmission of chronic wasting disease prions to squirrel monkeys (Saimiri sciureus)." J Virol 79(21): 13794-6.
Mathiason, C., J. G. Powers, et al. (2006). "Infectious Prions in the Saliva and Blood of Deer with Chronic Wasting Disease." Science in press.

Miller, M. W., E. S. Williams, et al. (2004). "Environmental sources of prion transmission in mule deer." Emerg Infect Dis 10(6): 1003-6.
Prusiner, S. B. (1982). "Novel proteinaceous infectious particles cause scrapie." Science 216(4542): 136-44.
Race, R., A. Jenny, et al. (1998). "Scrapie infectivity and proteinase K-resistant prion protein in sheep placenta, brain, spleen, and lymph node: implications for transmission and antemortem diagnosis." J Infect Dis 178(4): 949-53.
Race, R., M. Oldstone, et al. (2000). "Entry versus blockade of brain infection following oral or intraperitoneal scrapie administration: role of prion protein expression in peripheral nerves and spleen." J Virol 74(2): 828-33.
Robertson, D. (2004). Primer on the autonomic nervous system. Boston, Academic Press.
Salman, M. D. (2003). "Chronic wasting disease in deer and elk: scientific facts and findings." J Vet Med Sci 65(7): 761-8.
Schneider, K., H. Fangerau, et al. (2008). "The early history of the transmissible spongiform encephalopathies exemplified by scrapie." Brain Res Bull 77(6): 343-55.
Scott, M., D. Foster, et al. (1989). "Transgenic mice expressing hamster prion protein produce species-specific scrapie infectivity and amyloid plaques." Cell 59(5): 847-57.
Scott, M. R., J. Safar, et al. (1997). "Identification of a prion protein epitope modulating transmission of bovine spongiform encephalopathy prions to transgenic mice." Proc Natl Acad Sci U S A 94(26): 14279-84.
Sigurdson, C. J. (2008). "A prion disease of cervids: chronic wasting disease." Vet Res 39(4): 41.
Sigurdson, C. J. and M. W. Miller (2003). "Other animal prion diseases." Br Med Bull 66: 199-212.
Sigurdson, C. J., T. R. Spraker, et al. (2001). "PrP(CWD) in the myenteric plexus, vagosympathetic trunk and endocrine glands of deer with chronic wasting disease." J Gen Virol 82(Pt 10): 2327-34.
Sigurdson, C. J., E. S. Williams, et al. (1999). "Oral transmission and early lymphoid tropism of chronic wasting disease PrPres in mule deer fawns (Odocoileus hemionus)." J Gen Virol 80 (Pt 10): 2757-64.
Soto, C. and J. Castilla (2004). "The controversial protein-only hypothesis of prion propagation." Nat Med 10 Suppl: S63-7.
Tamguney, G., K. Giles, et al. (2006). "Transmission of elk and deer prions to transgenic mice." J Virol 80(18): 9104-14.
van Keulen, L. J., A. Bossers, et al. (2008). "TSE pathogenesis in cattle and sheep." Vet Res 39(4): 24.
van Keulen, L. J., B. E. Schreuder, et al. (2000). "Pathogenesis of natural scrapie in sheep." Arch Virol Suppl(16): 57-71.
van Keulen, L. J., M. E. Vromans, et al. (2008). "Pathogenesis of bovine spongiform encephalopathy in sheep." Arch Virol 153(3): 445-53.
Weissmann, C. and E. Flechsig (2003). "PrP knock-out and PrP transgenic mice in prion research." Br Med Bull 66: 43-60.

Wilesmith, J. W., G. A. Wells, et al. (1988). "Bovine spongiform encephalopathy: epidemiological studies." Vet Rec 123(25): 638-44.
Will, R. G. (1993). "Epidemiology of Creutzfeldt-Jakob disease." Br Med Bull 49(4): 960-70.
Will, R. G., J. W. Ironside, et al. (1996). "A new variant of Creutzfeldt-Jakob disease in the UK." Lancet 347(9006): 921-5.
Williams, E. S. (2005). "Chronic wasting disease." Vet Pathol 42(5): 530-49.
Williams, E. S. and S. Young (1980). "Chronic wasting disease of captive mule deer: a spongiform encephalopathy." J Wildl Dis 16(1): 89-98.

CHAPTER 1:

Pathogenesis of Chronic Wasting Disease in Cervidized Transgenic Mice.

ABSTRACT

Chronic Wasting Disease (CWD) is a fatal, endemic prion disease of wild and captive cervids, including deer, elk, and moose. Typical of prion diseases, CWD is characterized by the conversion of the native, protease-sensitive protein PrP^{C} to a protease-resistant isoform, denoted PrP^{CWD}. Here I employed a line of transgenic mice expressing the normal cervid prion protein (1536 Tg[CerPrP] mice) to study the expression of cervid PrP^{C} and the multi-route susceptibility and pathogenesis of CWD infection. Using tissue-based *in situ* immunohistochemistry protocols, I identified cervid PrP^{C} expression in the lymphoid, nervous, hemopoietic, endocrine, and certain epithelial tissues of Tg[CerPrP] mice. Tg[CerPrP] mice were inoculated with CWD via one of 4 routes: intracerebral (IC), intravenous (IV), intraperitoneal (IP), and oral (PO). All groups developed spongiform encephalopathy, although the oral route required a larger infecting dose. Incubation periods were 184 ± 13, 218 ± 15, 200 ± 7, and 350 ± 27 days post-inoculation (dpi), respectively. I identified PrP^{CWD} in the brain, spleen, Peyer's patches, lymph nodes, pancreatic islets of Langerhans, bone marrow, and salivary glands in both pre-clinical and terminal mice. In addition, I documented horizontal transmission of CWD from inoculated mice and to un-inoculated cohabitant cage-mates. This work affirms that Tg[CerPrP] mice represent a robust model system to study CWD infection, pathogenesis, and lateral transmission.

BACKGROUND

The transmissible spongiform encephalopathies (TSEs), or prion diseases, are uniformly-fatal, chronic and progressive neurodegenerative diseases that affect humans (kuru and Creutzfeldt-Jakob disease [CJD]), sheep and goats (scrapie), cattle (bovine spongiform encephalopathy [BSE]), felids (feline spongiform encephalopathy [FSE]), and cervids (chronic wasting disease [CWD]). Prion diseases are so named based upon their association with aggregates of conformationally-altered and post-translationally modified isoforms (denoted PrP^{RES}) of the normal cellular prion protein (denoted PrP^{C}). Chronic wasting disease (CWD) is a prion disease affecting captive and wild cervid populations including mule deer, white-tailed deer, elk, and moose. CWD was first recognized in captive mule deer in Colorado in 1967 and, 11 years later, was identified as a TSE. CWD is unique among TSE's in infecting free-ranging wildlife species and in its highly transmissible nature (Miller and Williams 2003). Although the mechanism(s) of this facile spread remains uncertain, experimental and epidemiological evidence suggest lateral transmission.(Williams and Young 1992; Miller, Wild et al. 1998; Miller and Wild 2004)

While mice of *Mus* species are substantially resistant to CWD infection, mice engineered to express the normal cervid prion protein transgenically (i.e. cervidized mice, Tg[CerPrP] mice) have been shown susceptible to CWD infection by intracerebral inoculation.(Browning, Mason et al. 2004; Kong, Huang et al. 2005; Angers, Browning et al. 2006; LaFauci, Carp et al. 2006; Tamguney, Giles et al. 2006; Trifilo, Ying et al. 2007) In the present study I used a series of immunohistochemical (IHC) techniques to:

i) map the distribution of PrP^{C} in naïve Tg[CerPrP] mice; ii) determine the CWD susceptibility of these mice following exposure via a presumed natural route [oral; (PO)] and three parenteral routes [intravenous (IV), and intraperitoneal (IP), and intracerebral (IC)]; iii) assess the longitudinal accumulation of PrP^{RES} in tissues of inoculated mice; and iv) evaluate the possibility of CWD horizontal transmission to naïve, cohabitating mice, thereby simulating lateral transmission in the native cervid host.

MATERIALS and METHODS

Generation and genotyping of Tg[CerPrP] mice:

The transgenic mice used in this study (1536 Tg[CerPrP] mice) were created and their susceptibility to CWD established in the Telling laboratory (Browning, Mason et al. 2004). Line 1536 was generated as follows: the open reading frame (ORF) cassette of the CerPrP S2 allele (Gen-Bank accession no.AF009180) was released from plasmid sequences following digestion with SalI and XhoI and purified ORF fragments were ligated to the SalI-cut cosSHa.Tet cosmid expression vector. The cosSHa.Tet cosmid expression vector contains a 49-kb DNA fragment encompassing the Syrian hamster PrP gene and has been used to produce numerous Tg models of prion diseases, including mice in which the species barriers to Syrian hamster, human, and bovine prions were eliminated (Scott, Kohler et al. 1992; Telling, Scott et al. 1994; Telling, Scott et al. 1995; Scott, Safar et al. 1997; Telling 2000; Baron 2002; Browning, Mason et al. 2004; Angers, Browning et al. 2006). To increase CerPrP expression in transgenic mice, the CerPrP S2 allele plasmid nucleotide sequence was modified by site-directed mutagenesis immediately upstream of the initiating ATG to produce a consensus Kozak translation initiation sequence. Two founders were generated by microinjection of fertilized embryos from *Prnp*$^{0/0}$ knockout mice on an FVB/N background (FVB/*Prnp*$^{0/0}$), from which a colony of 1536 Tg[CerPrP] mice was developed. Tail-tip DNA was screened for the presence and appropriate orientation of the CerPrP transgene by conventional and real-time PCR (RT-PCR) (Browning, Mason et al. 2004). The PrP$^{0/0}$ mice used in the PrP^{C} mapping studies were kindly donated by Mark Zabel.

Inoculum preparation:

The CWD inoculum (D-10) was prepared as a brain homogenate derived from a terminally-ill, naturally infected CWD-positive captive mule deer (Dr. Michael Miller, Colorado Division of Wildlife, Wildlife Research Center). This inoculum has proven infectious for both deer and the 1536 Tg[CerPrP] mice in previous studies (Sigurdson, Williams et al. 1999; Browning, Mason et al. 2004). The negative control inoculum was a brain homogenate originating from a CWD-negative white-tailed deer originating outside of the CWD endemic area (courtesy of David Osborn, University of Georgia). Both inocula were homogenized in sterile phosphate-buffered saline (PBS) using a reciprocal homogenizer and diluted to a final concentration of 1% (wt/vol) using sterile PBS containing penicillin-streptomycin (100 U/ml).

Inoculation protocol:

Five experimental groups were utilized in these studies (Fig. 1.1). Four of the groups consisted of 4- to 6-week old, mixed-sex, 1536 Tg[CerPrP] mice that were inoculated with CWD prions via one of four routes: IC, IP, IV, or PO. The fifth group consisted of age and sex-matched, naïve 1536 Tg[CerPrP] mice that were included to assess for the possibility of horizontal transmission (described below). In each cage, 2 inoculated mice were housed with 1 sentinel, non-inoculated mouse. For intracerebral (IC) inoculation, mice were sedated through the IP injection of a mixture of ketamine and xylazine at 120 and 16 mg/kg, respectively. Mice were then inoculated with 30 µl of a 1% brain homogenate via a 29-gauge needle through the calvarium into the left parietal

lobe of the cerebral cortex. For IP inoculation, 100 µl of a 1% brain homogenate was instilled via a 29-gauge needle through the skin and subcutaneous tissues of the right lateral aspect of the caudal ventral abdomen. For IV inoculation, 30 µl of a 1% brain homogenate was injected through either the left or right tail vein. PO inoculations were performed by oral instillation of 100 µl of a 1% brain homogenate, which was administered 50 µl per day for 2 consecutive days. Mice were not sedated for the IP, IV, or PO inoculations. A second oral inoculation study employed whole brain and is described separately below. Negative control mice (n = 6 per route) were similarly inoculated with 1% brain homogenate obtained from a CWD-negative white-tailed deer originating outside of the CWD endemic area (per above).

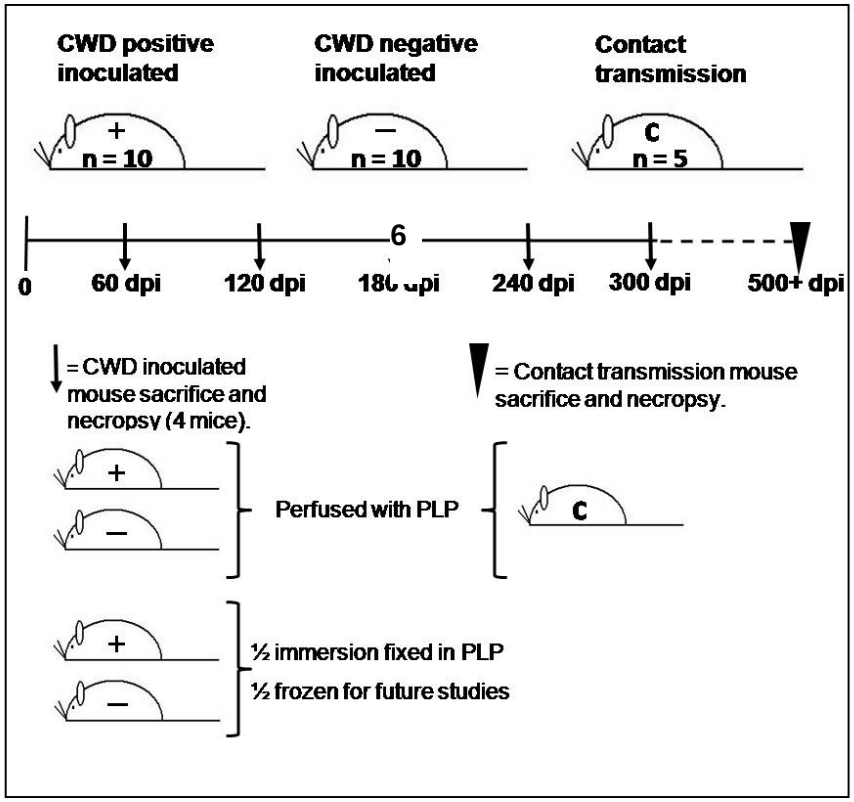

Figure 1.1 The transmission of CWD to Tg[CerPrP] mice. Mice were inoculated via one of four routes with a varied amount of a 1% CWD^{+} or CWD^{-} brain homogenate. Mice were sacrificed at 60 day intervals and tissues were evaluated for neuropathology on hematoxylin-and-eosin (H&E) stained sections, and for PrP^{CWD} deposition using IHC.

Animal evaluation, euthanasia, and necropsy:

Following inoculation, Tg[CerPrP] mice were sacrificed at either: 1) a predetermined time-point, 2) the onset of the terminal neurologic disease associated with prion infection, or 3) the onset of severe clinical disease not associated with prion infection but necessitating humane euthanasia. The criteria used for the diagnosis of central nervous dysfunction in prion-inoculated mice have been previously published (Carlson, Kingsbury et al. 1986) and consist of: severe ataxia, difficulty in righting from a supine position, tail rigidity, generalized tremors, and/or severe mental obtundation. For the multi-route CWD-susceptibility and PrP^{RES} sequential accumulation studies, Tg[CerPrP] mice sacrifice time-points were chosen based upon the previously reported 220-day survival period following IC inoculation (Browning, Mason et al. 2004), and were as follows: 60 days-post-inoculation (dpi), 120 dpi, 180 dpi, 240 dpi, and terminal disease. By contrast, the sentinel, co-habitant mice were euthanized at either the onset of terminal neurological disease or other clinical disease necessitating humane euthanasia.

At each pre-determined sacrifice-point, 3 mice per inoculation group were sacrificed (2 mice from the CWD infected group and 1 mouse from the sham-inoculated group) for a total of 12 mice at each time-point. One of the two mice from each CWD-inoculated group was perfusion fixed with paraformaldehyde-lysine-periodate (PLP) fixative and necropsied. The second mouse from this group and the single sham-inoculated mouse were euthanized via IP injection of pentobarbital (Sleepaway®, Fort Dodge Animal Health) and necropsied. Tissues from this group were split between frozen storage (at -80^{o} centigrade) and PLP immersion fixation. At necropsy, samples

from all tissues were obtained, including both nervous (brain and spinal cord) and non-nervous (peripheral) tissues. Following necropsy, all fixed tissues were immersed in PLP fixative for 24 hours before being moved into 70% ethanol for long-term storage.

Following less than 5 days in ethanol, tissues were routinely trimmed for histologic processing. Whole brains were sectioned coronally to generate a series of 2-3 mm thick tissue slices, representing the following regions of the brain: (i) neocortex (at the level of the caudate nucleus), (ii) hippocampus and hypothalamus, (iii) midbrain (at the level of the colliculi) (iv) hindbrain (including the pons and the cerebellum), and (v) caudal brain stem (at the level of the obex).

Tissue collection and processing:

For detection of PrP^{C}, Tg[CerPrP] and $PrP^{0/0}$ mice were perfusion or immersion fixed with one of 2 fixatives: 10% neutral buffered formalin (NBF) or PLP. In all cases, perfusion fixation was performed using a commercially available, gravity-feed system (AutoMate Scientific™) and modification of a published protocol which employs left ventricular fixative injection and right atrial exsanguination.(Heinlich and Bullock 2004) Following perfusion, tissues were post-fixed in their respective fixative for 12-24 hours and transferred to 70% ethanol for long-term storage. For detection of PrP^{RES}, tissues obtained from CWD-inoculated mice were perfusion fixed with PLP as described above. To ablate PrP^{C} immunoreactivity, cassetted tissues were immersed in 88% formic acid for 1 hour followed by rinsing in running tap water for 1 hour prior to histologic processing. 6 micron sections were prepared and immunostained as described above.

Histology and immunohistochemistry:

For all experiments, paraffin-embedded tissue sections (6 µm) were mounted onto positively charged glass slides; deparaffinized in a heated oven followed by successive immersions in xylene, and rehydrated through graded ethanol. To enhance detection, tissues were subjected to Heat Induced Epitope Retrieval (HIER) using an automated antigen-retrieval system (Retriever™) and a proprietary buffer solution (DakoCytomation™ Target Retrieval Solution).

For the detection of PrP^C, tissues were stained using one of 7 anti-prion protein antibodies (Table 1.1).

Table 1.1. Anti-PrP antibodies used in the detection of PrP^C in 1536 Tg[CerPrP] mice.*

Ab designation	Origin	Ig isotype	Source
BAR-224	Mouse monoclonal	IgG_1	Cayman
F99 / 97.6.1	Mouse monoclonal	IgG_1	VMRD
6D11	Mouse monoclonal	IgG_{2a}	Signet
7D9	Mouse monoclonal	IgG_1	Signet
12B2	Mouse monoclonal	IgG_1	Jan Langeveld
9A2	Mouse monoclonal	IgG_1	Jan Langeveld
R505.5	Rabbit polyclonal		Jan Langeveld

* For each of the antibodies, the following tissue fixation techniques were evaluated:

1. Immersion fixation with 10% NBF.
2. Perfusion fixation with 10% NBF.
3. Immersion fixation with PLP.
4. Perfusion fixation with PLP.

The R505.5 antibody was elicited in rabbits by immunization with the ovine prion protein peptide 100-111 (SQWNKPSKPKTN). The reactivity and specificity of this antibody for the prion protein has been demonstrated using Pepscan and Western blot analysis and ELISA and Radio-immunoprecipitation.(Garssen, Van Keulen et al. 2000)] The primary and secondary antibody type, concentration, and/or tissue pre-treatment

varied as detailed below. Antibody deposition was visualized using DAB (Dako Cytomation™) and slides were counterstained with hematoxylin and incubated with a bluing reagent (0.1% sodium bicarbonate). Following immunostaining, slides were dehydrated through graded ethanol, cleared with xylene, and coverslipped.

For the detection of PrP^{CWD}, an IHC protocol was used that combined either a one- or two-step immunostaining procedure with tyramide signal amplification (TSA). Previous work in our laboratory has demonstrated this methodology to be more sensitive in the detection of PrP^{CWD} than traditional, two-step indirect IHC protocols (Sigurdson, Barillas-Mury et al. 2002) (Fig 1.2).

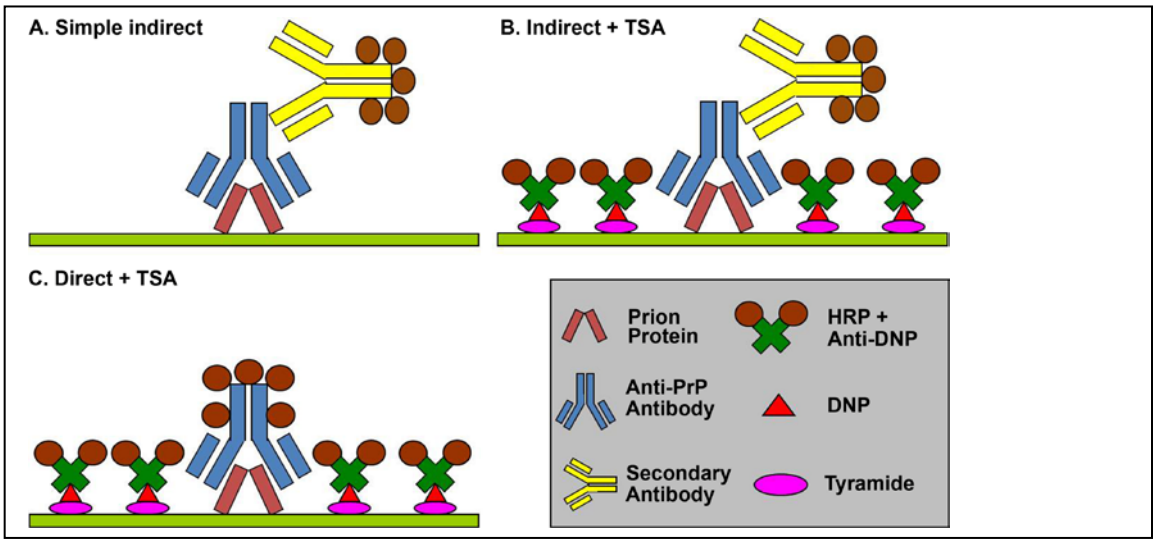

Figure 1.2 Techniques used in the IHC detection of the prion protein in Tg[CerPrP] mice. For the detection of PrP^{C}, a simple, 2-step, indirect method was used (A). For the detection of PrP^{CWD}, one of two protocols incorporating TSA was used, either indirect (B) or direct (C) in nature. In the latter, so as to eliminate the secondary antibody, the HRP-conjugated antibody BAR224 was used. For each of the protocols, labeled antigen was detected using either DAB or AEC. Abbreviations: TSA = Tyramide Signal Amplification, PrP = Prion protein, HRP = Horseradish peroxidase, DNP = Dinitrophenol, DAB = 3,3'-Diaminobenzidine, AEC = 3-amino-9-ethyl-carbazole.

The TSA-PrP^{CWD} protocol used a proprietary TSA-detection kit (Perkin-Elmer™) and was conducted as follows. Following slide rehydration and HIER (as described

above), tissue section endogenous peroxidase activity was blocked using 3% H_2O_2 for 60 minutes. Sections were further blocked using a proprietary protein block (TNB, Perkin-Elmer™) for 60 minutes and 10% goat serum for 30 minutes. Slides were incubated with one of two anti-prion antibodies, either the R505.5 antibody or the HRP-conjugated antibody BAR-224.

In protocols incorporating the R505.5 antibody, slides were incubated with an HRP-conjugated anti-rabbit secondary antibody. Between all incubation steps, slides were washed three times (5 minutes each) in a TNT wash buffer (0.1M Tris-HCl, pH 7.5, 0.15M NaCl, and 0.05% Tween-20). Following the application of the antibodies, slides were sequentially incubated with two proprietary TSA reagents: 1) DNP Amplification Reagent (Perkin-Elmer™) for 4 minutes and 2) anti-DNP-HRP (Perkin-Elmer™) for 30 minutes. Antibody deposition was visualized using DAB and slides were counterstained with hematoxylin and incubated with a bluing reagent (0.1% sodium bicarbonate). Following immunostaining, slides were dehydrated through graded ethanol, cleared with xylene, and coverslipped.

Peptide blocking studies:

To confirm the specificity of the anti-PrP^{CWD} IHC detection protocols, I conducted a series of complementary peptide-blocking IHC studies in which the anti-prion protein antibody (either R505.5 or HRP-conjugated BAR-224) was pre-incubated with its eliciting peptide prior to incubation on the tissue section. To confirm the specificity of the PrP^{CWD} detection protocol, the anti-prion protein antibody BAR-224

was pre-incubated with the peptide FGSDYEDRYYR, which corresponds with its eliciting antigen, residues 141-151 of the ovine prion protein. The R505.5 antibody was pre-incubated with the peptide SQWNKPSKPKTN, which corresponds to residues 100-111 of the ovine prion protein. The reactivity and specificity of this antibody for the prion protein has been demonstrated using Pepscan and Western blot analysis and ELISA and Radio-immunoprecipitation.(Garssen, Van Keulen et al. 2000) In such peptide blocking reactions, the remainder of the immunostaining protocol was identical to that described for the detection of PrP^{CWD}, however antibody deposition was visualized using the chromagen 3-amino-9-ethyl-carbazole (AEC, Dako Cytomation^{TM}) rather than DAB.

Whole brain oral inoculation studies:

As a follow-up to the PO-inoculation studies described above, a study was initiated to evaluate the effect of dose on the susceptibility of 1536 Tg[CerPrP] mice to oral inoculation with CWD prions. Two groups of naïve, 4-6 week old mice (n = 5 per group) were orally-inoculated with whole brain obtained from either a known CWD-positive or CWD-negative white-tailed deer. Mice were orally inoculated with 0.2 – 0.25 grams of whole brain material introduced directly into the oral cavity. Mice were not sedated for this procedure. Following inoculation, mice were monitored for the development of clinical neurologic disease as described above and euthanized at the onset of either terminal neurologic disease or any other severe clinical disease necessitating humane euthanasia. Upon euthanasia, mice were perfusion fixed with PLP fixative and tissues prepared for immunohistochemical evaluation.

Ethics Statement:

The animal experiments were conducted under the guidelines developed by the Colorado State University Animal Care and Use Committee.

RESULTS

Immunohistochemical detection of PrP^C in naïve 1536 Tg[CerPrP] mice:

In order to determine the systemic, tissue-specific distribution profile of the cervid prion protein (PrP^C) in naïve 1536 Tg[CerPrP] mice, I developed IHC protocols to detect PrP^C in paraffin-embedded tissues by evaluating 8 primary antibodies, 2 fixation techniques (perfusion and immersion), and 2 fixatives (PLP and 10% NBF). Although most antibody-fixative combinations were effective at generating some degree of immunoreactivity, the most sensitive PrP^C detection method combined perfusion fixation with PLP and the primary polyclonal anti-PrP antibody R505.5. Cervid PrP^C expression was identified in a surprisingly wide variety of tissues, including those of the nervous, lymphoid, gastrointestinal, hemopoietic, and endocrine systems (Figure 1.3, Table 1.2). Morphologically, the pattern of immunostaining was generally uniform among all PrP^C–expressing tissue types. Within the cytoplasm, in which immunostaining was most common, immunoreactivity was usually finely granular; whereas in the CNS, the immunoreactivity was most commonly fine to coarsely granular with heavy reactivity within the neuropil and within the perikaryon.

CNS PrP^C expression:

Within the CNS, immunoreactivity was identified in a variety of nucleated cell populations (Fig. 1.3 A). Although dual labeling studies were not performed to precisely identify the PrP^C-positive cells, morphologically these cells were consistent with neurons and glial cells (astrocytes and oligodendrocytes). Additionally, marked PrP^C immunoreactivity was observed within the extracellular neuropil. In contrast, PrP^C expression was not identified within components of the peripheral nervous system, including sections of peripheral nerves identified in skeletal muscle and the plexi of the enteric nervous system.

Lymphoid PrP^C expression:

In the lymphoid system, PrP^C immunoreactivity was identified in a spectrum of cell types within the tissues of the primary (lymph nodes) and secondary lymphoid organs, including the spleen, thymus, and Peyer's patches (Fig. 1.3 B). In the lymph nodes, PrP^C was identified in the lymphocytes of the lymphoid follicles of the cortex as well as within large cells within the cortical germinal centers, paracortical, and medullary regions, which likely represent macrophages and/or dendritic cells (Fig. 1.3 K). Within the spleen, immunoreactivity was localized to the white pulp, including cells within both the splenic lymphoid nodules and the periarterial lymphatic sheaths (PALs). Morphologically, the cells demonstrating PrP^C immunoreactivity were consistent with lymphocytes (discrete cells with scant cytoplasm and round nuclei) and macrophages and/or dendritic cells (Fig. 1.3 B, K). Within the thymus, immunoreactivity was confined

to the lymphoid population of the medulla and cortex, whereas the thymic epithelial cell population was negative.

Gastrointestinal PrP^C expression:

Within the gastrointestinal (GI) tract, PrP^C expression was sparsely identified within cells of the lamina propria of the alimentary canal (oral cavity, esophagus, stomach, intestine, and colon). Morphologically, these cells were consistent with small lymphocytes and dendritic cells. The remaining cell types, including the epithelial cell, nervous, muscular, and serosal populations of the alimentary canal were uniformly negative. In the extramural tissues of the GI tract, PrP^C immunoreactivity was identified in the glandular epithelial cells of the salivary glands, but not within the ductular epithelium (Fig. 1.3 C). Additionally, heavy PrP^C immunoreactivity was seen in the cells of the lingual taste buds (Fig. 1.3 J). In the liver, PrP^C expression was identified only within the resident macrophage population (Kupfer cells) (Fig. 1.3 L) whereas in the pancreas, it was limited to the endocrine, islet epithelial cells (Fig. 1.3 I).

Urogenital PrP^C expression:

In the urogenital system, PrP^C immunoreactivity was identified within the kidney, urinary bladder, and male and female reproductive systems. In the kidney, PrP^C expression was limited to cells of the tubular system, largely those of the proximal nephron, and transitional epithelium lining the renal pelvis with rare expression seen in the renal glomerulus (Fig. 1.3 D). Similar to the kidney, in the urinary bladder, PrP^C expression was limited to the transitional epithelium. In the male reproductive tract,

prominent PrP^C expression was identified in the cells of the testes and in the epithelial cells of the accessory sex glands including the prostate and vesicular glands. The coagulating gland was negative.

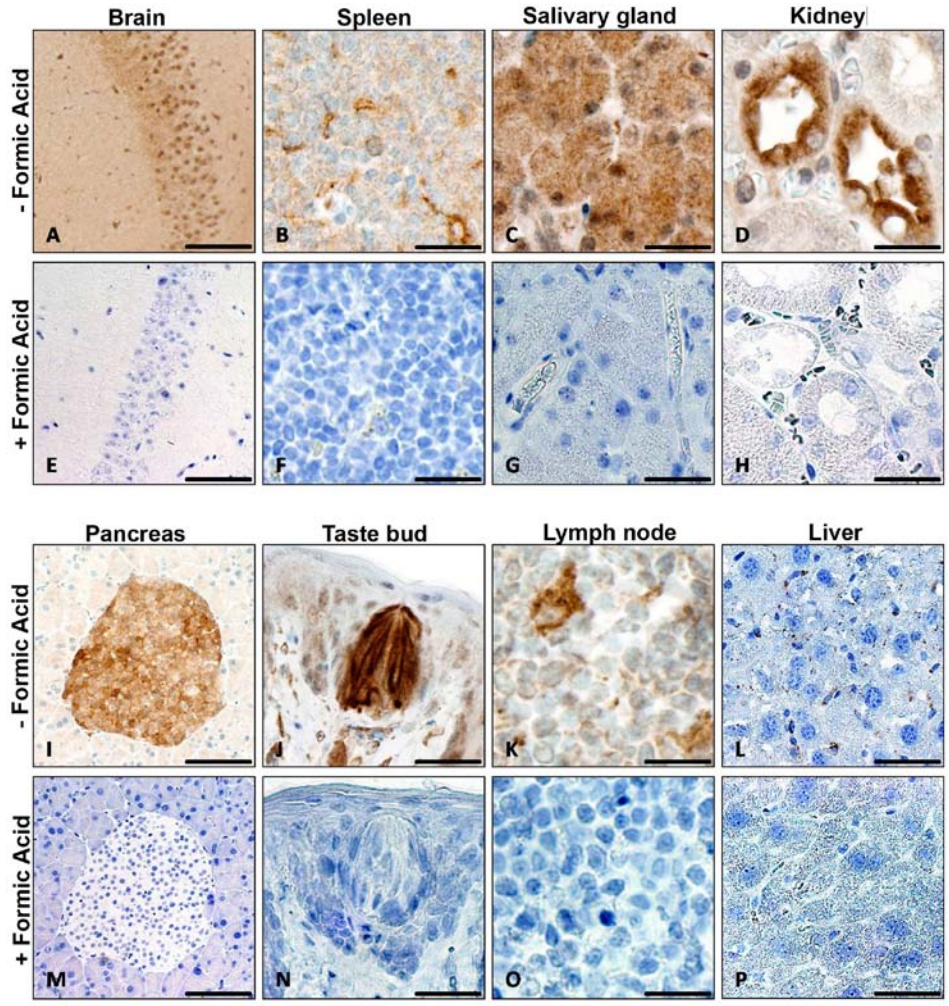

Figure 1.3 Cervid PrP^C expression within tissues of Tg[CerPrP] mice.
Each paired set of rows represents identical tissues both of which have been stained with the R505.5 antibody. The bottom row of each set represents tissues which have been twice treated with 88% formic acid. PrP^C immunoreactivity present (brown) in (a) neurons and neuropil, (b) splenic nucleated cells, (c) salivary gland epithelial cells, (d) renal tubular epithelial cells, (i) pancreatic islet cells, (j) lingual taste buds, (k) lymph node nucleated cells, and (l) hepatic Kupfer cells. Note the lack of PrP^C immunoreactivity in tissues treated with 88% formic acid (Rows 2 & 4). Bars = 100 µm (A, E, I), 40 µm (B, F, J), 40 µm (C, G, K), 30 µm (D, H, L), 120 µm (M), 45 µm (N), 25 µm (O), and 20 µm (P).

Respiratory PrP^C expression:

In the respiratory system, PrP^C immunoreactivity was identified only a small number of cells within the inter-alveolar interstitium, likely interstitial macrophages. The remaining cell types, including the ciliated epithelial cells of the upper and lower respiratory tract and the type I and II alveolar cells, were negative.

Endocrine PrP^C expression:

Within the endocrine system, PrP^C was identified in the epithelial cells of the pancreatic islets (Fig. 1.3 I), and the adrenal, thyroid glands, and parathyroid glands.

Hematopoietic PrP^C expression:

In the hematopoietic system, PrP^C immunoreactivity was identified within the bone marrow, in which expression was limited to megakaryocytes and cells of apparent myeloid lineage.

Additionally, PrP^C immunoreactivity was not detected in tissues fixed with NBF or in tissues immunostained with either a negative control antiserum or in tissues obtained from a $PrP^{0/0}$ mouse. Moreover, as accurate and specific detection of PrP^{CWD} requires the complete abrogation of PrP^C immunoreactivity, I examined tissue and slide treatment strategies which most effectively allow us to make such a distinction. As demonstrated in Figure 1, complete abrogation of PrP^C immunoreactivity can be obtained through a two-step series of immersions in 88% formic acid (Figure 1.3 E-H and M-P). Finally, to confirm the specificity of the PrP^C detection protocol, matching tissues from

$PrP^{0/0}$ mice were identically immunostained and in such animals, no PrP^{C} immunoreactivity was observed nor was immunoreactivity identified in sections immunostained with a protocol incorporating a negative control antiserum.

CENTRAL NERVOUS SYSTEM		**UROGENITAL SYSTEM**	
Neuronal cell bodies	**Positive**	Renal tubules	**Positive**
Oligodendrocytes	Negative	Glomerulus	**Positive**
Astrocytes	Negative	Transitional epithelium	Negative
Neuropil	**Positive**	Prostate	**Positive**
Ependymal cells	**Positive**	Vesicular gland	**Positive**
		Coagulating gland	Negative
PERIPHERAL NERVOUS SYSTEM		Testes	**Positive**
Ganglia neuronal cells.	Negative	Uterine endometrium	Negative
Axons	Negative	Vaginal epithelium	Negative
		Ovary	**Positive**
CARDIOVASCULAR SYSTEM			
Cardiac myocytes	Negative	**RESPIRATORY SYSTEM**	
Endothelial cells	**Positive**	Respiratory epithelium	Negative
		Type I pneumocytes	Negative
LYMPHOID SYSTEM		Type II pneumocytes	Negative
Lymph node cortical follicles	**Positive**	Alveolar macrophages	**Positive**
Lymph node paracortex	**Positive**		
Lymph node medulla	**Positive**	**ENDOCRINE SYSTEM**	
Splenic lymphatic sheaths	**Positive**	Pancreatic islet cells	**Positive**
Thymus	**Positive**	Adrenal medullary cells	**Positive**
		Adrenal cortical cells	**Positive**
GASTROINTESTINAL SYSTEM		Thyroid epithelium	N/A
Salivary glands	Negative	Parathyroid epithelium	N/A
Tongue epithelium	Negative		
Taste buds	**Positive**	**OTHER TISSUES**	
Esophagus	Negative	Myocytes	Negative
Gastric epithelium	Negative	Bone marrow	**Positive**
Submucosal glands	Negative	Adipose tissue	Negative
Peyer's patches	**Positive**	Keratinocytes	Negative

Table 1.2 PrP^{C} expression in the tissues of 1536 Tg[CerPrP] cervidized transgenic mice. All evaluated tissues were obtained from PLP-perfusion fixed, adult 1536 Tg[CerPrP] mice and stained using the R505.5 primary antibody and the IHC protocol detailed in the text. In the tissues denoted as positive, PrP^{C} immunoreactivity varied in intensity, but the reactivity was uniformly cytoplasmic and granular.

Transmission of CWD to 1536 Tg[CerPrP] mice:

The inoculation of the Tg[CerPrP] mice with mule-deer origin CWD prions resulted in clinical disease in the IC, IP, and IV inoculated animals with the following survival periods IC: 184 (± 13 dpi), IP: 218 (± 15 dpi), and IV: 200 (± 7 dpi), respectively (Table 1.3). In affected animals, clinical disease was characterized by ataxia, hyperactivity, tail rigidity, and terminal mental obtundation.

	Route of inoculation					
	IC	*IP*	*IV*	*PO – 1%*	*Contact*	*PO – WB*
Days to disease	184 ± 13 d.	218 ± 15 d.	200 ± 7 d.	N/A	See text	350 ± 27 d.
# ill mice / total # mice	3/3	3/3	3/3	0/10	3/20	3/5

Table 1.3 The transmission of CWD prions to transgenic mice following multiroute inoculation. Time-to-clinical disease and number of mice evaluated at the time of terminal disease is represented for the IC, IP, IV, and PO-inoculated 1536 Tg[CerPrP] mice. The results of two PO-inoculation studies are summarized – one performed with a 1% inoculum (PO-1%) and the second with a whole-brain (PO-WB) inoculum (see text for details). The contact transmission mice represent naïve transgenic mice which were cohabitant with inoculated counterparts (see text for details). For all animals, CWD-infectivity was confirmed by IHC. None of the sham-inoculated mice (n = 6 per route) developed clinical neurologic disease nor demonstrated PrP^{res} accumulations in the brain.

Moreover, in addition to neurologic signs, IV, IP, and IC inoculated mice demonstrated a clinical syndrome characterized by hyperphagia and weight gain, which presaged both the previously described neurologic disease and terminal weight loss (Table 1.4). Finally, the initial group of PO-inoculated and the sham-inoculated Tg[CerPrP] mice remained healthy for more than 700 days.

	Days Post Inoculation	Mean weight of CWD-infected mice	Mean weight of sham-infected mice	Percent difference
IC	120	38.3 (n=8)	33.3 (n=5)	+15%
IP	120	39.8 (n=8)	35.3 (n=5)	+13%
PO	120	32.8 (n=8)	32.6 (n=5)	+0.01%
IV	120	35.8 (n=8)	34.3 (n=5)	+4.3%

Table 1.4 Mean body weights of CWD-infected and uninfected transgenic mice.
Note the increase in mean body weight in the IC, IP, and IV inoculation groups as compared to the nominal change in the PO group.

Neuropathology in inoculated 1536 Tg[CerPrP] mice:

Independent of inoculation route, CWD-infected mice developed similar histopathological lesions. These changes in the hippocampus, hypothalamus, cerebellum, and brainstem, consisted of raggedy rarefaction of the neuropil and perikaryon (spongiform degeneration) with the adjacent deposition of pale eosinophilic, plaques. The most extensive lesions were identified in the cellular layers of the hippocampus and the cerebellum. In the cerebellum, there was extensive neuronal loss within the Purkinje cell and granular layers with rarefaction of the neuropil and plaque accumulation (Figure 1.4 C). Similarly, in the hippocampus, there was loss of neurons within cellular layers as well as neuropil rarefaction and eosinophilic plaque accumulation (Figure 1.4 B). No lesions were observed in sham-inoculated Tg[CerPrP] mice (Figures 1.4 B and D).

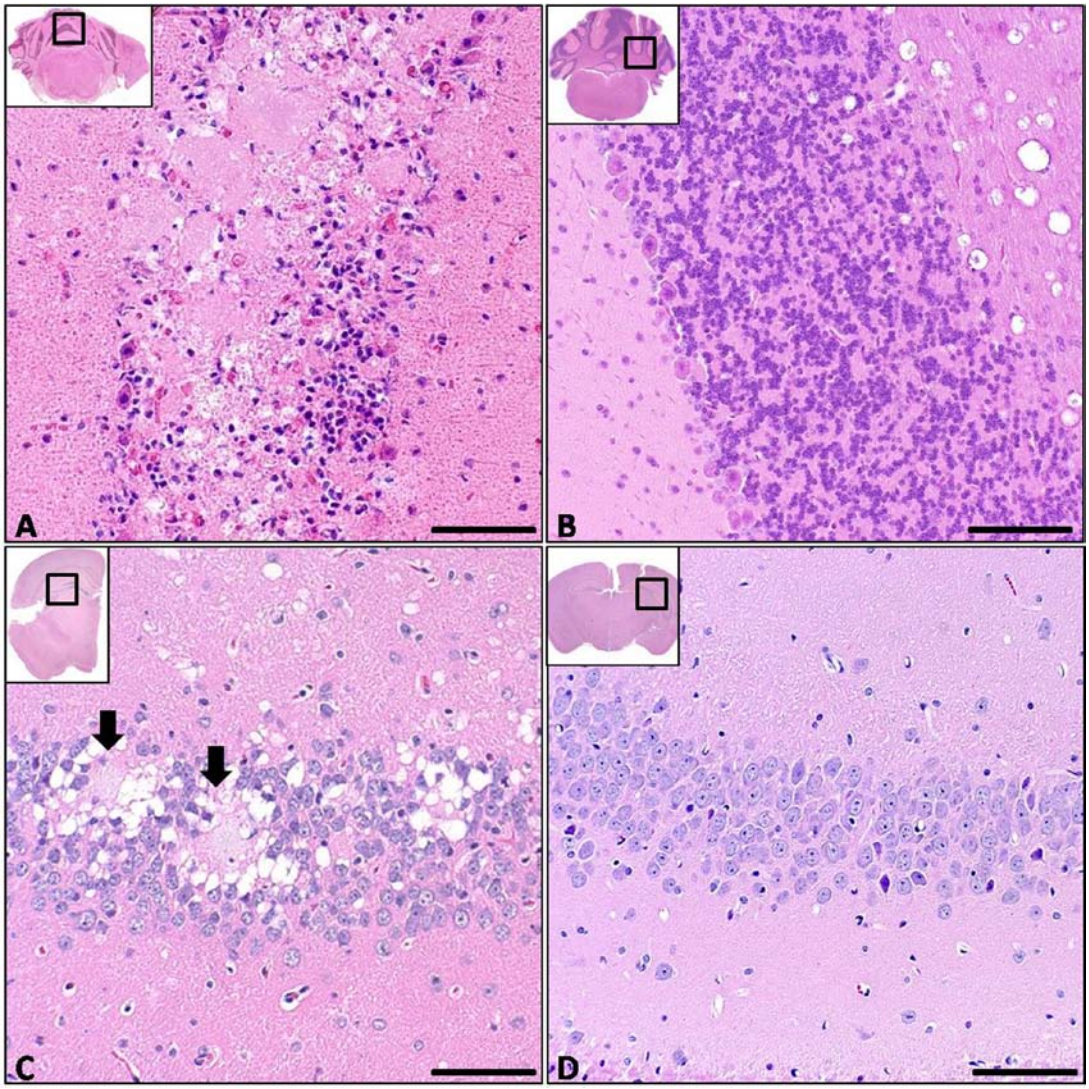

Figure 1.4 Neuropathology in CWD-infected 1536 Tg[CerPrP] mice. All tissues were obtained from inoculated, PLP-perfused mice and were routinely stained with hematoxylin and eosin. The panels on the left (Panels A and C) demonstrate tissues obtained from a terminal, CWD-positive, IV-inoculated Tg[CerPrP] mouse sacrificed at 201 dpi. The panels on the right (Panels B and D) demonstrate tissues obtained from a CWD-negative, sham-IV-inoculated Tg[CerPrP] mouse sacrificed at 201 dpi. Panel A demonstrates a loss of neuronal cell bodies within the granular and Purkinje cell layers of the cerebellum, raggedy rarefaction of the neuropil, and the accumulation of irregularly shaped, extracellular, eosinophilic plaques (outlined by arrows). Panel C demonstrates a similar loss of neuronal cell bodies within the hippocampus, as well as raggedly rarefaction of the neuropil and the accumulation of extracellular eosinophilic plaques (denoted by arrows). In contrast, a lack of neuropathology was identified in matched, sham-inoculated negative controls (Panels B and D). Bars = 50 µm (A), 40 µm (B), and 75 µm (C and D).

Detection of PrP^{CWD} in tissues of Tg[CerPrP] mice:

The most effective strategy for the detection of PrP^{CWD} in the tissues of the CWD-inoculated mice involved PLP fixation of tissues, a two step treatment with 88% formic acid, and an immunodetection protocol incorporating one of two anti-prion antibodies – rabbit polyclonal R505.5 or HRP-BAR224. In contrast to simple, either direct or two-step IHC protocols, the incorporation of TSA technology into the immunodetection of PrP^{CWD} in the tissues of the inoculated Tg[CerPrP] mice resulted in a dramatically increased sensitivity (Fig. 1.5 B & D). Moreover, TSA allowed for the re-classification of the IV- and IP-inoculated mice sacrificed at 60 dpi, which were originally deemed to be CWD-negative.

In mice successfully infected by the IC, IP, and IV- routes, PrP^{CWD} depositions differed chiefly in the sequence of first detection in target organs and cell populations and, in some instances as noted, in the spectrum of PrP^{CWD}-positive cell phenotype (Fig. 1.6). The earliest detection of PrP^{CWD} in the CNS was at 60 dpi, in the gray and white matter of the frontal cortex, the hippocampus, and the hypothalamus, most commonly in regions of neuropil spongiosis. The earliest detection of PrP^{CWD} in a peripheral tissue was at 60 dpi in the spleen, liver, and mesenteric lymph nodes. PrP^{CWD} was not detected at any time point in any tissues from the following systems: musculoskeletal, reproductive, peripheral nervous, respiratory, or cardiovascular. Moreover, PrP^{CWD} was not identified in any of the tissues obtained from the sham-inoculated 1536 Tg[CerPrP] mice. Route of inoculation specifics are detailed below.

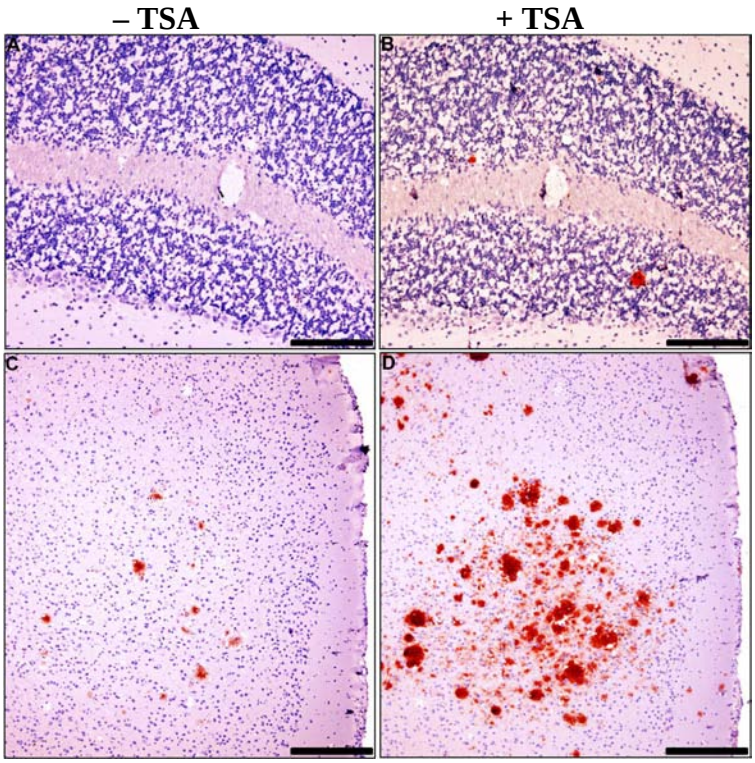

Figure 1.5 Enhanced PrP^{CWD} detection using TSA-IHC.
In paired, PLP-perfused tissue sections, the incorporation of TSA resulted in either the detection of novel deposits of PrP^{CWD} (A vs. C) or greatly enhanced signal from previously identified, PrP^{CWD}-positive sites (B vs. D). Abbreviations:
Bar: A-D = 1000 µm.

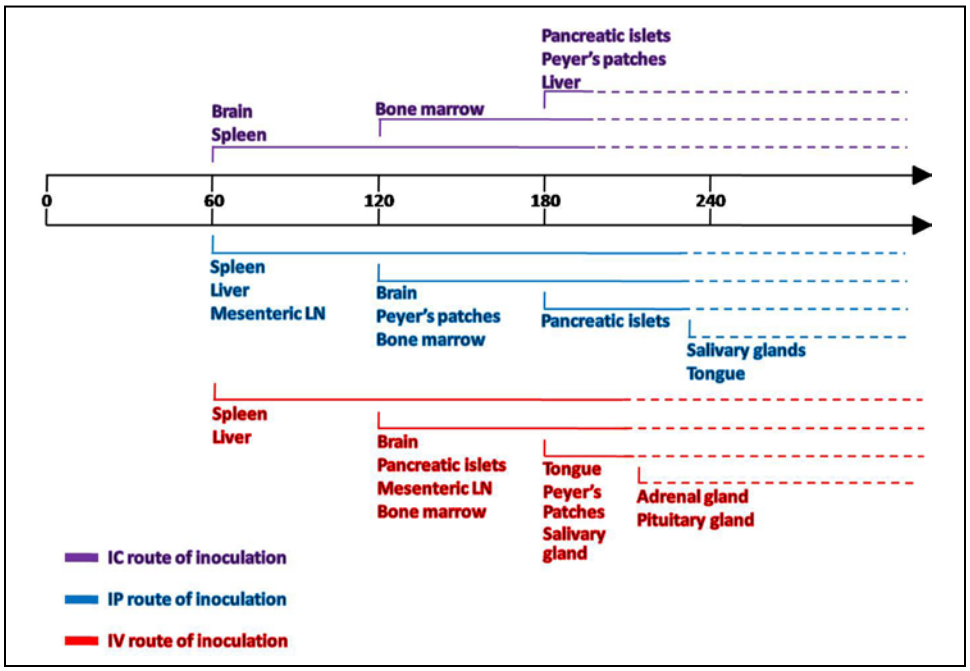

Figure 1.5 Longitudinal PrP^{CWD} detection in Tg[CerPrP] mice.
For each of three routes of inoculation (purple = IC, blue = IP, and red = IV), tissues are listed by earliest sacrifice time point (60, 120, 180, and 240 dpi) at which PrP^{CWD} was detected by IHC. For each time point and each route, listed are only those tissues in which the identification of PrP^{CWD} represented a new appearance. The transition from solid to dashed line represents the approximate onset of terminal clinical disease. Tissues listed at the last time-point represent IHC findings in terminal animals.

PrP^{CWD} in 1536 Tg[CerPrP] mice after intracerebral (IC) inoculation:

In the two IC-inoculated mice sacrificed at 60 dpi, PrP^{CWD} was detected in the brain and in the spleen. Within the brain, PrP^{CWD} immunoreactivity was limited to the gray and white matter of the frontal cortex, the hippocampus, and the hypothalamus. In these areas, the immunoreactivity was granular to clumped, extracellular, and commonly seen in regions of neuropil spongiosis (Fig. 1.6 A). No immunoreactivity was detected in the cerebellum, brain stem, or spinal cord. Within the spleen, the PrP^{CWD} staining appeared as granular deposits arranged in cytoplasmic processes suggestive of follicular dendritic cells (FDCs) within lymphoid follicles (Figure 1.6 B). In the mice sacrificed at 120 dpi, PrP^{CWD} was detected in the brain, spleen, and bone marrow. Within the brain and spleen, the anatomic distribution and morphology of the PrP^{CWD} deposits were identical to that reported at 60 dpi. Within the bone marrow, immunoreactivity was finely granular to coarsely clumped and was localized to a small number of nucleated cells (Figure 1.6 C). On H&E sections, these cells were round to polygonal in shape and contain a modest amount of eosinophilic cytoplasm. Morphologically, these cells were interepreted to be of myeloid origin (non-erythroid / non-lymphoid). In mice sacrificed at 180 dpi and in mice sacrificed at terminal disease, PrP^{CWD} was detected in the brain, spleen, liver, Peyer's patches, pancreatic islets, and bone marrow. In the pancreas, PrP^{CWD} immunoreactivity was limited to the islets of Langerhans, and in these sections immunoreactivity was finely granular to clumped and unevenly distributed throughout the cytoplasm (Figure 1.6 D).

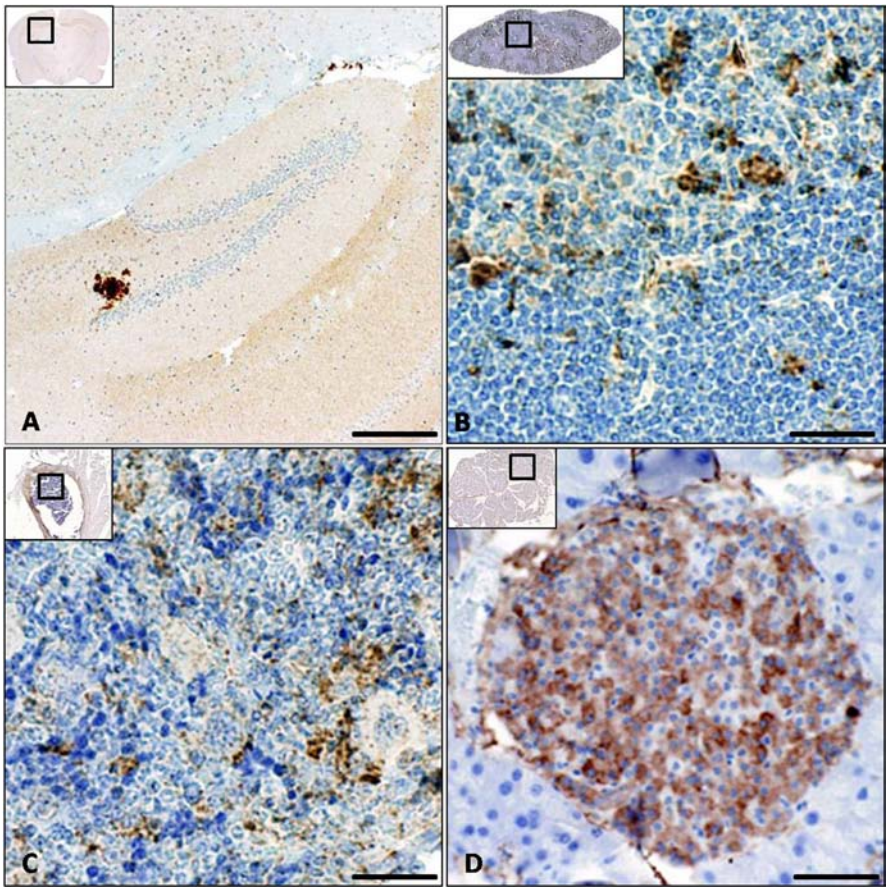

Figure 1.6. PrP^{CWD} in tissues of IC-inoculated 1536 Tg[CerPrP] mice.
All tissues were obtained from PLP-perfused, IC-inoculated mice, immunostained using a TSA-based IHC protocol with either the R505.5 polyclonal antibody or the HRP BAR224 monoclonal antibody. Each panel demonstrates PrP^{CWD} immunoreactivity (brown) in selected tissues. Panel A shows the accumulation of PrP^{CWD} in the hippocampus of the brain at 60 dpi. Specifically, aggregates of extracellular PrP^{CWD} are identified within the hilus fasciae dentatae. Panel B demonstrates the accumulation of PrP^{CWD} within the spleen, most notably within large cells of the marginal zone likely representing macrophages and/or dendritic cells at 60 dpi. Panel C demonstrates the accumulation of PrP^{CWD} within the bone marrow at 193 dpi. Panel D shows the presence of PrP^{CWD} isolated to the islet cells of the endocrine pancreas at 193 dpi. Bars = 200 µm (A), 50 µm (B), and 25 µm (C and D).

PrP^{CWD} in 1536 Tg[CerPrP] mice after intraperitoneal (IP) inoculation:

In IP-inoculated mice sacrificed at 60 dpi, PrP^{CWD} was detected in the liver, spleen, and mesenteric lymph nodes. In the liver, the granular to clumped PrP^{CWD} deposits were identified in a small number of angular, sinusoid-lining cells suggestive of

Kupfer cells (Fig. 1.7 A). Within the spleen and lymph nodes, PrP^{CWD} was present in cells, likely FDCs, similar to that seen in the IC-inoculated mice (Fig. 1.7 B). In mice at 120 dpi, PrP^{CWD} was detected in the brain, liver, spleen, Peyer's patches, mesenteric lymph nodes, and bone marrow. In the brain, PrP^{CWD} was identified within the hippocampus, hypothalamus, and overlying neocortex, and often localized to areas affected by regionally extensive areas of neuropil spongiosis (Fig. 1.7 C). The deposits within the brain were extracellular, coarse, and irregularly shaped in nature. In the remaining affected tissues, the morphology and pattern of immunostaining was identical to that seen in previously examined mice. In IP-inoculated mice sacrificed at 180 dpi, PrP^{CWD} was detected in the brain, spleen, liver, Peyer's patches, pancreas, mesenteric lymph nodes, and bone marrow. In the pancreas, PrP^{CWD} was identified exclusively within the islets of Langerhans. At terminal disease in IP-inoculated mice, PrP^{CWD} immunoreactivity was detected in the brain, spleen, Peyer's patches, liver, salivary glands, tongue, pancreatic islets, mesenteric lymph nodes, and bone marrow. In the salivary glands, PrP^{CWD} was identified within the serous epithelial cells of the submandibular salivary gland (Fig. 1.7 D). In the tongue, the immunoreactivity was finely granular to coarse and identified in two cellular populations – the lingual taste-buds and the lingual glands. In each of these tissues, the immunoreactivity was intracytoplasmic and fine to coarsely granular in nature.

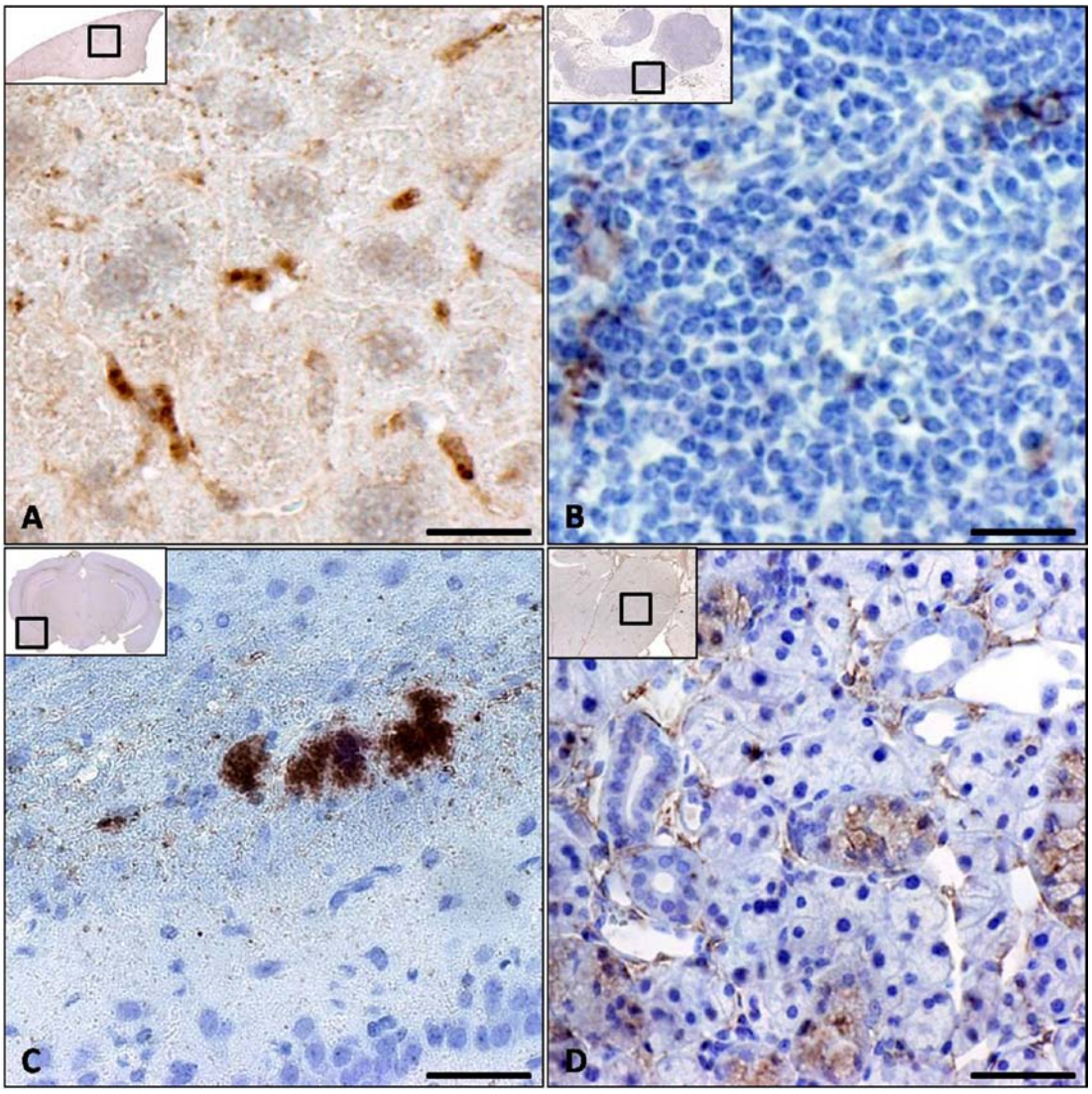

Figure 1.7 PrP^{CWD} in tissues of IP-inoculated 1536 Tg[CerPrP] mice.
All tissues were obtained from PLP-perfused, IP-inoculated mice, immunostained using a TSA-based IHC protocol and either the R505.5 polyclonal antibody or the HRP-BAR224 monoclonal antibody. Each panel demonstrates PrP^{CWD} (brown) in selected tissues. Panel A shows the presence of PrP^{CWD} in the sinusoidal lining cells of the liver (probable Kupfer cells) at 60 dpi. Panel B demonstrates the accumulation of PrP^{CWD} within the mesenteric lymph node, most notably within large cells likely representing macrophages and/or dendritic cells at 60 dpi. Panel C demonstrates the accumulation of PrP^{CWD} within the hippocampus. Specifically, aggregates of extracellular PrP^{CWD} were seen in the laminal principalis interna areae entorhinalis of the hippocampus at 233 dpi. Panel D shows the presence of PrP^{CWD} isolated to the serous cells of the submandibular salivary gland at 233 dpi. Bars = 10 µm (A), 60 µm (B), 50 µm (C), and 25 µm (D).

PrP^{CWD} in 1536 Tg[CerPrP] mice after intravenous (IV) inoculation:

In tissues from IV-inoculated mice sacrificed at 60 dpi, PrP^{CWD} was detected in the spleen and liver in cells morphologically identical to those described in previous tissue sections, namely compatible with FDCs and Kupfer cells, respectively. In mice sacrificed at 120 dpi, PrP^{CWD} was detected in the brain, spleen, liver, pancreatic islets of Langerhans, mesenteric lymph nodes, and bone marrow. The tissue distribution of PrP^{CWD} was identical between the mice sacrificed at 180 dpi and the mice sacrificed at terminal disease (sacrificed at 194 and 201 dpi). In the tissues of these mice, PrP^{CWD} immunoreactivity was detected in the brain, spleen, mesenteric lymph nodes, Peyer's patches, liver, salivary glands, tongue, pancreatic islets, adrenal gland, pituitary gland, and bone marrow. In all affected tissues, the pattern and morphologic nature of the immunoreactivity was identical to that seen in previously described tissues. Within the tongue, PrP^{CWD} was detected in: 1) the cells of the taste bud and 2) the mucus glands of the tongue. Within the taste bud, PrP^{CWD} immunoreactivity was moderate to marked in intensity and granular-to-clumped in the nature (Fig. 1.8 A). Within lingual mucus glands (Fig. 1.8 B), the immunoreactivity was granular to coarse. Within the adrenal gland, PrP^{CWD} immunoreactivity was observed within the cells of the adrenal medulla (Fig. 1.8 D). The cells of the adrenal cortex were negative for PrP^{CWD} immunoreactivity. Within one of two terminal, IV-inoculated mice, PrP^{CWD} deposition was detected in the pituitary gland (Fig. 1.8 C). In the pituitary gland, PrP^{CWD} immunoreactivity was detected in cells morphologically consistent with cells of the neurohypophysis.

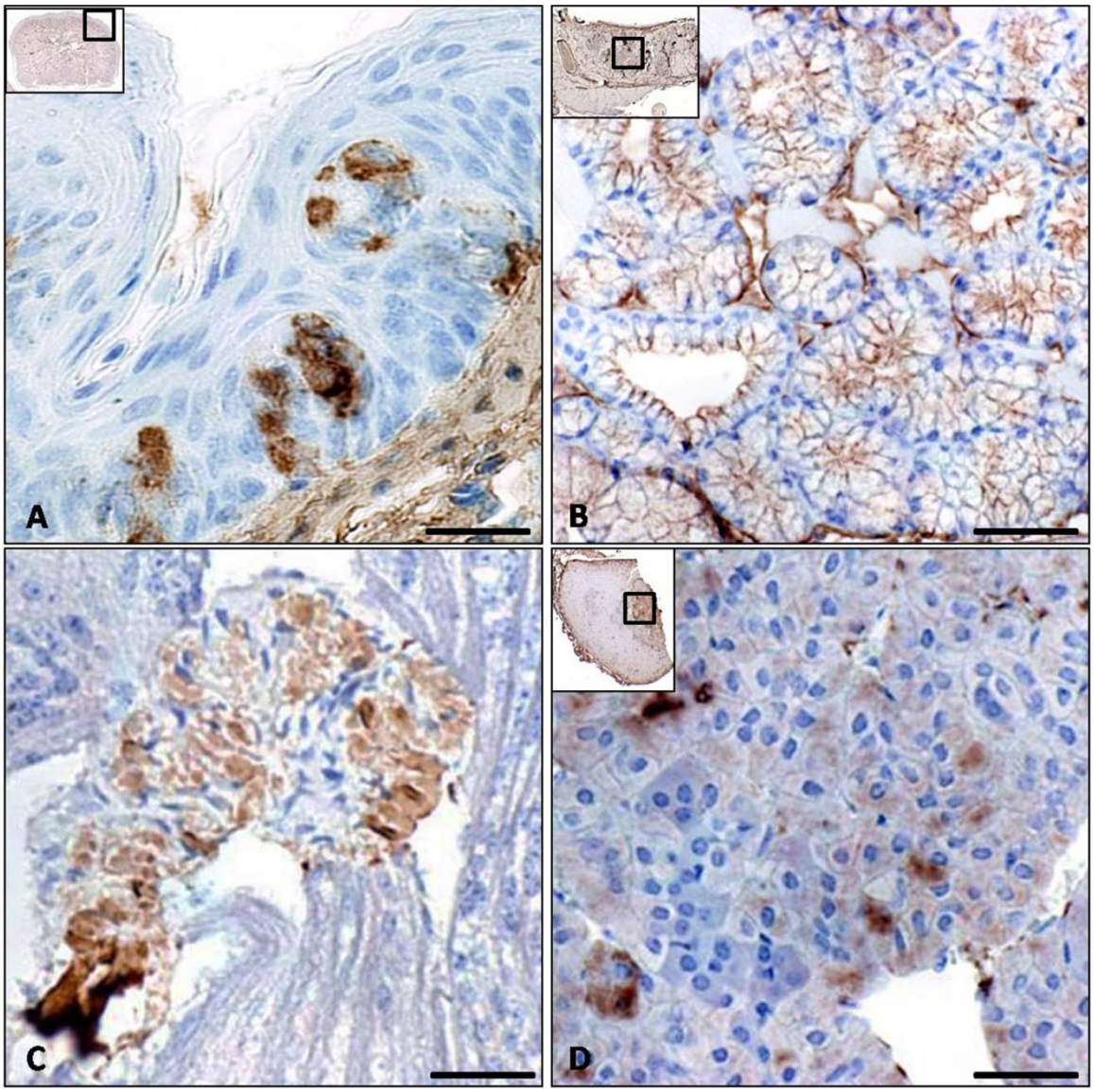

Figure 1.8 PrP^{CWD} in tissues of IV-inoculated 1536 Tg[CerPrP] mice.
All tissues were obtained from PLP-perfused, IV-inoculated mice, immunostained using a TSA-based IHC protocol and either the R505.5 polyclonal antibody or the HRP-BAR224 monoclonal antibody. All tissues are from a terminally-ill mouse sacrificed at 201 dpi. Each panel demonstrates PrP^{CWD} immunoreactivity (brown) in selected tissues. Panel A shows the presence of PrP^{CWD} in the cells of the lingual taste bud. Panel B demonstrates the accumulation of PrP^{CWD} within cells of the mucus lingual glands. Panel C demonstrates the accumulation of PrP^{CWD} within neurohypophysis of the pituitary gland. Panel D shows the presence of PrP^{CWD} isolated to the glandular cells of the adrenal medulla. Bars = 25 µm (A), 60 µm (B), and 50 µm (C and D).

Successful transmission of CWD to orally (PO) inoculated Tg[CerPrP] mice:

In the initial 1% PO-inoculation study, none of the inoculated Tg[CerPrP] mice developed neurologic disease (>700 dpi) or accumulated PrP^{CWD} in either brain or spleen. To determine the role of inoculum dose in oral susceptibility, I inoculated a second group (n=5) of Tg[CerPrP] mice with whole, undiluted CWD-positive or CWD-negative brain. Three of the five CWD-inoculated mice developed progressive and terminal neurologic disease characterized by ataxia and mental obtundation at 323, 350, and 378 dpi, and accumulated PrP^{CWD} in nervous and non-nervous tissues (Fig. 1.9). The largest and most numerous immunoreactive aggregates were detected in the caudal aspects of the brain (obex, brain stem, and cerebellum) with decreasing amounts in the mid- and fore-brain regions, including the hippocampus and hypothalamus with rare PrP^{CWD} detected in the neocortex. In the non-CNS tissues from these 3 mice, PrP^{CWD} was detected in the spleen (3/3), Peyer's patches (3/3), mesenteric lymph nodes (3/3), and pancreatic islets (2/3). PrP^{CWD} was not detected in the remainder of the peripheral tissues evaluated, including all remaining tissues from the gastrointestinal, urogenital, endocrine, and musculoskeletal systems. None of the sham-inoculated animals developed clinical disease nor did tissues from these mice contain PrP^{CWD} immunoreactivity. Thus a 100-fold increment in CWD brain homogenate dosage produced infection and disease by the oral route.

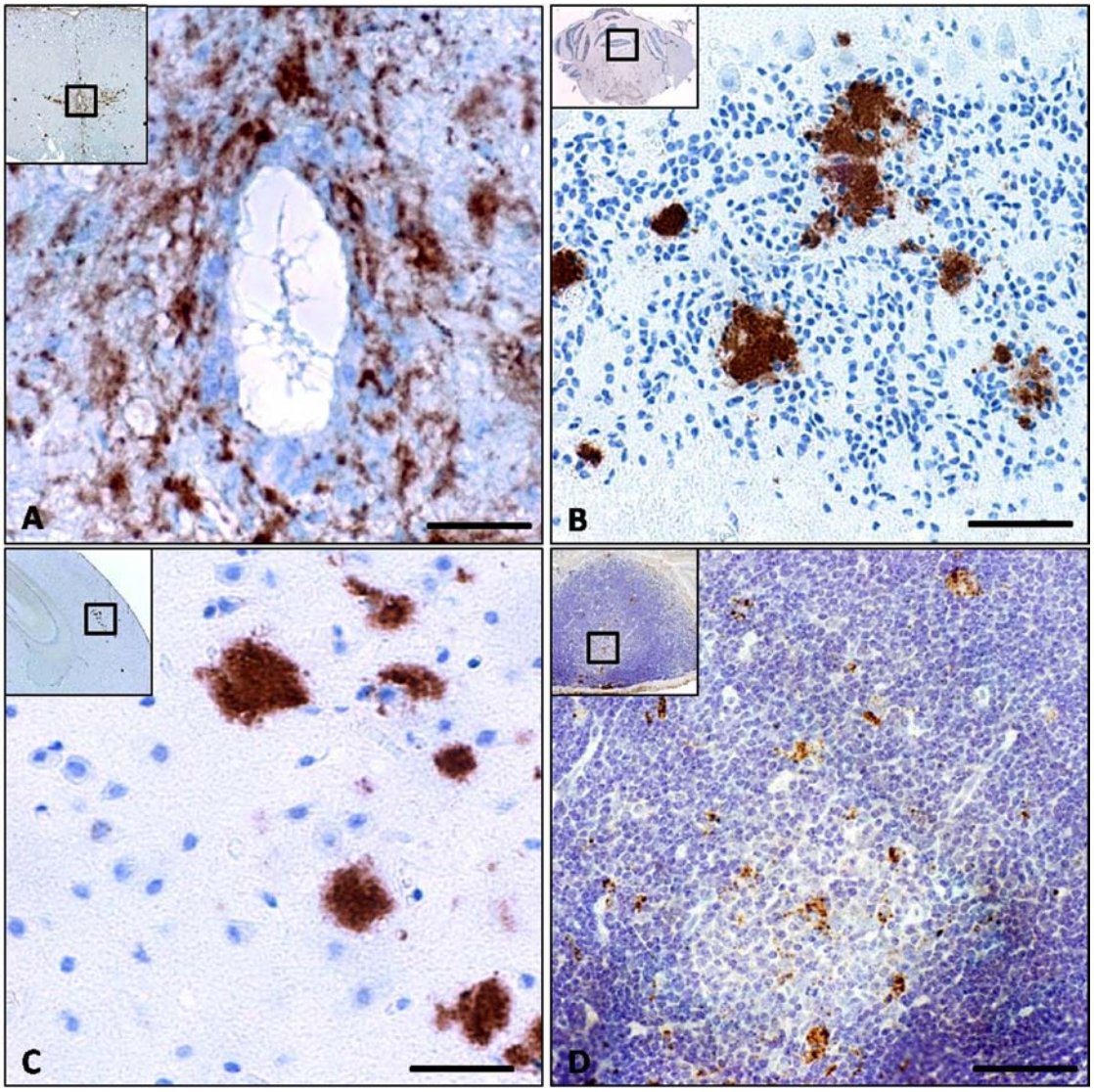

Figure 1.9 PrP^{CWD} in tissues of whole brain, orally-inoculated 1536 Tg[CerPrP] mice. All tissues were obtained from a terminally ill, PLP-perfused, PO-inoculated mouse sacrificed at 350 dpi and immunostained using a TSA-based IHC protocol and either the R505.5 polyclonal antibody or the HRP-BAR224 monoclonal antibody. Each panel demonstrates PrP^{CWD} immunoreactivity (brown) in selected tissues. Panel A shows the accumulation of marked amounts of PrP^{CWD} in the cervical spinal cord, including heavy deposition surrounding the central canal. Panel B demonstrates the moderate-to-marked accumulation of PrP^{CWD} within the granular layer of the cerebellum. Panel C demonstrates the minimal accumulation of PrP^{CWD} in the neocortex. Panel D shows the presence of PrP^{CWD} within the cells of the Peyer's patch which, based upon size and cytomorphologic characteristics, are likely macrophages and/or dendritic cells. Bars = 25 µm (A), 75 µm (B), 20 µm (C), and 200 µm (D).

Horizontal transmission of CWD to contact-exposed sentinel Tg[CerPrP] mice:

To evaluate for the possibility of horizontal CWD transmission in Tg[CerPrP] mice, 1 naïve Tg[CerPrP] mouse was housed as a co-habitant with 2 CWD-inoculated mice. At each of the pre-determined sacrifice time-points (60, 120, 180, and 240 dpi), 2 CWD-inoculated mice and 1 sham-inoculated mouse were euthanized and necropsied. Thus, at the completion of each of these sacrifices, 1 of the 5 cohabitant mice assigned per inoculation group was left alone in the cage resulting in sentinel mice that were exposed to the CWD-inoculated mice for either 60, 120, 180, 240 days, or until terminal disease developed in inoculated cage-mates (171 to 233 days).

Following the sacrifice of their inoculated cage-mates, the co-habitant mice were allowed to live out the remainder of the study (600 dpi) or until the onset of either: 1) clinical neurological disease or 2) clinical signs of any other disease which necessitated humane euthanasia. Of these 20 sentinel mice, three demonstrated clinical neurologic dysfunction and had immunohistochemically detectable PrP^{CWD} within the brain, although only 15 were observed over a long enough observation period (600 dpi) to allow for detection of infection and disease. The first affected mouse was housed with two IC-inoculated mice for 193 days and was sacrificed at 543 days post exposure (dpe). The second affected mouse was housed with two IP-inoculated mice for 233 days and was sacrificed at 562 dpe. The third affected mouse was housed with two IV-inoculated mice for 201 days and was sacrificed at 551 dpe. These three mice lived for 350, 329, and 350 days respectively after the sacrifice of their inoculated cage-mates. Thus, of the 15 mice

exposed to infected cage mates which survived to the end of the study (600 dpi), 3 developed TSE.

Lesions and PrP^{CWD} in horizontally-infected Tg[CerPrP] mice:

Neuropathologic findings in the affected Tg[CerPrP] mice were identical to those seen in the IC, IP, and IV-inoculated mice. PrP^{CWD} distribution in the brains of horizontally infected mice were similar to that in the high dose PO-inoculated mice, with heavy PrP^{CWD} deposits in the obex, brain stem, and cerebellum (Fig. 1.10 A) and smaller, less frequent PrP^{CWD} deposits in the hippocampus, hypothalamus, and neocortex (Fig. 1.10 B). PrP^{CWD} was also detected in the spleen, Peyer's patches, and pancreatic islets (Fig. 1.10 C, D). PrP^{CWD} was not detected in the remainder of the peripheral tissues evaluated, including all remaining tissues from the gastrointestinal, urogenital, endocrine, and muscuoloskeletal systems.

Abrogation of PrP^{CWD} immunoreactivity using peptide blocking:

To confirm the specificity of the PrP^{CWD} IHC detection protocols, tissues previously identified as PrP^{CWD} positive were subjected to an IHC protocol which incorporated a pre-incubation of the primary, anti-prion antibody with its eliciting peptide. In these experiments, there was near-complete to complete abrogation of PrP^{CWD} immunoreactivity when such a peptide, pre-incubation step was incorporated (Figure 1.11).

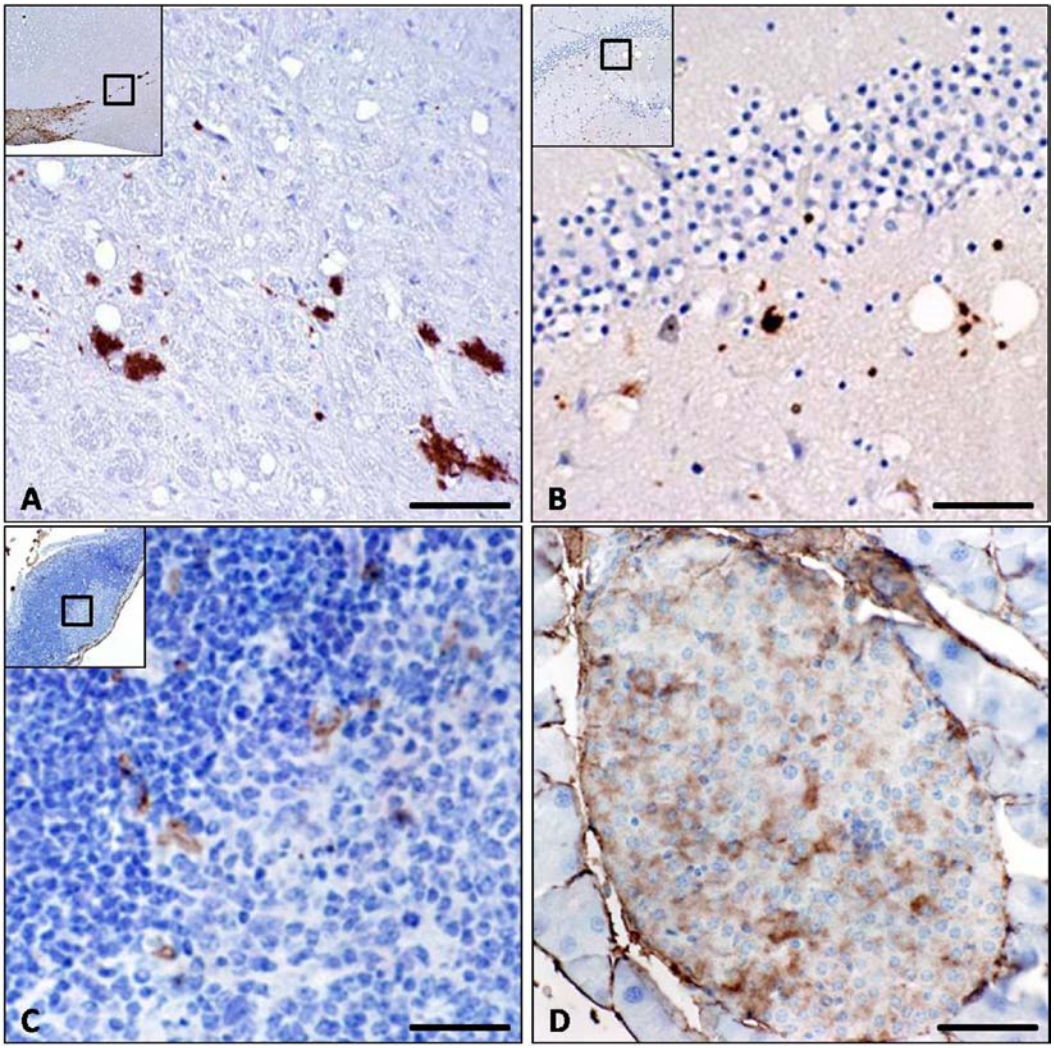

Figure 1.10 PrP^{CWD} in tissues of horizontally-infected 1536 Tg[CerPrP] mice. All tissues were obtained from a terminally ill, PLP-perfused, non-inoculated mouse which cohabitated with an IC-inoculated mice that was sacrificed at terminal neurologic disease. All tissues were immunostained using a TSA-based IHC protocol and either the R505.5 polyclonal antibody or the BAR-224 monoclonal antibody. Each panel demonstrates PrP^{CWD} immunoreactivity (brown) in selected tissues. Panel A shows the accumulation of marked amounts of PrP^{CWD} in the brainstem. Panel B demonstrates the minimal accumulation of PrP^{CWD} within the hippocampus, specifically within the hilus fasciae dentatae. Panel C demonstrates the accumulation of PrP^{CWD} in association with cells of the Peyer's patch which, given their large size and vesicular nuclei, are likely macrophages and/or dendritic cells. Panel D shows the presence of PrP^{CWD} within the cells of the pancreatic islets. Bars = 25 µm (A), 60 µm (B), and 50 µm (C and D).

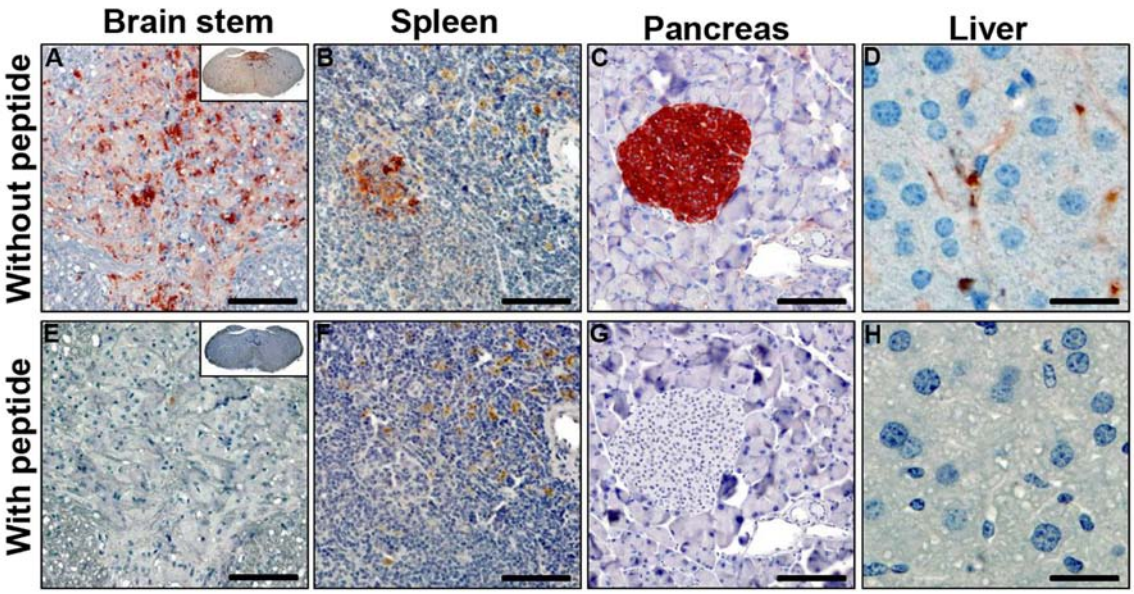

Figure 1.11 Blocking of PrP^{CWD} immunoreactivity using peptide pre-incubation.
All tissues were obtained from a terminally ill, PLP-perfused, IP-inoculated mouse sacrificed at 233 dpi. All tissues were immunostained using an IHC protocol incorporating the BAR-224 monoclonal antibody, amplification using TSA reagents, and the presence (row 2) or absence (row 1) of a peptide blocking step. Top row: Moderate to marked PrP^{CWD} immunoreactivity (red) in (a) brain stem neuropil, (b) splenic nucleated cells, (c) pancreatic islet epithelial cells, and (d) hepatic Kupfer cells. Bottom row: Pre-application incubation of the primary antibody with its eliciting peptide results in complete to near-complete abrogation of PrP^{CWD} immunoreactivity in matched tissue sections (e-h). Bars = 100 µm (A, E), 100 µm (B, F), 80 µm (C, G), and 27.5 µm (D, H).

DISCUSSION

Although the effectiveness of peripheral inoculation in prion diseases appears to rely, in part, upon the expression of PrP^C in peripheral (non-CNS) tissues, there are little published data regarding the systemic expression patterns of PrP^C in the tissues of transgenic mice expressing PrP^C of alternate species.(Brandner, Isenmann et al. 1996; Blattler, Brandner et al. 1997; Glatzel and Aguzzi 2000; Le Pichon and Firestein 2008) In the initial characterization of the 1536 Tg[CerPrP] strain utilized in these studies, cervid PrP was detected only in the brain by dot and western blotting using monoclonal antibody 6H4.(Browning, Mason et al. 2004) To expand upon this initial characterization of 1536 Tg[CerPrP] mice, I used PLP-fixation and the polyclonal anti-prion antibody R505.5 to identify PrP^C expression in cell populations in the nervous, lymphoid, endocrine, reproductive, gastrointestinal, and hematopoietic systems (Table 1.2)--a pattern of expression similar to that reported for expression of native species PrP^C in rodents and cervids.(Mathiason, Foos et al. ; Burthem, Urban et al. 2001; Liu, Li et al. 2001; Ford, Burton et al. 2002; Zhang, Steele et al. 2006) Morphologically, the pattern of PrP^C immunoreactivity varied widely between individual cell and tissue types from finely granular to punctate to aggregate in nature. Such a pattern of PrP^C immunoreactivity is similar to that described in other PrP^C mapping studies in the adult mouse (Brown, Ritchie et al. 2000; Ford, Burton et al. 2002), and may be reflective of the varied, and often high, level of protein expressed in the immunopositive cells. In certain cell types (i.e., splenic lymphocytes, brain neurons) the high levels of protein might saturate the detection system resulting in aggregation of the chromagen. Based upon the lack of

corresponding immunoreactivity in the $PRP^{0/0}$ mice, I am confident that the protocol used to detect PrP^{C} produced accurate and specific results. Finally, these findings provide the first evidence suggesting that the cosTet vector system is capable of manifesting peripheral expression of a heterologous species' prion protein, and compliment recent work confirming this vector system as capable of manifesting widespread prion protein expression in the mouse.(Scott, Foster et al. 1989; Prusiner, Scott et al. 1990; Telling, Scott et al. 1994; Telling, Scott et al. 1995; Scott, Safar et al. 1997; Asante, Linehan et al. 2002; Browning, Mason et al. 2004; Kong, Huang et al. 2005; Angers, Browning et al. 2006; LaFauci, Carp et al. 2006; Tamguney, Giles et al. 2006; Tremblay, Bouzamondo-Bernstein et al. 2007; Trifilo, Ying et al. 2007)

In these studies, I utilized the combination of clinical disease and the immunohistochemical detection of PrP^{CWD} to document successful CWD infection in the inoculated Tg[CerPrP] mice. The use of such an approach is justified by previously published prion pathogenesis and PrP^{CWD} mapping studies, including those evaluating longitudinal patterns of CWD prion accumulation in native cervid species.(Sigurdson, Williams et al. 1999; Sigurdson, Spraker et al. 2001; Sigurdson, Barillas-Mury et al. 2002) While I did not include concurrent immunoblot analysis of all tissue samples, I believe the sensitivity of the TSA-based immunohistochemical detection techniques used provided more than equivalent sensitivity to tissue homogenate western blotting. Moreover, I believe that the results from the peptide blocking and $PrP^{0/0}$ studies confirm the specificity of the PrP^{CWD} longitudinal mapping results.

I demonstrate the susceptibility of Tg[CerPrP] mice to CWD following inoculation via the IC, IV, IP, and PO routes, expanding upon previously published work. (Browning, Mason et al. 2004) Although this is the first report documenting the susceptibility of Tg[CerPrP] 1536 mice to infection with CWD following IP, IV, and PO routes of inoculation, this is not the first report documenting oral susceptibility of cervidized mice to CWD. Trifilo et al. demonstrated that oral inoculation of two other lines of cerPrP transgenic mice produced clinical TSE in both lines at 370 ± 26 and 381 ± 55 dpi, respectively (Trifilo, Ying et al. 2007), which is similar to our findings of 350 ± 27 dpi. The failure of the initial group of orally inoculated mice to demonstrate susceptibility to CWD is likely the result of an insufficient inoculum dose, a point which is emphasized by both the successful inoculation of 3 of 5 mice fed a whole brain inoculum and the successful PO-inoculation study cited above, in which a more concentrated (5%) brain homogenate proved successful.(Trifilo, Ying et al. 2007)

Through serial sacrifice, I was able to demonstrate longitudinal patterns of PrP^{CWD} tissue tropism suggestive of a three phase pathogenesis - 1) an early lymphoreticular (LRS)-associated phase characterized by the accumulation of PrP^{CWD} in lymphoid compartments (spleen and/or lymph node), 2) a neuroinvasive phase, whereby PrP^{CWD} became detectable in the CNS, and 3) the terminal accumulation of PrP^{CWD} within peripheral tissues. The first two phases are most evident in the temporal patterns of PrP^{CWD} accumulation in the IV and IP-inoculated mice in which the early LRS-accumulation phase was demonstrated. In these tissues, PrP^{CWD} was observed within likely follicular dendritic cells (FDCs), cells which have been shown to be important

enablers of prion disease propagation and neuroinvasion (Kimberlin and Walker 1989; Muramoto, Kitamoto et al. 1993; Mabbott, Mackay et al. 2000; Huang, Farquhar et al. 2002; Sigurdson, Barillas-Mury et al. 2002; Mabbott, Young et al. 2003; Mohan, Bruce et al. 2005; Mabbott and MacPherson 2006).

Detection of splenic PrP^{CWD} at a time point (60 dpi) preceding PrP^{CWD} detection in the brain (120 dpi) suggests that splenic-mediated neuroinvasion plays a role in Tg[CerPrP] mice, as has been theorized for scrapie prion transit via nerve fibers associated with FDC-rich splenic germinal centers as conduits to the thoracic spinal cord.(Glatzel, Heppner et al. 2001; Prinz, Heikenwalder et al. 2003) Although splenic-mediated neuroinvasion remains the most likely possibility, I cannot exclude the possibility of hematogenous neuroinvasion. This phenomenon, while little investigated, finds support in the literature by work demonstrating infectious prions in blood.(Hunter, Foster et al. 2002; Banks, Niehoff et al. 2004; Llewelyn, Hewitt et al. 2004; Peden, Head et al. 2004; Mathiason, Powers et al. 2006; Saa, Castilla et al. 2006; Viegas, Chaverot et al. 2006)

The third phase of CWD pathogenesis in Tg[CerPrP] mice was marked by the accumulation of PrP^{CWD} in peripheral tissues (denoted terminal PrP^{CWD} dissemination). In this phase, PrP^{CWD} deposits were detected in the bone marrow, pancreatic islets, Peyer's patches, mesenteric lymph nodes, adrenal gland, pituitary gland, tongue, and salivary gland. Such a pattern is typical of the progressive, vagal- and sympathetic nervous system-mediated, centrifugal dissemination of prions from the brain in the later to terminal stages of prion disease as described in previous mouse, sheep, and hamster

models.(Borchelt, Koliatsos et al. 1994; Blattler, Brandner et al. 1997; Moya, Hassig et al. 2004; Mulcahy, Bartz et al. 2004; Beekes and McBride 2007)

In the successfully infected Tg[CerPrP] mice, there were exceptions to the proposed 2-3 step pathogenesis, i.e., instances in which PrP^{CWD} was identified in peripheral tissues either prior to, or simultaneous with, its identification in the CNS. Such cases included the identification of PrP^{CWD} in the spleen or liver of IV-, IP-, and IC-inoculated mice sacrificed at 60 dpi, or in the pancreatic islets of IV-inoculated animals sacrificed at 120 dpi. These findings support the presence of a transient, post-inoculation period of hematogenous prion trafficking, which results in the delivery of inoculum-origin prions to peripheral tissues. Such a phenomenon, described as a spillover "prionemia," has been reported following the IP- or IC-inoculation of scrapie or CJD prions, such that infectious prions accumulate in peripheral tissues (bone marrow, adrenal gland, salivary gland, spleen) either prior to or coincident with, the identification of prions in the brain and that infectious prions can be detected in the blood immediately after IP- and IC-inoculation.(Field, A. et al. 1968; Millson, Kimberlin et al. 1979; Bruce 1985; Kimberlin and Walker 1989)

The more novel detection of PrP^{CWD} in the salivary glands, bone marrow, neuroendocrine system, and neurosensory cells of the tongue confirms the utility of Tg[CerPrP] mice as effective surrogates for CWD infection. Moreover, serial sacrifice-derived PrP^{CWD} accumulation data offer insights into the manner by which prions traffic to these tissues. In the salivary glands, I identified PrP^{CWD} only after it was identified in the CNS, which suggests that centrifugal spread along neural pathways is responsible for

prion delivery. The salivary glands secrete in response to stimuli provided by the autonomic nervous system, including fibers of both the parasympathetic and sympathetic systems via the medulla oblongata and lateral hypothalamus.(Zoukhri and Kublin 2001; Proctor and Carpenter 2007) Although I did not track the accumulation of prions along specific peripheral and cranial nerve tracts, in our terminal IV- and IP-inoculated mice I did identify significant deposits of PrP^{CWD} within the pons and the ventromedial hypothalamus, which have been described as the salivary centers of the brain.(Proctor and Carpenter 2007) Finally, the pattern of PrP^{CWD} deposition in the salivary glands, with PrP^{CWD} accumulations present on the surface of acinar epithelial cells, is similar to that reported in an IHC study published in scrapie-affected sheep (Vascellari, Nonno et al. 2007) and suggests that salivary secretion of prions may result from normal, physiologic activity of glands during the process of saliva secretion.(McManaman, Reyland et al. 2006)

The demonstration of PrP^{CWD} in the bone marrow of Tg[CerPrP] mice, while novel in the CWD system, is consistent with our identification of PrP^{C} in this compartment and with published work in murine models of scrapie and GSS.(Eklund, Kennedy et al. 1967; Kimberlin and Walker 1989; Takakura, Yamaguchi et al. 2008) While the route by which PrP^{CWD} accumulated in the bone marrow is uncertain, the weight of the evidence suggests a pathway of hematogenous trafficking, as demonstrated by studies showing the feasibility of blood-borne transmission in several prion diseases (BSE, scrapie, CWD, and nvCJD), as well as work detecting prions in the blood of pre-clinical, scrapie-infected hamsters and CWD-infected deer.(Hunter, Foster et al. 2002;

Llewelyn, Hewitt et al. 2004; Peden, Head et al. 2004; Mathiason, Powers et al. 2006; Saa, Castilla et al. 2006) Identification of PrP^{CWD} in the endocrine system of cervidized mice has not been reported previously, but resembles findings in orally-inoculated and naturally-infected mule deer, in which PrP^{CWD} was demonstrated in the adrenal medulla, islets of Langerhans, and pituitary of animals with late stage CWD.(Sigurdson, Spraker et al. 2001; Fox, Jewell et al. 2006) PrP^{RES} has also been seen in the pancreas of goats and sheep with natural scrapie, and in hamsters and mice with experimental scrapie.(Pattison and Millson 1960; McBride, Eikelenboom et al. 1992; Ye, Carp et al. 1994) As PrP^{CWD} was detectable in endocrine tissues only after its detection in the brain, centrifugal dissemination via the vagus nerve, splanchnic nerves, and fibers from the hypothalamus to the pancreatic islets, adrenal gland, and pars nervosa of the pituitary gland, respectively, is likely.(Kesse, Parker et al. 1988; Loewy, Franklin et al. 1994)

The identification of PrP^{CWD} in the lingual taste buds and glands is intriguing. PrP^{RES} has been previously reported in the tongues of hamsters IC-inoculated with transmissible mink encephalopathy (TME), in hamsters PO-inoculated with scrapie, in transgenic mice PO-inoculated with CWD, and in sheep with natural scrapie.(Thomzig, Kratzel et al. 2003; Andreoletti, Simon et al. 2004; DeJoia, Moreaux et al. 2006; Trifilo, Ying et al. 2007) Using IHC and confocal microscopy, Bessen and colleagues (Mulcahy, Bartz et al. 2004) demonstrated that PrP^{RES} accumulates within the nerve fibers, taste buds, and the stratified squamous epithelium in the fungiform papillae as well as within nerve fascicles and skeletal muscle cells. Trifilo et al. (Trifilo, Ying et al. 2007) demonstrated PrP^{CWD} in occasional taste buds of PO-inoculated cervidized transgenic

mice. I found PrP^{CWD} in the tongue only late in disease (180-240 dpi), after its appearance in the brain, again suggesting centrifugal spread, likely via cranial nerve fibers (facial [VII] and trigeminal [V]) - a pathway proven in hamsters inoculated with TME (DeJoia, Moreaux et al. 2006). In addition to taste buds, I identified PrP^{CWD} in the lingual glands, consistent with the findings of Trifilo et al.(Trifilo, Ying et al. 2007) suggesting centrifugal dissemination via the hypoglossal nerve.(Saraswathi 2003; Trifilo, Ying et al. 2007)

Disappointingly, the initial group of orally inoculated mice failed to demonstrate susceptibility to CWD, which is in contrast to published work detailing the successful oral inoculation of cervidized transgenic mice.(Trifilo, Ying et al. 2007) While the precise cause for this failure is uncertain, given the results of the successful follow-up whole-brain inoculation study, it is likely the result of an insufficient inoculum dosage. In the successful study documenting the oral susceptibility of cervidized transgenic mice to CWD infection cited above, the researchers used 100 µL of a 5% brain homogenate, whereas I inoculated our mice with an identical volume (100 µL) of a 1% brain homogenate. While dose-dependent failure seems the most likely interpretation of these results, it remains possible that these animals were successfully infected, but suffered from subclinical disease.

Subclinical prion disease is a phenomenon characterized by the accumulation of prion infectivity in the absence of either clinical disease or detectable PrP^{RES}, as determined by conventional assays (including IHC).(Hill and Collinge 2003) It has been suggested that the phenomenon of subclinical prion disease is, in part, related to the dose

of the initial inoculum.(Thackray, Klein et al. 2002) The nature of this phenomenon is uncertain, but the infectious component may represent a fraction of PrP^{RES} which is proteinase K- and formic acid-sensitive, thus rendering it undetectable by conventional assays.(Pastrana, Sajnani et al. 2006) Finally, although serial sacrifice data is not available for successfully-infected, PO-inoculated mice, the pattern of PrP^{CWD} accumulation in these mice - which included deposits in tissues of nervous, lymphoreticular, gastrointestinal, and endocrine systems - mimics what has been observed in studies evaluating tissues from terminal elk, mule deer, and white-tailed deer with natural and PO-inoculated, experimental CWD.(Sigurdson, Spraker et al. 2001; Sigurdson, Barillas-Mury et al. 2002; Spraker, Zink et al. 2002; Spraker, Zink et al. 2002; Fox, Jewell et al. 2006; Hamir, Gidlewski et al. 2006)

In association with the direct CWD inoculation studies, I demonstrated, for the first time, the horizontal transmission of CWD prions in a rodent model system. While lateral transmission is a prominent feature of CWD and scrapie, little published information exists in rodent models (Morris, Gajdusek et al. 1965; Miller and Williams 2003; Williams 2005). While questions remain regarding the nature of this transmission, based upon the identical pattern of PrP^{CWD} accumulation seen in naturally and experimentally (PO-) infected cervids orally-infected mice in this study, I reason that the contact-exposed mice were infected by the oral route (Sigurdson, Williams et al. 1999; Sigurdson, Barillas-Mury et al. 2002; Spraker, Zink et al. 2002; Spraker, Zink et al. 2002; Fox, Jewell et al. 2006). Precedent for the horizontal transmission of pathogens between cohabitant cage mates is provided by work detailing the horizontal spread of hantavirus

and *H. pylori* between murine cage-mates (Botten, Mirowsky et al. 2002; Karita, Matsumoto et al. 2005). The vehicle responsible for the spread of prions between cage-mates is uncertain, but other studies in cervids and rodent model systems support the plausibility of biologic fluids and excreta as transmission vehicles (Mathiason, Powers et al. 2006; Safar, Lessard et al. 2008; Haley 2009). Given the presence of PrP^{CWD} in the taste-buds of inoculated Tg[CerPrP] mice, horizontal spread could be linked to the shedding of prion-infected cells into oronasal secretions (DeJoia, Moreaux et al. 2006). In addition to direct animal-to-animal contact or animal-to-excreta contact, coprophagy is also plausible, as evidenced by the transmission of CWD and scrapie by exposure of naïve animals to a contaminated environment (Miller, Williams et al. 2004; Safar, Lessard et al. 2008).

Mice in three of the inoculation groups demonstrated a syndrome of hyperphagia and weight gain, which presaged terminal clinical disease and weight loss. This finding mimics studies in our laboratory conducted in CWD-infected white-tailed deer, in which animals maintained in controlled indoor housing conditions remain hyperphagic during terminal disease, suggestive of central perturbation of appetite regulation mechanisms Furthermore, given previous work which has revealed a syndrome of metabolic dysfunction in scrapie-infected mice, sheep, and goats (Schelcher, Picard-Hagen et al. 1999; Busiguina, Fernandez et al. 2000; Gayrard, Picard-Hagen et al. 2000; Viguie, Chilliard et al. 2004) (Kim, Carp et al. 1987; Carp, Kim et al. 1989), it seems equally likely that such a phenomenon is present in the CWD-infected mice. Moreover, the early and often heavy accumulation of PrP^{CWD} in centers of appetite regulation, namely the

hypothalamus and hippocampus, mimics rodent models of scrapie in which hypothalamic and hippocampal dysfunction is considered to be a leading factor in the genesis of scrapie-induced obesity owing to the presence of prion-disease associated pathology in these two regions.(Ye, Scallet et al. 1997; Carp, Meeker et al. 1998; Ye, Scallet et al. 1999)

In summary, cervidized transgenic mice substantially recapitulate the clinical disease, neuropathologic features, PrP^{CWD} tropism, as well as transmission patterns reported in the native cervid species (Sigurdson, Spraker et al. 2001; Sigurdson, Barillas-Mury et al. 2002; Spraker, Zink et al. 2002; Spraker, Zink et al. 2002; Fox, Jewell et al. 2006; Hamir, Gidlewski et al. 2006) and studies in Tg[CerPrP] mice can provide additional insights into the trafficking, shedding, and lateral transmission of CWD prions.

ACKNOWLEDGEMENTS

I would like to thank Jan Langeveld for his generous gift of anti-prion antibody R505.5. I thank Jeanette Hayes-Klug, Heather Bender, Kelly Anderson, Erin McNulty, and Kate Bruner for their excellent care and management of the Tg mice used in these studies. I thank Mark Zabel for his helpful comments on this work and for provision of the $PrP^{0/0}$ mice. This work was supported by contract NO1-AI-25491 from NIH, NIAID from T32-RR07072 from NIH, NCRR.

REFERENCES

Andreoletti, O., S. Simon, et al. (2004). "PrPSc accumulation in myocytes from sheep incubating natural scrapie." Nat Med 10(6): 591-3.

Angers, R. C., S. R. Browning, et al. (2006). "Prions in skeletal muscles of deer with chronic wasting disease." Science 311(5764): 1117.

Asante, E. A., J. M. Linehan, et al. (2002). "BSE prions propagate as either variant CJD-like or sporadic CJD-like prion strains in transgenic mice expressing human prion protein." EMBO J 21(23): 6358-66.

Banks, W. A., M. L. Niehoff, et al. (2004). "Passage of murine scrapie prion protein across the mouse vascular blood-brain barrier." Biochem Biophys Res Commun 318(1): 125-30.

Baron, T. (2002). "Mouse models of prion disease transmission." Trends Mol Med 8(10): 495-500.

Beekes, M. and P. A. McBride (2007). "The spread of prions through the body in naturally acquired transmissible spongiform encephalopathies." FEBS J 274(3): 588-605.

Blattler, T., S. Brandner, et al. (1997). "PrP-expressing tissue required for transfer of scrapie infectivity from spleen to brain." Nature 389(6646): 69-73.

Borchelt, D. R., V. E. Koliatsos, et al. (1994). "Rapid anterograde axonal transport of the cellular prion glycoprotein in the peripheral and central nervous systems." J Biol Chem 269(20): 14711-4.

Botten, J., K. Mirowsky, et al. (2002). "Shedding and intracage transmission of Sin Nombre hantavirus in the deer mouse (Peromyscus maniculatus) model." J Virol 76(15): 7587-94.

Brandner, S., S. Isenmann, et al. (1996). "Normal host prion protein necessary for scrapie-induced neurotoxicity." Nature 379(6563): 339-43.

Brown, K. L., D. L. Ritchie, et al. (2000). "Detection of PrP in extraneural tissues." Microsc Res Tech 50(1): 40-5.

Browning, S. R., G. L. Mason, et al. (2004). "Transmission of prions from mule deer and elk with chronic wasting disease to transgenic mice expressing cervid PrP." J Virol 78(23): 13345-50.

Bruce, M. E. (1985). "Agent replication dynamics in a long incubation period model of mouse scrapie." J Gen Virol 66 (Pt 12): 2517-22.

Burthem, J., B. Urban, et al. (2001). "The normal cellular prion protein is strongly expressed by myeloid dendritic cells." Blood 98(13): 3733-8.

Busiguina, S., A. M. Fernandez, et al. (2000). "Neurodegeneration is associated to changes in serum insulin-like growth factors." Neurobiol Dis 7(6 Pt B): 657-65.

Carlson, G. A., D. T. Kingsbury, et al. (1986). "Linkage of prion protein and scrapie incubation time genes." Cell 46(4): 503-11.

Carp, R. I., Y. S. Kim, et al. (1989). "Scrapie-induced alterations in glucose tolerance in mice." J Gen Virol 70 (Pt 4): 827-35.

Carp, R. I., H. Meeker, et al. (1998). "Analysis of the incubation periods, induction of obesity and histopathological changes in senescence-prone and senescence-

resistant mice infected with various scrapie strains." J Gen Virol 79 (Pt 11): 2863-9.
DeJoia, C., B. Moreaux, et al. (2006). "Prion infection of oral and nasal mucosa." J Virol 80(9): 4546-56.
Eklund, C. M., R. C. Kennedy, et al. (1967). "Pathogenesis of scrapie virus infection in the mouse." J Infect Dis 117(1): 15-22.
Field, E. J., C. E. A., et al. (1968). "Scrapie agent in blood." Vet Rec 83: 109-10.
Ford, M. J., L. J. Burton, et al. (2002). "Selective expression of prion protein in peripheral tissues of the adult mouse." Neuroscience 113(1): 177-92.
Fox, K. A., J. E. Jewell, et al. (2006). "Patterns of PrPCWD accumulation during the course of chronic wasting disease infection in orally inoculated mule deer (Odocoileus hemionus)." J Gen Virol 87(Pt 11): 3451-61.
Garssen, G. J., L. J. Van Keulen, et al. (2000). "Applicability of three anti-PrP peptide sera including staining of tonsils and brainstem of sheep with scrapie." Microsc Res Tech 50(1): 32-9.
Gayrard, V., N. Picard-Hagen, et al. (2000). "Major hypercorticism is an endocrine feature of ewes with naturally occurring scrapie." Endocrinology 141(3): 988-94.
Glatzel, M. and A. Aguzzi (2000). "PrP(C) expression in the peripheral nervous system is a determinant of prion neuroinvasion." J Gen Virol 81(Pt 11): 2813-21.
Glatzel, M., F. L. Heppner, et al. (2001). "Sympathetic innervation of lymphoreticular organs is rate limiting for prion neuroinvasion." Neuron 31(1): 25-34.
Haley, N. J. (2009). "Detection of CWD prions in urine and saliva of deer by transgenic mouse bioassay." PLoS ONE.
Hamir, A. N., T. Gidlewski, et al. (2006). "Preliminary observations of genetic susceptibility of elk (Cervus elaphus nelsoni) to chronic wasting disease by experimental oral inoculation." J Vet Diagn Invest 18(1): 110-4.
Heinlich, H. and G. Bullock (2004). The laboratory mouse. London, Academic.
Henry, B. A. (2003). "Links between the appetite regulating systems and the neuroendocrine hypothalamus: lessons from the sheep." J Neuroendocrinol 15(7): 697-709.
Hill, A. F. and J. Collinge (2003). "Subclinical prion infection." Trends Microbiol 11(12): 578-84.
Huang, F. P., C. F. Farquhar, et al. (2002). "Migrating intestinal dendritic cells transport PrP(Sc) from the gut." J Gen Virol 83(Pt 1): 267-71.
Hunter, N., J. Foster, et al. (2002). "Transmission of prion diseases by blood transfusion." J Gen Virol 83(Pt 11): 2897-905.
Karita, M., S. Matsumoto, et al. (2005). "Direct transmission of H. pylori from challenged to nonchallenged mice in a single cage." Dig Dis Sci 50(6): 1092-6.
Kesse, W. K., T. L. Parker, et al. (1988). "The innervation of the adrenal gland. I. The source of pre- and postganglionic nerve fibres to the rat adrenal gland." J Anat 157: 33-41.
Kim, Y. S., R. I. Carp, et al. (1987). "Scrapie-induced obesity in mice." J Infect Dis 156(2): 402-5.
Kimberlin, R. H. and C. A. Walker (1989). "The role of the spleen in the neuroinvasion of scrapie in mice." Virus Res 12(3): 201-11.

Kong, Q., S. Huang, et al. (2005). "Chronic wasting disease of elk: transmissibility to humans examined by transgenic mouse models." J Neurosci 25(35): 7944-9.
LaFauci, G., R. I. Carp, et al. (2006). "Passage of chronic wasting disease prion into transgenic mice expressing Rocky Mountain elk (Cervus elaphus nelsoni) PrPC." J Gen Virol 87(Pt 12): 3773-80.
Le Pichon, C. E. and S. Firestein (2008). "Expression and localization of the prion protein PrP(C) in the olfactory system of the mouse." J Comp Neurol 508(3): 487-99.
Liu, T., R. Li, et al. (2001). "Normal cellular prion protein is preferentially expressed on subpopulations of murine hemopoietic cells." J Immunol 166(6): 3733-42.
Llewelyn, C. A., P. E. Hewitt, et al. (2004). "Possible transmission of variant Creutzfeldt-Jakob disease by blood transfusion." Lancet 363(9407): 417-21.
Loewy, A. D., M. F. Franklin, et al. (1994). "CNS monoamine cell groups projecting to pancreatic vagal motor neurons: a transneuronal labeling study using pseudorabies virus." Brain Res 638(1-2): 248-60.
Mabbott, N. A., F. Mackay, et al. (2000). "Temporary inactivation of follicular dendritic cells delays neuroinvasion of scrapie." Nat Med 6(7): 719-20.
Mabbott, N. A. and G. G. MacPherson (2006). "Prions and their lethal journey to the brain." Nat Rev Microbiol 4(3): 201-11.
Mabbott, N. A., J. Young, et al. (2003). "Follicular dendritic cell dedifferentiation by treatment with an inhibitor of the lymphotoxin pathway dramatically reduces scrapie susceptibility." J Virol 77(12): 6845-54.
Mathiason, C., T. Foos, et al. Cervid PrPc Quantitation and Tissue Mapping. Fort Collins, Colorado State University - Microbiology, Immunology, and Pathology.
Mathiason, C. K., J. G. Powers, et al. (2006). "Infectious prions in the saliva and blood of deer with chronic wasting disease." Science 314(5796): 133-6.
McBride, P. A., P. Eikelenboom, et al. (1992). "PrP protein is associated with follicular dendritic cells of spleens and lymph nodes in uninfected and scrapie-infected mice." J Pathol 168(4): 413-8.
McManaman, J. L., M. E. Reyland, et al. (2006). "Secretion and fluid transport mechanisms in the mammary gland: comparisons with the exocrine pancreas and the salivary gland." J Mammary Gland Biol Neoplasia 11(3-4): 249-68.
Miller, M. W. and M. A. Wild (2004). "Epidemiology of chronic wasting disease in captive white-tailed and mule deer." J Wildl Dis 40(2): 320-7.
Miller, M. W., M. A. Wild, et al. (1998). "Epidemiology of chronic wasting disease in captive Rocky Mountain elk." J Wildl Dis 34(3): 532-8.
Miller, M. W. and E. S. Williams (2003). "Prion disease: horizontal prion transmission in mule deer." Nature 425(6953): 35-6.
Miller, M. W., E. S. Williams, et al. (2004). "Environmental sources of prion transmission in mule deer." Emerg Infect Dis 10(6): 1003-6.
Millson, G. C., R. H. Kimberlin, et al. (1979). "Early distribution of radioactive liposomes and scrapie infectivity in mouse tissues following administration by different routes." Vet Microbiol 5: 89-99.
Mohan, J., M. E. Bruce, et al. (2005). "Follicular dendritic cell dedifferentiation reduces scrapie susceptibility following inoculation via the skin." Immunology 114(2): 225-34.

Morris, J. A., D. C. Gajdusek, et al. (1965). "Spread of scrapie from inoculated to uninoculated mice." Proc Soc Exp Biol Med 120(1): 108-10.
Moya, K. L., R. Hassig, et al. (2004). "Enhanced detection and retrograde axonal transport of PrPc in peripheral nerve." J Neurochem 88(1): 155-60.
Mulcahy, E. R., J. C. Bartz, et al. (2004). "Prion infection of skeletal muscle cells and papillae in the tongue." J Virol 78(13): 6792-8.
Muramoto, T., T. Kitamoto, et al. (1993). "Accumulation of abnormal prion protein in mice infected with Creutzfeldt-Jakob disease via intraperitoneal route: a sequential study." Am J Pathol 143(5): 1470-9.
Pastrana, M. A., G. Sajnani, et al. (2006). "Isolation and characterization of a proteinase K-sensitive PrPSc fraction." Biochemistry 45(51): 15710-7.
Pattison, I. H. and G. C. Millson (1960). "Further observations on the experimental production of scrapie in goats and sheep." J Comp Pathol 70: 182-93.
Peden, A. H., M. W. Head, et al. (2004). "Preclinical vCJD after blood transfusion in a PRNP codon 129 heterozygous patient." Lancet 364(9433): 527-9.
Prinz, M., M. Heikenwalder, et al. (2003). "Positioning of follicular dendritic cells within the spleen controls prion neuroinvasion." Nature 425(6961): 957-62.
Proctor, G. B. and G. H. Carpenter (2007). "Regulation of salivary gland function by autonomic nerves." Auton Neurosci 133(1): 3-18.
Prusiner, S. B., M. Scott, et al. (1990). "Transgenetic studies implicate interactions between homologous PrP isoforms in scrapie prion replication." Cell 63(4): 673-86.
Saa, P., J. Castilla, et al. (2006). "Presymptomatic detection of prions in blood." Science 313(5783): 92-4.
Safar, J. G., P. Lessard, et al. (2008). "Transmission and detection of prions in feces." J Infect Dis 198(1): 81-9.
Saraswathi, P. (2003). "Neurohistological observations on the tongue of the monkey (macaca radiata)." Journal of the Anatomical Society of India 52(2): 7-12.
Schelcher, F., N. Picard-Hagen, et al. (1999). "Corticoid concentrations are increased in the plasma and urine of ewes with naturally occurring scrapie." Endocrinology 140(5): 2422-5.
Scott, M., D. Foster, et al. (1989). "Transgenic mice expressing hamster prion protein produce species-specific scrapie infectivity and amyloid plaques." Cell 59(5): 847-57.
Scott, M. R., R. Kohler, et al. (1992). "Chimeric prion protein expression in cultured cells and transgenic mice." Protein Sci 1(8): 986-97.
Scott, M. R., J. Safar, et al. (1997). "Identification of a prion protein epitope modulating transmission of bovine spongiform encephalopathy prions to transgenic mice." Proc Natl Acad Sci U S A 94(26): 14279-84.
Sigurdson, C. J., C. Barillas-Mury, et al. (2002). "PrP(CWD) lymphoid cell targets in early and advanced chronic wasting disease of mule deer." J Gen Virol 83(Pt 10): 2617-28.
Sigurdson, C. J., T. R. Spraker, et al. (2001). "PrP(CWD) in the myenteric plexus, vagosympathetic trunk and endocrine glands of deer with chronic wasting disease." J Gen Virol 82(Pt 10): 2327-34.

Sigurdson, C. J., E. S. Williams, et al. (1999). "Oral transmission and early lymphoid tropism of chronic wasting disease PrPres in mule deer fawns (Odocoileus hemionus)." J Gen Virol 80 (Pt 10): 2757-64.
Spraker, T. R., R. R. Zink, et al. (2002). "Distribution of protease-resistant prion protein and spongiform encephalopathy in free-ranging mule deer (Odocoileus hemionus) with chronic wasting disease." Vet Pathol 39(5): 546-56.
Spraker, T. R., R. R. Zink, et al. (2002). "Comparison of histological lesions and immunohistochemical staining of proteinase-resistant prion protein in a naturally occurring spongiform encephalopathy of free-ranging mule deer (Odocoileus hemionus) with those of chronic wasting disease of captive mule deer." Vet Pathol 39(1): 110-9.
Takakura, Y., N. Yamaguchi, et al. (2008). "Bone marrow stroma cells are susceptible to prion infection." Biochem Biophys Res Commun 377(3): 957-61.
Tamguney, G., K. Giles, et al. (2006). "Transmission of elk and deer prions to transgenic mice." J Virol 80(18): 9104-14.
Telling, G. C. (2000). "Prion protein genes and prion diseases: studies in transgenic mice." Neuropathol Appl Neurobiol 26(3): 209-20.
Telling, G. C., M. Scott, et al. (1994). "Transmission of Creutzfeldt-Jakob disease from humans to transgenic mice expressing chimeric human-mouse prion protein." Proc Natl Acad Sci U S A 91(21): 9936-40.
Telling, G. C., M. Scott, et al. (1995). "Prion propagation in mice expressing human and chimeric PrP transgenes implicates the interaction of cellular PrP with another protein." Cell 83(1): 79-90.
Thackray, A. M., M. A. Klein, et al. (2002). "Chronic subclinical prion disease induced by low-dose inoculum." J Virol 76(5): 2510-7.
Thomzig, A., C. Kratzel, et al. (2003). "Widespread PrPSc accumulation in muscles of hamsters orally infected with scrapie." EMBO Rep 4(5): 530-3.
Tracy, A. L., L. E. Jarrard, et al. (2001). "The hippocampus and motivation revisited: appetite and activity." Behav Brain Res 127(1-2): 13-23.
Tremblay, P., E. Bouzamondo-Bernstein, et al. (2007). "Developmental expression of PrP in the post-implantation embryo." Brain Res 1139: 60-7.
Trifilo, M. J., G. Ying, et al. (2007). "Chronic wasting disease of deer and elk in transgenic mice: oral transmission and pathobiology." Virology 365(1): 136-43.
Vascellari, M., R. Nonno, et al. (2007). "PrPSc in salivary glands of scrapie-affected sheep." J Virol 81(9): 4872-6.
Viegas, P., N. Chaverot, et al. (2006). "Junctional expression of the prion protein PrPC by brain endothelial cells: a role in trans-endothelial migration of human monocytes." J Cell Sci 119(Pt 22): 4634-43.
Viguie, C., Y. Chilliard, et al. (2004). "Alterations of somatotropic function in prion disease in sheep." J Endocrinol 183(2): 427-35.
Williams, E. S. (2005). "Chronic wasting disease." Vet Pathol 42(5): 530-49.
Williams, E. S. and S. Young (1992). "Spongiform encephalopathies in Cervidae." Rev Sci Tech 11(2): 551-67.

Ye, X., R. I. Carp, et al. (1994). "Hyperplasia and hypertrophy of B cells in the islets of Langerhans in hamsters infected with the 139H strain of scrapie." J Comp Pathol 110(2): 169-83.
Ye, X., A. Scallet, et al. (1999). "Abnormal periodic acid-Schiff (PAS)-positive substance in the islets of Langerhans, pituitaries and adrenal glands of 139H scrapie-infected hamsters." Histol Histopathol 14(3): 673-8.
Ye, X., A. C. Scallet, et al. (1997). "The 139H scrapie agent produces hypothalamic neurotoxicity and pancreatic islet histopathology: electron microscopic studies." Neurotoxicology 18(2): 533-45.
Zhang, C. C., A. D. Steele, et al. (2006). "Prion protein is expressed on long-term repopulating hematopoietic stem cells and is important for their self-renewal." Proc Natl Acad Sci U S A 103(7): 2184-9.
Zoukhri, D. and C. L. Kublin (2001). "Impaired neurotransmitter release from lacrimal and salivary gland nerves of a murine model of Sjogren's syndrome." Invest Ophthalmol Vis Sci 42(5): 925-32.

CHAPTER 2:

Trafficking of CWD Prions via the Autonomic and Enteric Nervous Systems in Tg[CerPrP-E] Mice

ABSTRACT

Chronic wasting disease (CWD) is an efficiently transmitted spongiform encephalopathy of cervids. In native species, horizontal spread of the disease is likely the result of the oral ingestion of a prion-containing excreta, including urine, saliva, or feces. While cervid prion protein expressing transgenic (Tg[CerPrP]) mice have been shown to be effective surrogates of natural CWD, questions remain regarding the mechanisms by which CWD prions traffic *in vivo*. Chief among these is the manner in which prions travel to and within the CNS, and how prions transit across the epithelial barrier of the gastrointestinal (GI) tract. Here, I show through light microscopy and immunohistochemistry (IHC) that the cells and fibers of the enteric and autonomic nervous systems (ENS and ANS) serve as significant pathways for the centripetal and centrifugal spread of CWD prions in infected Tg[CerPrP] mice. Additionally, I demonstrate that PrP^{CWD} is associated with the cell bodies and processes of enteric glial cells (EGCs) within the ENS. Through this work, I demonstrate the importance of the peripheral and central autonomic networks in CWD neuroinvasion and neuropathogenesis, and that enteroglial cells may facilitate the invasion and shedding of prions via the GI tract.

BACKGROUND

Chronic wasting disease (CWD) of white-tailed deer (WTD), mule deer, elk, and moose is a prion disease first identified in the Rocky Mountain region and now recognized in 19 states, Canada, and one Asian country.(Williams and Young 1980; Williams 2005; 2010) Typical of all transmissible spongiform encephalopathies (TSEs) including scrapie, bovine spongiform encephalopathy (BSE) and human Creutzfeldt-Jakob Disease (CJD), CWD is caused by the conversion of normal protease-sensitive prion protein (PrP^{C}) to a misfolded protease-resistant conformation (PrP^{CWD}), which accumulates in the CNS and lymphoid system and leads to wasting and spongiform encephalopathy.(Sigurdson, Williams et al. 1999; Sigurdson, Barillas-Mury et al. 2002; Spraker, Zink et al. 2002) To date, the abnormal form of the prion protein, abbreviated either generically as PrP^{RES} or by the more CWD-specific PrP^{CWD}, represents the only available marker of prion disease and its demonstration in affected tissues has been shown to correlate strongly with infectivity and disease.(Bolton, Rudelli et al. 1991; Race, Jenny et al. 1998) Moreover, like other TSEs, CWD is characterized by a constellation of 4 microscopic brain lesions, including: 1) neuronal degeneration and/or loss, 2) neuronal and neuropil degenerative spongiosis, 3) reactive gliosis (astrocytosis) with absent-to-minimal inflammation, and 4) the deposition of protease-resistant (amyloid) plaques of PrP^{CWD}. Because *in vivo* susceptibility studies in cervids are protracted (with incubation periods in excess of 20 months), costly, and logistically challenging, a comprehensive analysis of CWD pathogenesis in a facile murine model species remains vital to furthering our understanding of this disease.

While there is an ever increasing number of reports documenting successful CWD infection of cervidized transgenic mice,(Browning, Mason et al. 2004; Kong, Huang et al. 2005; Angers, Browning et al. 2006; LaFauci, Carp et al. 2006; Tamguney, Giles et al. 2006; Haley 2009; Haley, Mathiason et al. 2009; Seelig, Mason et al. 2010) none have utilized a serial sacrifice strategy to map the progressive temporal-spatial pattern of PrP^{CWD} accumulation in tissues of the lymphoid system, the peripheral nervous system (PNS) and the CNS. Such an approach has proven invaluable in seminal work discerning the pathogenic features of scrapie and other TSEs.(Kimberlin, Field et al. 1983; Muramoto, Kitamoto et al. 1992; Muramoto, Kitamoto et al. 1993; Beekes, McBride et al. 1998) Following peripheral prion infection such serial sacrifice studies have demonstrated initial accumulations of PrP^{RES} in tissues of the lymphoreticular system (LRS) followed by those of the PNS and ultimately the CNS. While the precise details are lacking in CWD, mapping of sequential PrP^{RES} accumulations in scrapie strongly implicates all three peripheral branches of the autonomic nervous system (ANS) – the parasympathetic (PaNS), sympathetic (SNS), and enteric nervous systems (ENS) – in the process of prion CNS neuroinvasion.(van Keulen, Schreuder et al. 2000) Outside of the CNS, early accumulation of PrP^{RES} in the Peyer's patches and enterocytes of orally-infected animals confirms that prions cross the enteric epithelial barrier, yet the manner by which enteroinvasion occurs is unknown.(Maignien, Lasmezas et al. 1999; Beekes and McBride 2000; Shmakov and Ghosh 2001) However, one likely site is the ENS, which has been shown to be the first neural tissue in which PrP^{RES} can identified in orally-infected sheep and hamsters with scrapie.(Beekes and McBride 2000; van Keulen, Schreuder et al. 2000)

The ease by which CWD spreads among cervids is unique among TSEs and likely reflects the transmission of infectious prions from the saliva, urine, and/or feces of infected cervids.(Mathiason, Powers et al. 2006; Safar, Lessard et al. 2008) In addition to uncertainties regarding prion enteroinvasion, questions remain regarding the manner in which prion infectivity is conferred to the feces of CWD afflicted cervids. One such candidate mediator of trans-gastrointestinal (GI) trafficking of prions, based upon its connections with the PaNS and the SNS, is the ENS.

The ENS is a complex and extensive component of the ANS which controls several aspects of GI function, including motility, blood flow, nutrient uptake, epithelial secretion of fluids and intestinal barrier function. It is organized into a series of plexi throughout the intestinal wall and consists of a heterogenous population of specialized neurons and enteric glial cells (EGCs), the latter of which show morphologic and functional similarities to CNS astrocytes.(Savidge, Newman et al. 2007) The EGCs reside throughout the entire intestinal tract and their cellular processes extend the length of intestinal villi where they lie in close proximity to intestinal epithelial cells and to submucosal blood vessels (Fig. 2.1), thus providing an anatomic roadmap by which the EGCs may facilitate early and late events in CWD prion trans-GI trafficking.(Ruhl 2005; Savidge, Sofroniew et al. 2007) Support for the involvement of the ENS in the pathogenesis of CWD is demonstrated by studies in CWD-infected cervids and cervidized mice, which have identified PrP^{CWD} in the ENS either coincident with, or following, its detection in the CNS.(Fox, Jewell et al. 2006; Trifilo, Ying et al. 2007)

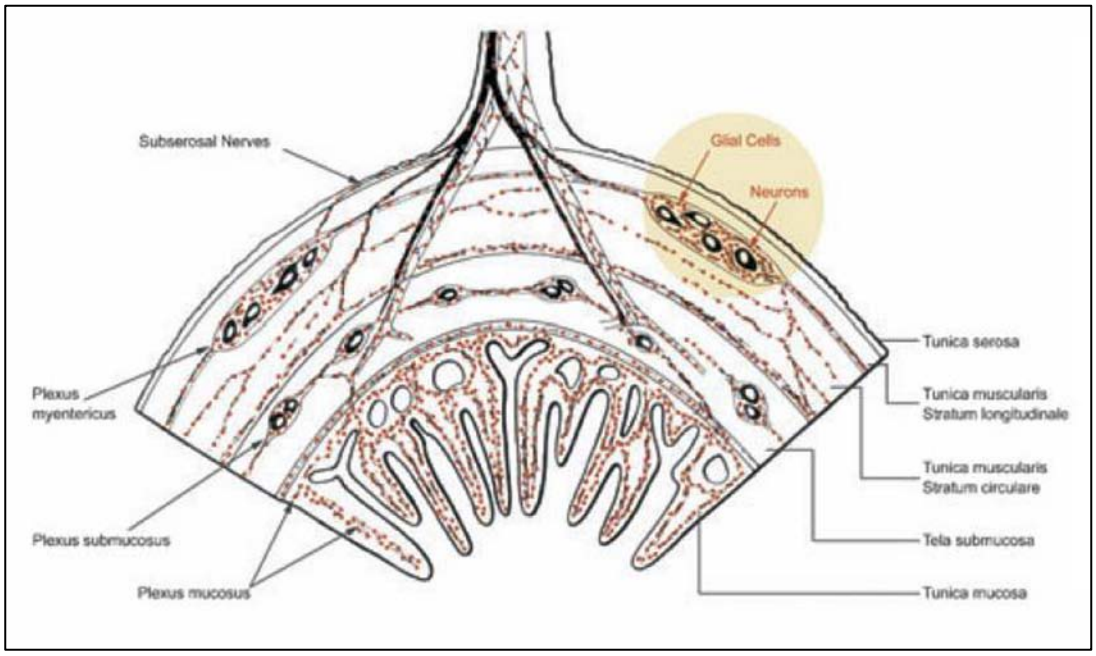

Figure 2.1 Anatomy of Enteric Glial Cells within ENS.
The EGCs form a network of cells and processes throughout all layers of the GI tract wall, from mucosa to serosa. Enteric glia are symbolized by red dots (from Ref. 15)

The principal aim of these investigations was to determine the progressive pattern of PrP^{CWD} accumulation within the PNS and CNS of CWD-inoculated Tg[CerPrP] mice with emphasis placed on the central and peripheral components of the ANS, notably the central autonomic network (CAN), the PaNS, the SNS, and the ENS. To address these mechanisms, I inoculated a lineage of cervidized, transgenic mice (5037 Tg[CerPrP-E] mice) via one of four routes (intracerebral [IC], intraperitoneal [IP], intravenous [IV], and oral [PO]) and mapped progressive accumulations of PrP^{CWD} through serial sacrifice and enhanced IHC. Here I report that cells and fiber tracts of the ANS and CAN serve as major pathway by which prions spread to and within the CNS of CWD-infected mice. Furthermore, to address questions regarding the role of the ENS in CWD infection, I developed a series of single and dual-labeling immunostaining protocols to identify

relationships between PrP^{CWD} and cells of the ENS. Through this work, I demonstrate that intimate relationships between PrP^{CWD} and EGCs may facilitate the transit of CWD prions across the GI mucosal barrier.

MATERIALS AND METHODS

Ethics Statement:

The animal experiments were conducted under the guidelines developed by the Colorado State University Animal Care and Use Committee.

Generation and genotyping of 5037 Tg[CerPrP-E] mice:

The transgenic mice expressing the elk PrP coding sequence utilized in these studies (5037 Tg[CerPrP-E]) were created and their susceptibility to CWD was established in the Telling laboratory.(Angers, Seward et al. 2009) In brief, to generate the elk PrP coding sequence, codon 226 of the deer PrP gene was mutated from Q to E by site-directed mutagenesis. This resultant coding sequence was inserted into the MoPrP.Xho expression vector and the purified transgene was microinjected into FVB/$Prnp^{0/0}$ oocytes. The $PrP^{0/0}$ mice used in the PrP^{C} mapping studies were kindly donated by Dr. Mark Zabel at Colorado State University.

Inoculum preparation:

The CWD inoculum (WTD-104) was prepared as a brain homogenate derived from a terminally-ill CWD-positive WTD, which was infected as part of other studies in

this laboratory. The negative control inoculum consisted of a brain homogenate from a CWD-negative white-tailed deer originating outside of the CWD endemic area (courtesy of David Osborn, Warnell School of Forestry, University of Georgia). Both inocula were homogenized in sterile phosphate-buffered saline (PBS) using a reciprocal homogenizer and diluted to a final concentration of 1% (wt/vol) using sterile PBS containing penicillin-streptomycin (100 U/ml).

Inoculation protocol:

Four experimental groups of 5037 Tg[CerPrP-E] mice (n = 10 per group) were utilized in these studies (Fig. 2.2), consisting of 4 to 6 week old, mixed-sex, Tg[CerPrP-E] mice inoculated with CWD prions via one of four routes: intracerebral (IC), intraperitoneal (IP), intravenous (IV), or oral (PO). For IC inoculation, mice were sedated through the IP injection of a mixture of ketamine (120 mg/kg) and xylazine (16 mg/kg). Mice were inoculated with 30µl of a 1% brain homogenate via a 29-gauge needle in the left parietal lobe of the cerebral cortex. For IP inoculation, 100µl of a 1% brain homogenate was injected via a 29-gauge needle into the right caudal ventral abdomen. For IV inoculation, 30µl of a 1% brain homogenate was injected through either the left or right tail vein. PO inoculations were performed by oral instillation of 50µl of a 1% brain homogenate administered on each of 2 consecutive days. Mice were not sedated for the IP, IV, or PO inoculations. Negative control mice (n = 6 per route) were inoculated by all routes above with 1% brain homogenate obtained from a CWD-negative white-tailed deer.

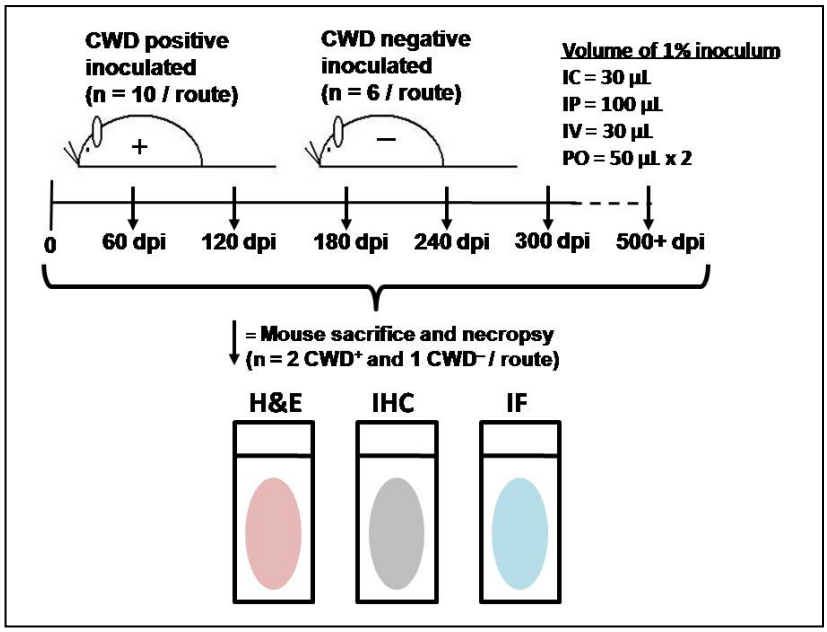

Figure 2.2 CWD infection of Tg[CerPrP-E] mice. Mice were inoculated via one of four routes with a varied amount of a 1% CWD^{+} or CWD^{-} brain homogenate. Mice were sacrificed at 60 day intervals and tissues were evaluated for neuropathology on hematoxylin-and-eosin (H&E) stained sections, and for PrP^{CWD} deposition using IHC, and immunofluorescence (IF).

Animal evaluation, euthanasia, and necropsy:

Following inoculation, Tg[CerPrP-E] mice were sacrificed at either: 1) a pre-determined time-point (Fig. 2.2); or 2) at the onset of terminal neurologic disease. The criteria used for the diagnosis of central nervous dysfunction in prion-inoculated mice have been previously published (Carlson, Kingsbury et al. 1986) and consist of: severe ataxia, difficulty in righting from a supine position, tail rigidity, generalized tremors, and/or severe mental obtundation. Tg[CerPrP-E] mice sacrifice time-points were chosen using the previously reported 220-day survival period following IC inoculation(Browning, Mason et al. 2004), and were as follows: 60 days-post-inoculation (dpi), 120 dpi, 180 dpi, 240 dpi, and terminal disease.

At each pre-determined sacrifice point, 3 mice per inoculation group were euthanized (2 mice from the CWD-inoculated group and 1 mouse from the sham-

inoculated group, for a total of 12 mice at each time-point). All animals were perfusion fixed with paraformaldehyde-lysine-periodate (PLP) using a commercially available, gravity-feed system (AutoMate Scientific™) and modification of a published protocol, which employs left ventricular fixative injection and right atrial exsanguination, (Heinlich and Bullock 2004) and necropsied. At necropsy, samples from all tissues were obtained, including those from both nervous (brain and spinal cord) and non-nervous (peripheral) systems. Following necropsy, all fixed tissues were immersion post-fixed in PLP fixative for 24 hours before transfer into 70% ethanol for long-term storage. Within 72-96 hours of necropsy, tissues were routinely trimmed for histologic processing. In order to standardize the evaluated neuroanatomic regions between mice, brains were identically sectioned using an acryl coronal brain matrix (Stoelting, Co.) to generate slices representing the following 5 neuroanatomic regions: i) the cerebral cortex, ii) the hippocampus, iii) the diencephalon, including the thalamus, iv) the cerebellum, and v) the medulla oblongata at the level of the obex and the pontine area. These regions have previously been determined useful in mouse models of scrapie.(Castilla, Gutierrez-Adan et al. 2004) In PrP^{CWD} detection studies, so as to ablate and enhance antigen detection, cassetted tissues were immersed in 88% formic acid for 1 hour then rinsed in running tap water for 1 hour prior to histologic processing. For the light microscopic evaluation of CNS neuropathology, 6 µm sections were stained using hematoxylin and eosin (H&E).

Histology and PrP^{CWD} immunohistochemistry:

For all experiments, paraffin-embedded tissue sections (4-6 µm) were mounted on positively charged glass slides; deparaffinized in a 64^{o} C oven followed by successive

immersions in xylene, and rehydrated through graded ethanol solutions. To enhance detection, tissues were subjected to Heat Induced Epitope Retrieval (HIER) using an automated antigen-retrieval system (Retriever™) and a proprietary buffer solution (DakoCytomation™ Target Retrieval Solution).

For the detection of PrP^{C}, tissues were stained using an automated immunostainer (DakoCytomation™), the primary prion protein antibody R505.5 (rabbit polyclonal, a generous gift from Dr. Jan Langeveld, Central Veterinary Institute of Wageningen University, The Netherlands) and a horseradish peroxidase (HRP) conjugated anti-rabbit secondary antibody (Vector Labs™). Prior to antibody application, endogenous peroxidase (EP) activity was quenched with 3% hydrogen peroxide (H_2O_2) in methanol and sections were blocked with a proprietary protein block (TNB, Perkin-Elmer™) for 60 minutes each. Antibody deposition was visualized using the chromagen 3,3'-diaminobenzidine (DAB) (DakoCytomation™); slides were counterstained with hematoxylin, and incubated with a bluing reagent (0.1% sodium bicarbonate). Following immunostaining, slides were coverslipped with an aqueous mounting media (Vector Labs™). To confirm specificity of PrP^{C} immunostaining tissue sections were immunostained using normal, non-stimulated rabbit serum (Vector Labs™) as a negative control.

For the detection of PrP^{CWD} an IHC protocol was used that combined a one-step immunostaining procedure with tyramide signal amplification (TSA). Previous work in our laboratory has demonstrated this methodology to be more sensitive in the detection of PrP^{CWD} than traditional, two-step indirect IHC protocols.(Sigurdson, Barillas-Mury et al.

2002; Seelig, Mason et al. 2010) The TSA-PrP^{CWD} protocol used a proprietary TSA-detection kit (Perkin-Elmer™) and was conducted as follows. Following slide rehydration, HIER, quenching of EP activity, and tissue blocking as described above, slides were incubated with an optimal dilution (Table 2.1) of the HRP-conjugated anti-prion protein antibody, BAR-224 (HRP-BAR224, Cayman Chemicals), which is a monoclonal prion protein antibody raised against amino acids 141-151 of the ovine prion protein. Between all incubation steps, slides were washed three times (5 minutes each) in TNT wash buffer (0.1M Tris-HCl, pH 7.5, 0.15M NaCl, and 0.05% TIen-20). Following the application of the antibodies, slides were sequentially incubated with two proprietary TSA reagents: 1) DNP Amplification Reagent (Perkin-Elmer™) for 4 minutes and 2) anti-DNP-HRP (Perkin-Elmer™) for 30 minutes. Antibody deposition was visualized using the chromagen 3-amino-9-ethylcarbazole (AEC, DakoCytomation™) and slides were counterstained with hematoxylin and incubated with a bluing reagent (0.1% sodium bicarbonate). Following immunostaining, slides were coverslipped with an aqueous mounting media (Vector Labs™).

Cell phenotype immunostaining:

For single-label immunophenotyping, tissue sections (4-6 µm) were mounted on positively charged glass slides, deparaffinized, rehydrated, subjected to HIER, quenched of EP activity, and blocked as described above. Next, slides were incubated with an anti-cell phenotype antibody at an optimal concentration (Table 2.1) for 2 hours and an appropriate species-specific, either HRP-conjugated or Alexa Fluor® 488 conjugated,

secondary antibody. Between all incubation steps, slides were washed three times (5 minutes each) in TNT wash buffer.

Antibody	Specificity	Isotype	Working Dilution	Source
HRP-BAR224	Prion protein	Mouse IgG_1	1:500-1:1000	Cayman
Ab7260	GFAP	Rabbit IgG	1:1000	Abcam
Ab14917 (LYVE-1)	Lymphatic endothelium	Rabbit IgG	1:1000	Abcam
16A11	Hu protein	Mouse IgG_{2b}	1:100-1:1000	Abcam
Ab112	Tyrosine hydroxylase	Rabbit IgG	1:500	Abcam
Ab9034	160 kD neurofilament medium	Rabbit IgG	1:500	Abcam

Table 2.1 Antibodies used for the detection and localization of PrP^{CWD} in the CNS and ENS of CWD-infected mice. Antibodies were chosen to: (i) evaluate the distribution of PrP^{CWD} in tissues of CWD-inoculated Tg[CerPrP-E] mice (HRP-BAR224) and (ii) evaluate for the association between PrP^{CWD} and cells of the ENS.

Dual-TSA immunofluorescent staining:

To evaluate for possible relationships between PrP^{CWD} and cells of the ENS, selected tissue sections were dual immunostained utilizing an IHC protocol with 2 consecutive TSA-based techniques. Tissue sections (4-6 µm) were mounted on positively charged glass slides, deparaffinized, rehydrated, and subjected to HIER as described above. Next, tissue section EP activity was quenched using 3% H_2O_2 for 60 minutes and sections were blocked with a 1% proprietary blocking reagent (Component D, Invitrogen) for 60 minutes. Following blocking, excess block was tapped off and slides were incubated with an anti-cell phenotype antibody at an optimal concentration (Table 2.1) for 2 hours. Slides were next incubated with a goat origin, HRP-conjugated anti-rabbit secondary antibody (Bethyl Labs™) diluted 1:100 in Component D for 30

minutes followed by diluted, fluorescently-labeled (Alexa Fluor® 488) tyramide amplification solution.

Next, the slides were incubated with HRP-BAR224 (1:500 in Component D) followed by diluted, fluorescently-labeled (Alexa Fluor® 568) tyramide amplification solution. At the completion of immunostaining, slides were washed, nuclei were labeled with 4´,6-diamidino-2-phenylindole, dihydrochloride (DAPI, Invitrogen), and slides were mounted with fluorescent mounting medium (ProLong® Gold Antifade Reagent, Invitrogen). Between all incubation steps, slides were washed three times (5 minutes each) in a TNT wash buffer (0.1M Tris-HCl, pH 7.5, 0.15M NaCl, and 0.05% TIen-20). To confirm the specificity of the immunostaining, and to prevent potential non-specific immunoreactivity resultant from newly deposited HRP associated with the TSA-reagents, following the completion of the first TSA-based protocol EP activity was re-quenched with 0.3% H_2O_2 for 30 minutes.

PrP^{CWD} co-localization studies:

To evaluate for the co-localization of PrP^{CWD} with cell phenotype antibodies, dual-labeled sections were evaluated with a confocal, laser scanning microscope **(**Zeiss Laser Scanning Axiovert Confocal Microscope, LSM510 meta).

RESULTS

Immunohistochemical detection of PrP^{C} in naïve 5037 Tg[CerPrP] mice:

In order to determine the distribution profile of the cervid prion protein (PrP^{C}) in 5037 Tg[CerPrP-E] mice, I utilized an IHC protocol, which has previously proven successful in a separate strain of cervidized transgenic mice.(Seelig, Mason et al. 2010)

Cervid PrP^C expression was identified in tissues of the nervous, lymphoid, gastrointestinal, hemopoietic and endocrine systems (Figure 2.3, Table 2.2). In general, immunoreactivity was most prominent in the cytoplasm, usually as finely granular, but in the CNS more coarsely aggregated immunostaining was seen in the neuropil.

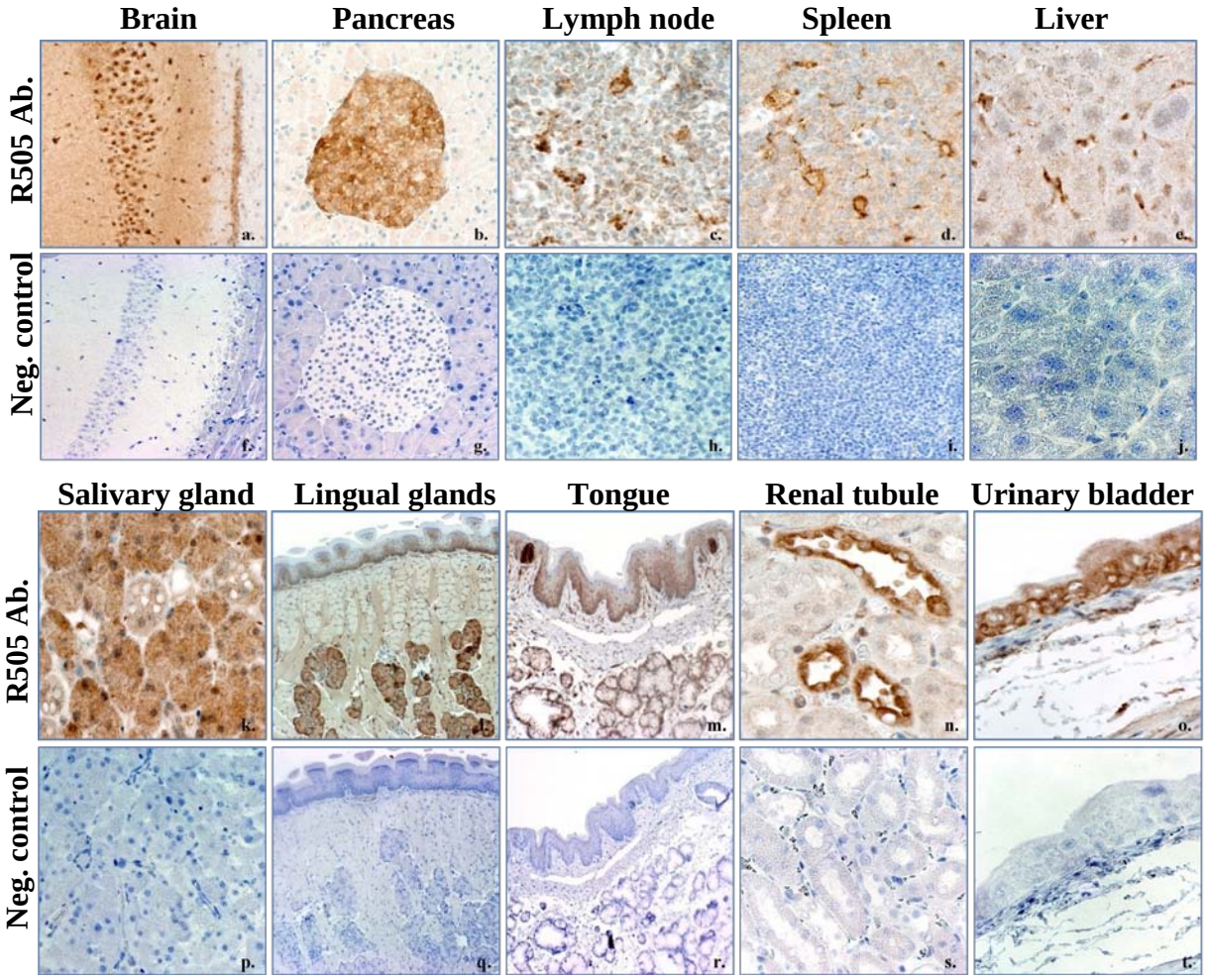

Figure 2.3 PrP^C expression in tissues of 5037 Tg[CerPrP] mice. All tissues were obtained from PLP-perfused naïve mice and stained using the IHC protocol detailed above. Each paired set of rows matches tissue types that have been stained with either the R505.5 antibody (rows 1 and 3) or a negative control anti-serum (rows 2 and 4). Row 1: PrP^C immunoreactivity (brown) in (a) neurons and neuropil, (b) pancreatic islet cells, (c) lymphoid dendritic cells, (d) splenic follicular dendritic cells, (e) hepatic Kupfer cells, (k) salivary gland epithelial cells, (l) lingual glands, (m) lingual epithelium and taste buds, (n) renal tubular epithelial cells, and (o) urinary bladder epithelial cells. PrP^C immunoreactivity is not seen in these same tissues stained with normal rabbit serum.

Table 2.2 – The Expression of PrP^C in 5037 Tg[CerPrP-E] Mice

CENTRAL NERVOUS SYSTEM	PrP^C Expression	UROGENITAL	PrP^C Expression
Neuronal cell bodies	Positive	Renal tubules	Positive
Oligodendrocytes	Negative	Glomerulus	Positive
Astrocytes	Negative	Urinary epithelium	Positive
Neuropil	Positive	Prostate	Positive
Ependymal cells	Positive	Vesicular gland	Positive
		Coagulating gland	Negative
PERIPHERAL NERVOUS SYSTEM		Testes	Positive
Ganglion neuronal cell bodies	Positive	Uterine endometrium	Negative
Axons	Negative	Vaginal epithelium	Negative
		Ovary	Positive
CARDIOVASCULAR			
Cardiac myocytes	Negative	**RESPIRATORY**	
Endothelial cells	Positive	Respiratory epithelium	Negative
		Type I pneumocytes	Negative
LYMPHOID SYSTEM		Type II pneumocytes	Negative
Lymph node cortical follicles	Positive	Alveolar macrophages	Positive
Lymph node paracortex	Positive		
Lymph node medulla	Positive	**ENDOCRINE**	
Splenic lymphatic sheaths	Positive	Pancreatic islet cells	Positive
Thymus	Positive	Adrenal medulla cells	Positive
		Adrenal cortical cells	Positive
GASTROINTESTINAL		Thyroid epithelium	N/A
Salivary glands	Negative	Parathyroid epithelium	N/A
Tongue epithelium	Negative		
Taste buds	Positive	**OTHER TISSUES**	
Esophagus	Negative	Skeletal myocytes	Negative
Gastric epithelium	Negative	Smooth muscle myocytes	Negative
Submucosal glands	Negative	Bone marrow	Positive
Peyer's patches	Positive	Adipose tissue	Negative
Enterocytes	Negative	Keratinocytes	Negative
Pancreatic exocrine cells	Negative	Cells of hair follicles and adnexal structures	Negative
Liver (hepatocyte population)	Negative	Osteocytes, osteoclasts, & chondrocytes	Negative
Liver (non-hepatocyte population)	Positive		

Transmission of CWD to 5037 Tg[CerPrP-E] mice:

The inoculation of the 5037 Tg[CerPrP-E] mice with WTD-origin CWD prions resulted in clinical disease in the IC-, IP-, and IV-inoculated animals with the following survival periods IC: 215 (± 13 dpi), IP: 232 (± 15 dpi), and IV: 220 (± 7 dpi), respectively (Table 2.3). Clinical disease was characterized by ataxia, hyperactivity, tail rigidity, and terminal mental obtundation. In contrast, Tg[CerPrP-E] mice orally with the same 1% CWD brain homogenate remained healthy for >700 dpi, as did all sham-inoculated controls (Table 2.3).

	Route of inoculation			
	IC	*IP*	*IV*	*PO – 1%*
Days to disease	215 ± 13 d.	232 ± 15 d.	220 ± 7 d.	N/A
# ill mice / total # mice	4/4	4/4	4/4	0/10

Table 2.3 Susceptibility of 5037 Tg[CerPrP-E] mice to CWD prions The inoculation of the 5037 Tg[CerPrP-E] mice with WTD-origin CWD prions resulted in clinical disease in the IC, IP, and IV inoculated animals. In terminal animals, CWD infection was determined by a combination of clinical disease and IHC.

Progressive accumulations of PrP^{CWD} in ANS-innervated tissues in CWD-infected Tg[CerPrP-E] mice:

In the IV- and IP-infected mice the patterns of accumulation within the peripheral tissues were similar, suggesting a similar pattern of prion trafficking. At the first sacrifice time-point (60 dpi), PrP^{CWD} was identified within the spleen and mesenteric lymph nodes (MLN). Within both tissues PrP^{CWD} appeared as granular to clumped deposits suggestive of cytoplasmic processes of follicular dendritic cells (FDCs) within

lymphoid follicles (Fig 2.4 A-B). At 120 dpi, prion neuroinvasion was first confirmed with PrP^{CWD} deposits seen in the CNS (detailed below). Finally, at 180 dpi PrP^{CWD} was first identified in the ENS and intestinal villi (detailed below), as well as in Peyer's patches (PPs) (Fig. 2.4 C). In the IC-infected mice, peripheral tissue accumulations of PrP^{CWD} - which were morphologically identically to that seen in the IV- and IP-inoculated mice - were first noted at 120 dpi with prions seen in the spleen, MLN and PPs. At 180 dpi, PrP^{CWD} was first noted in the GI tract of the IC-inoculated mice, including the ENS and the intestinal villi. In the PO-inoculated mice, PrP^{CWD} was detected only in one of two mice and only in the ENS (further detailed below).

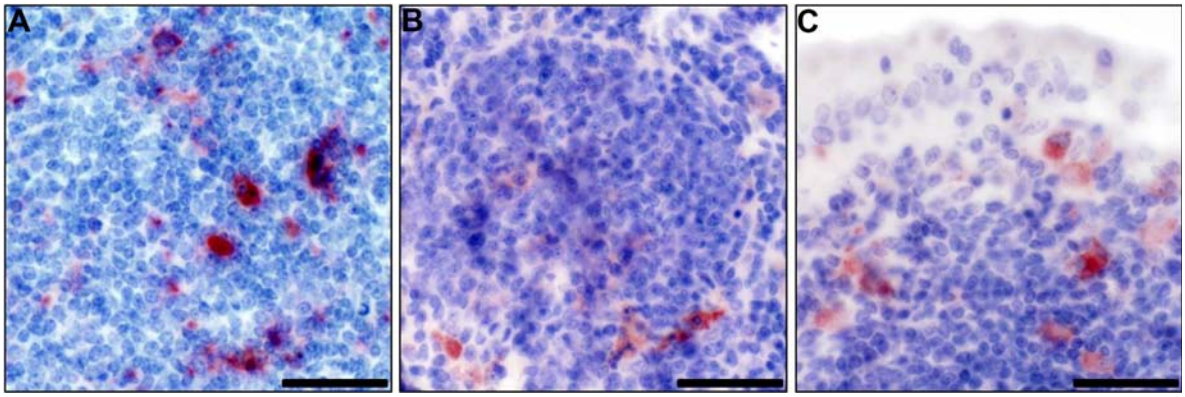

Figure 2.4 PrP^{CWD} in ANS-innervated peripheral tissues of 5037 Tg[CerPrP-E] mice. PrP^{CWD} immunoreactivity was detected in ANS-innervated peripheral tissues of the IC-, IV-, and IP-infected mice. All tissues were obtained from PLP-perfused mice and stained using the TSA-IHC protocol detailed above. A = spleen, B = mesenteric lymph node, C = Peyer's patches. Bar: A-C = 100 µm

Neuropathology in inoculated 5037 Tg[CerPrP-E] mice:

Detailed histopathologic evaluation of H&E stained brain coronal sections from all CWD-infected mice revealed a profile of neuropathology which varied little between groups and progressively worsened over the course of disease. In affected animals,

lesions consisted of a mixture of spongiform degeneration (spongiosis) and plaque formation. Spongiosis manifested as either: 1) a "discrete" form characterized by numerous, variably sized (2-20 μm), discrete to coalescing vacuoles within the neuropil and perikaryon (Fig 2.5 A) or 2) as a "raggedy" form with irregular, often regionally-extensive bands of coalescing neuropil vacuoles (Fig 2.5 B). In general the latter form was most commonly seen in animals with terminal disease. Plaques consisted of variably discrete, pale basophilic to eosinophilic irregularly shaped somewhat fibrillar bodies, which immunolabelled for PrP^{CWD} (Figure 2.5 B). While the general morphologic features of neuropathology were similar between inoculation groups, the anatomic distribution of affected areas was somewhat dependent upon route of inoculation.

In the IC-inoculated animals, the most severe neuropathology was observed within the hippocampal formation (HPF), with the CA (*Cornu Ammonis*) fields most significantly affected. In these areas "raggedy" spongiosis and plaque formation were most evident (Fig. 2.5 B). Contrastingly, in the IV- and IP-inoculated mice, regions of the medulla oblongata were mostly affected by "discrete" spongiosis predominantly in the dorsal motor nucleus of the vagus (DMNV) and nucleus of the solitary tract (NTS) (Fig. 2.5 A). Finally, some of the sham-inoculated animals had mild to modest neuropil vacuolization, but no intra-cellular vacuolization or plaque formation was detected (Fig 2.5 C-D).

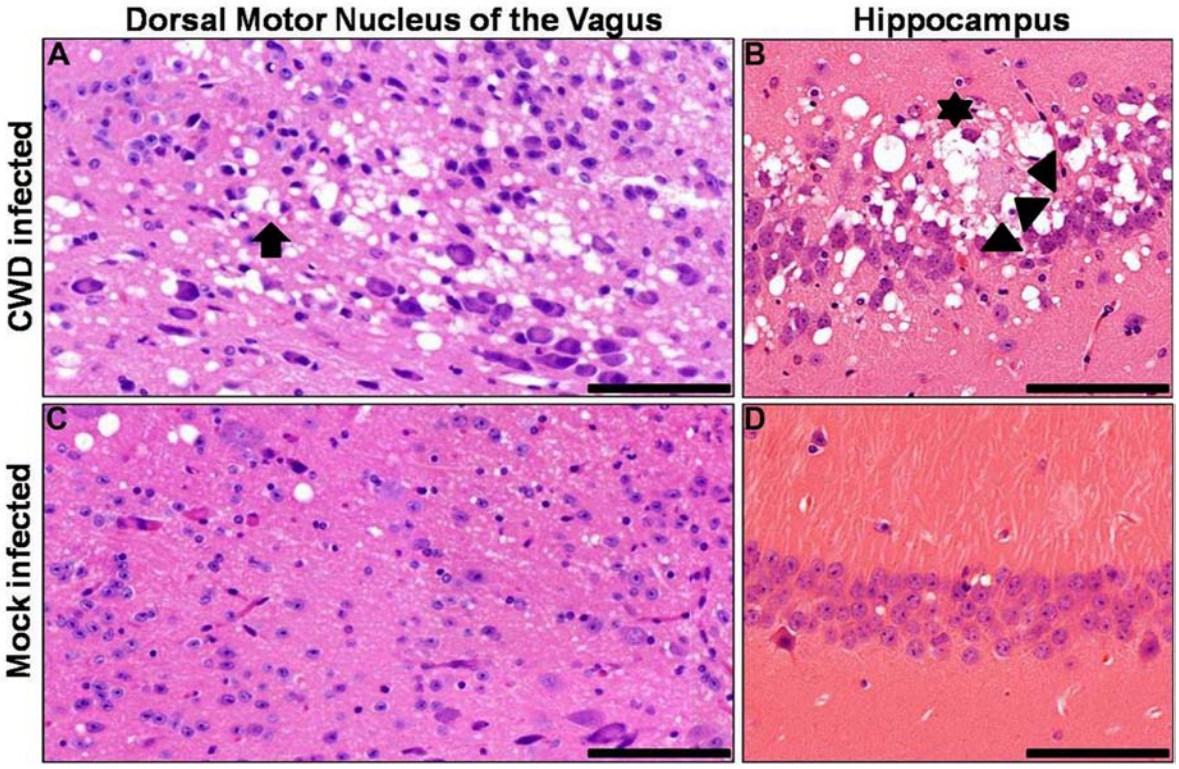

Figure 2.5 Neuropathology in CWD-infected Tg[CerPrP-E] mice.
H&E stained brain sections from CWD-infected mice revealed two forms of spongiosis – (A) a discrete form with neuropil and perikaryonic (arrow) vacuoles and (B) a raggedy form with coalescing neuropil vacuoles (star). Plaques (arrowheads) were most commonly observed in the hippocampal formation. Sham-infected mice (C, D) were devoid of such lesions. Bar: A-D = 100 µm.

<u>PrP^{CWD} in the CNS of CWD-inoculated Tg[CerPrP-E] mice:</u>

Morphology of PrP^{CWD} in CWD-inoculated Tg[CerPrP-E] mice:

In the CNS PrP^{CWD} immunostaining manifested in one of three ways, either as: 1) finely granular to somewhat clumped immunoreactive deposits, which were either cell-associated or disseminated throughout the neuropil ("diffuse" form) (Fig. 2.6.A), or 2) larger (often in excess of 100 µm in diameter) "florid" amyloid plaques, which ranged from dense plaques with a ill-formed core to those with a more fibrillar and radiating nature ("plaque" form) (Fig. 2.6.B), or 3) a combination of the two (Fig. 2.6 C). These

two patterns of immunoreactivity varied both with the time of sacrifice and between specific neuroanatomic areas.

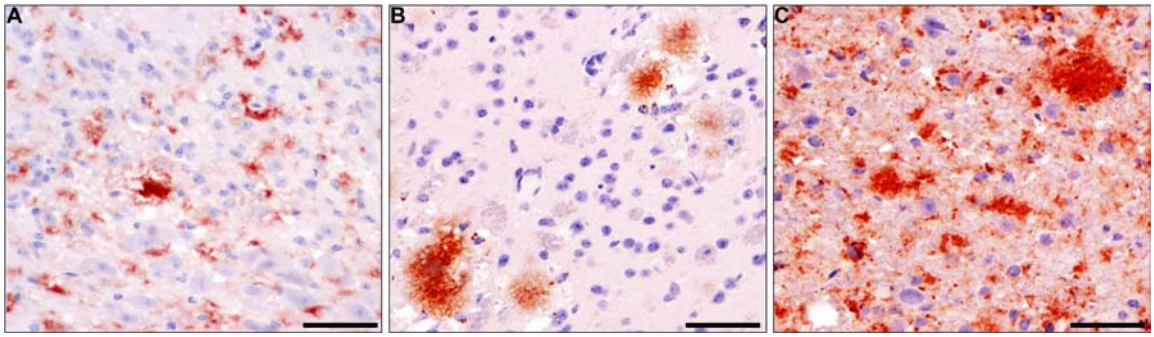

Figure 2.6 Plaque morphology in CWD-infected Tg[CerPrP-E] mice.
PrP^{CWD} immunoreactivity (red) manifested in 3 patterns: (A) a diffuse, granular form within the neuropil and cell cytoplasm, (B) a plaque form, and (C) a mixed form, composed of both the diffuse and plaque forms. Bar: A-C = 100 µm

Early in the course of disease, most notably within those animals sacrificed at 60 dpi, the "diffuse" form of PrP^{CWD} predominated. In these animals granular PrP^{CWD} deposits were seen within and adjacent to single and grouped neurons, within microglia and as dense punctate deposits scattered in gray matter neuropil. Moreover, this granular pattern of PrP^{CWD} immunoreactivity predominated within the cells and neuropil of the locus coeruleus (LC), the substantia nigra, the raphe nuclei, the hippocampal formation, the DMNV and the NTS. In contrast the plaque form was more evident later in disease (120 dpi – terminal disease) and was most prominent in the thalamus, hypothalamus, cerebral cortex, forebrain and cerebellum. The plaques were rarely seen at 60 dpi, with notable exceptions, including the pyramidal cell layer of the hippocampus in the IC-inoculated mice. However, late in disease, in all 3 groups the PrP^{CWD} immunoreactivity took on an increasingly mixed morphology, with nearly all affected areas containing a mixture of diffuse and plaque forms (Fig 2.6 C).

Progressive accumulation of PrP^{CWD} in IC-inoculated Tg[CerPrP-E] mice – 60 dpi:

In IC-inoculated animals, the first accumulations of PrP^{CWD} in the CNS were observed at 60 dpi and, while the amount of PrP^{CWD} immunoreactivity varied somewhat between individuals at this time-point, there was general consistency between mice regarding the areas with the most reproducible and intense PrP^{CWD} deposition. In two of two (2/2) sacrificed mice, PrP^{CWD} was most consistently identified in the HPF, most notably within the stratum lucidum, stratum radiatum, and the stratum pyramidale of CA1, CA2, and CA3 fields (Fig 2.7 A.).

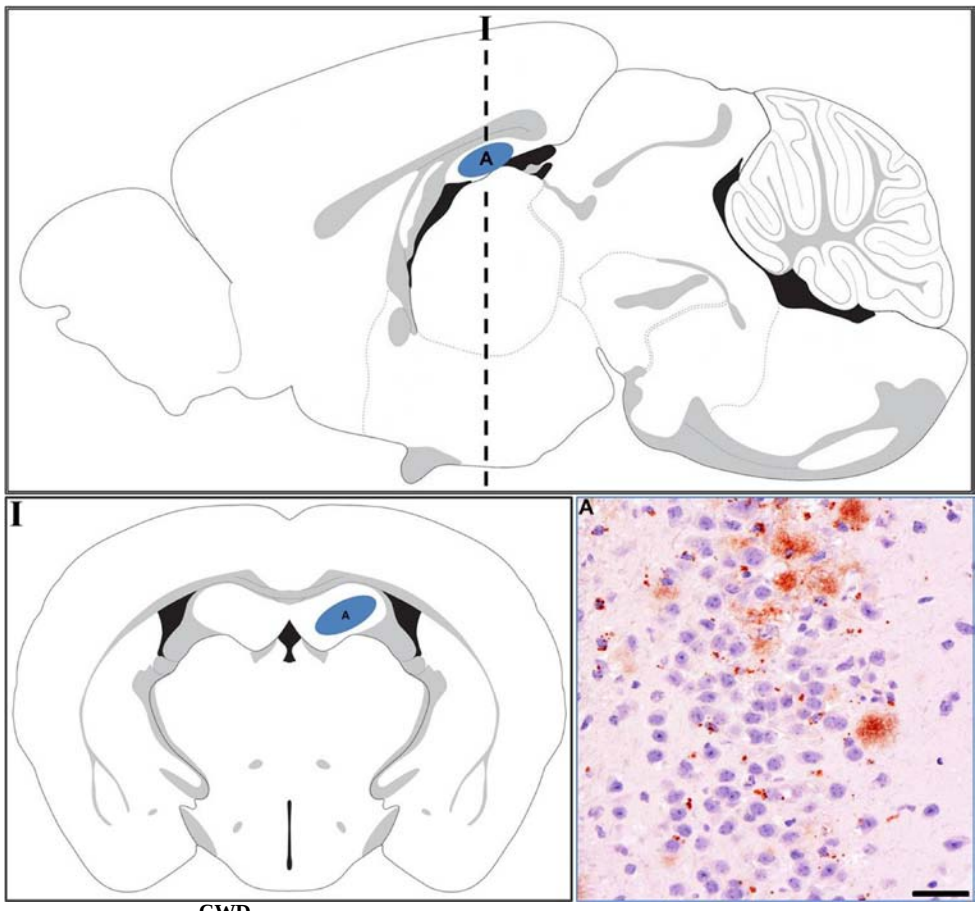

Figure 2.7 PrP^{CWD} in the CNS of IC-inoculated mice sacrificed at 60 dpi. In 2/2 animals, PrP^{CWD} immunoreactivity (red) was seen in the hippocampal formation. Note the presence of both granular to clumped, often cell-associated, immunoreactive deposits and the larger, neuropil-associated immunoreactive plaques. (Fig. 2.7 A). Bar = 75 µm.

Progressive accumulation of PrP^{CWD} in IC-inoculated Tg[CerPrP-E] mice – 120 dpi:

In the IC-inoculated mice sacrificed at 120 dpi, additional PrP^{CWD} was noted in the periaqueductal gray matter (PAGM), substantia nigra (SN), medial mammillary nucleus, amygdala, thalamus, habenular nucleus, cerebral cortex, lateral and 3rd ventricles, hypothalamus, caudoputamen, and accumbens nucleus (Fig. 2.8.B-O). Additionally, at this sacrifice time-point the first deposits of PrP^{CWD} were detected in the spinal cord, with accumulations noted in the gray matter, including the intermediolateral column of the cervical and rostral thoracic spinal cord segments. Morphologically the immunoreactive PrP^{CWD} deposits varied from diffuse to plaque-like with frequent regions of mixed morphology.

Progressive accumulation of PrP^{CWD} in IC-inoculated Tg[CerPrP-E] mice – 180 dpi / terminal disease:

In the IC-inoculated mice sacrificed at 180 dpi, additional deposits of PrP^{CWD} were identified in the cerebellum (confined to the molecular and granular cell layers), the DMNV, the NTS and the LC (Figure 2.9 P-U). Progressive caudal spreading of prions within the spinal cord continued, identifiable as accumulations of PrP^{CWD} in the mid-thoracic and lumbar segments. The patterns of immunoreactivity seen in the terminally-ill, IC-inoculated mice were identical to that seen in the mice sacrificed at the 180 dpi time-point.

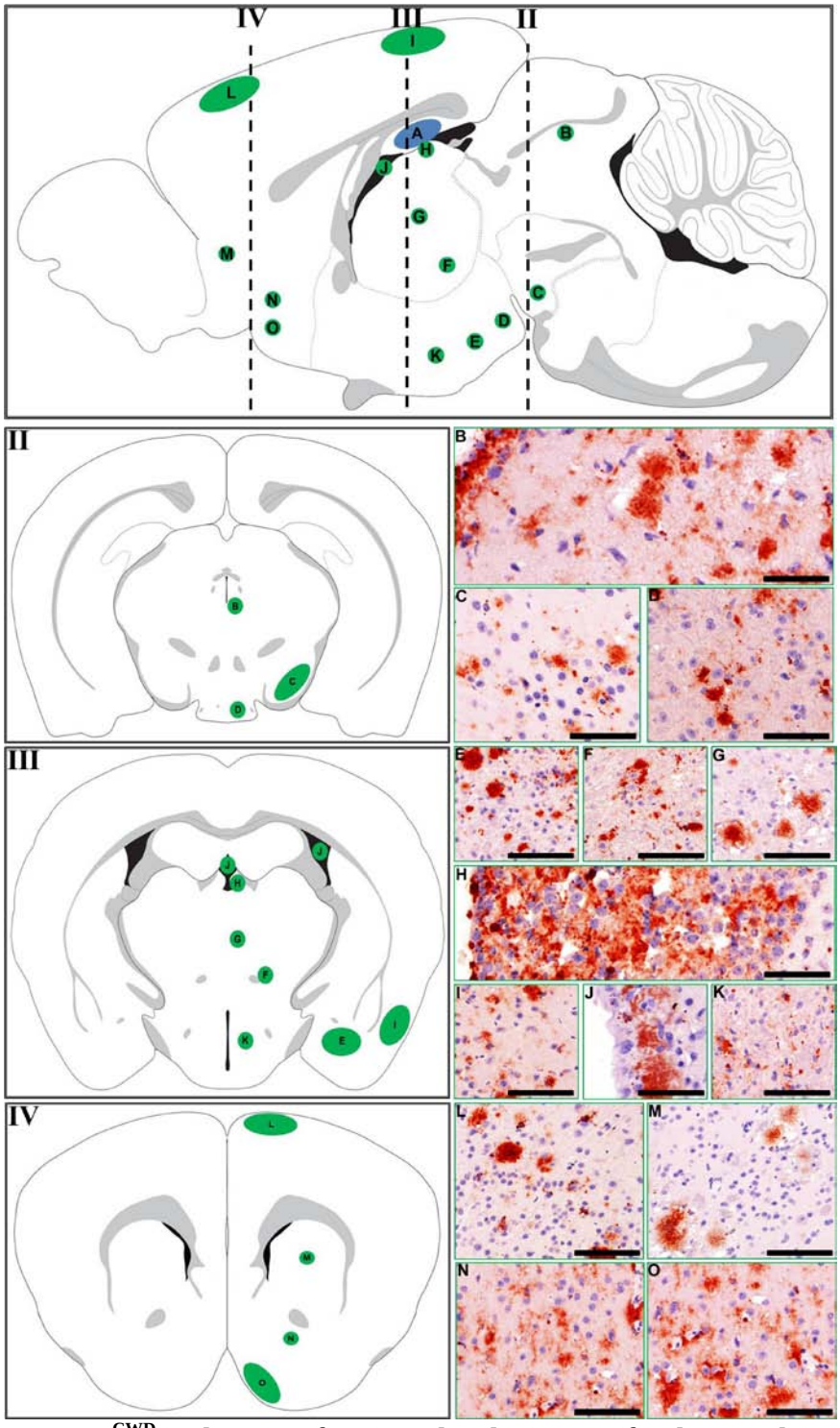

Figure 2.8 PrP^{CWD} in the CNS of IC-inoculated mice sacrificed at 120 dpi.
In 2/2 animals, PrP^{CWD} immunoreactivity (red) was seen in the periaqueductal gray matter (B), substantia nigra (C), medial mammillary nucleus (D), amygdala (E), thalamus (F, G), habenular nucleus (H), cerebral cortex (I, L, O), lateral and 3rd ventricles (J), hypothalamus (K), caudoputamen (M), and accumbens nucleus (N). Bar: B, H = 100 µm, C, D, J = 150 µm, E-G, I, K-O = 200 µm.

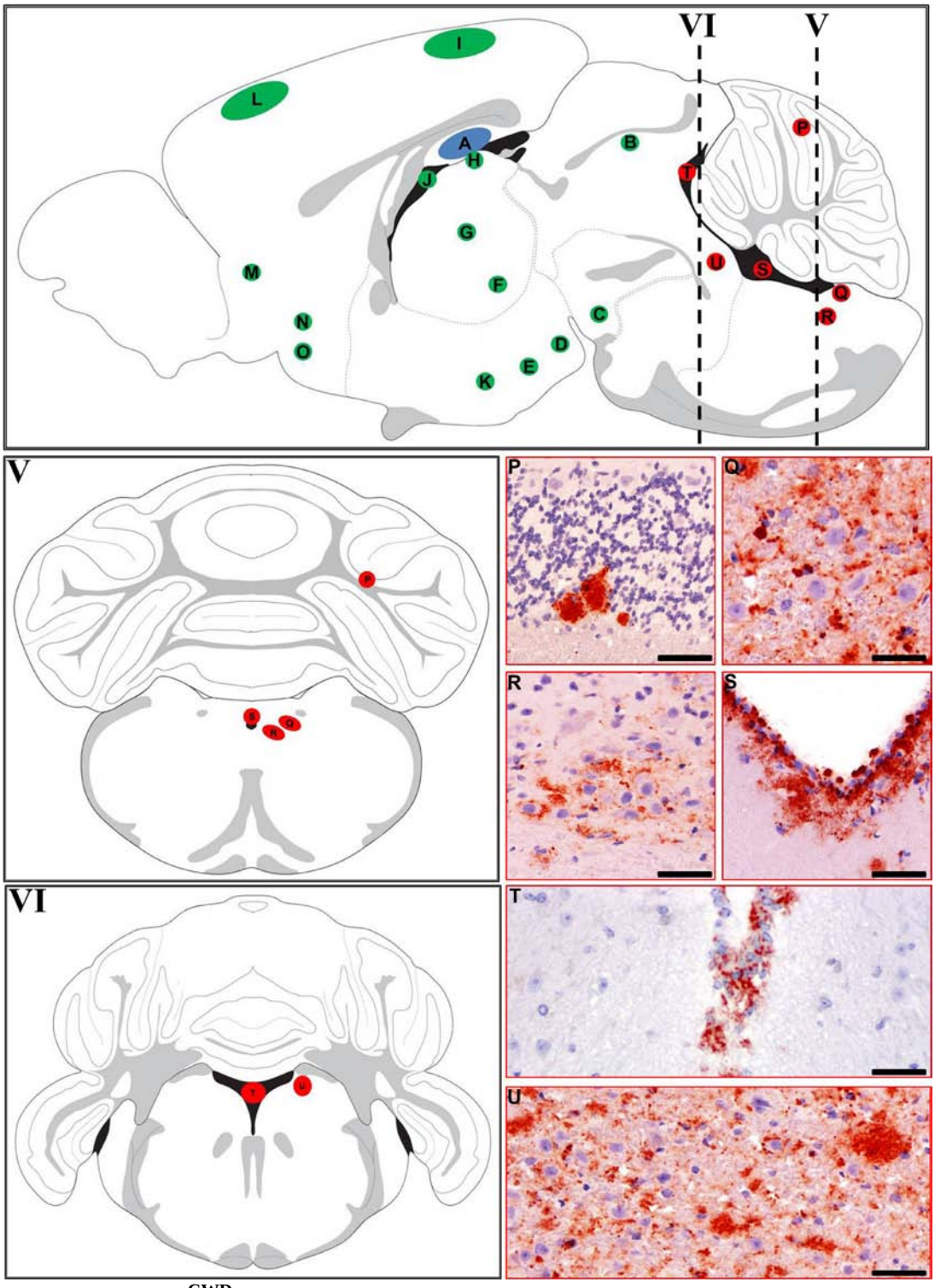

Figure 2.9 PrP^{CWD} in the CNS of IC-inoculated mice sacrificed at 180 dpi and at terminal disease.

In 2/2 animals, PrP^{CWD} immunoreactivity (red) was seen in the cerebellum (P), NTS (Q), DMNV (R), central canal (S), 4th ventricle (T), and LC (U). O), lateral Bar: P = 200 µm, Q = 75 µm, R-U = 100 µm.

PrP^{CWD} in central autonomic areas in IV- and IP-inoculated Tg[CerPrP-E] mice – 120 dpi:

In IV- and IP-inoculated animals the first accumulations of PrP^{CWD} in the CNS were observed at 120 dpi, with immunoreactivity seen in 4/4 animals in the NTS and the DMNV (Fig. 2.10 A, B). Less commonly, PrP^{CWD} was seen in the LC (2/4 animals) and the paraventricular nuclei of the hypothalamus (PVN) (3/4 animals). Moreover, in 4/4 animals, PrP^{CWD} was first noted in the cervical, caudal thoracic, and lumbar spinal cord segments with immunoreactivity located mainly in the gray matter including the central gray matter, the dorsal and ventral horns, and the intermediolateral cell column.

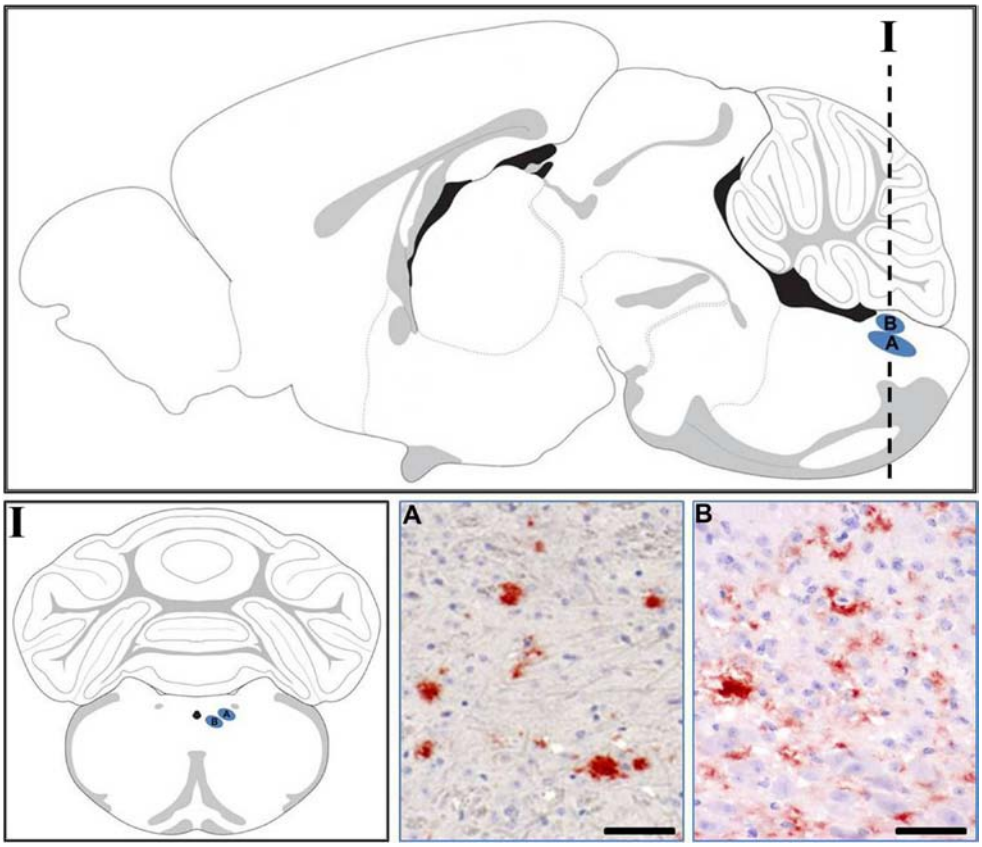

Figure 2.10 PrP^{CWD} in the CNS of IV- and IP-inoculated mice at 120 dpi.
In 4/4 mice, PrP^{CWD} immunoreactivity (red) was seen in the NTS (A) and DMNV (B). Bar: A = 200 µm, B = 100 µm.

PrP^{CWD} in central autonomic areas in IV and IP-inoculated Tg[CerPrP-E] mice – 180 dpi:

At 180 dpi, in all sacrificed mice, additional deposits of PrP^{CWD} immunoreactivity were seen in the raphe nuclei, gigantocellular nucleus, 4th ventricle, LC, cerebellar cortex, parabrachial nucleus, central canal, PAGM, hypothalamus, amygdala, and medial habenular nuclei (Fig. 2.11 C-N). Additionally, at this sacrifice time-point, PrP^{CWD} was seen throughout all segments of the spinal cord, including the cranial portions of the thoracic spinal cord.

PrP^{CWD} in central autonomic areas in IV- and IP-inoculated Tg[CerPrP-E] mice – terminal disease:

At terminal disease, in all sacrificed mice, additional deposits of PrP^{CWD} immunoreactivity were seen in the hippocampal formation, cerebral cortex, lateral and 3rd ventricles, subfornical organ, thalamus (T), and hypothalamus (U) (Fig. 2.12 O-W).

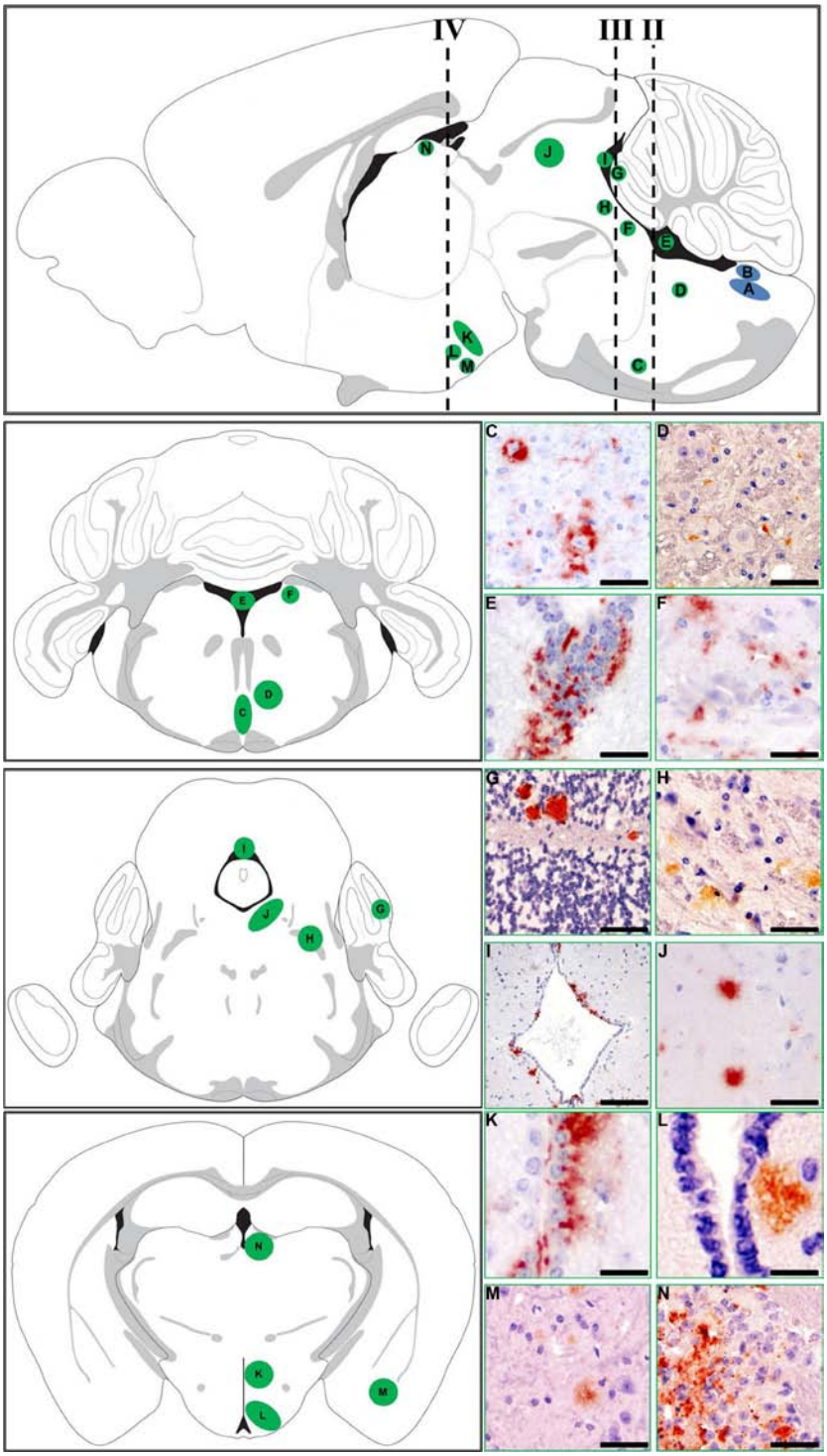

Figure 2.10 PrP^{CWD} in the CNS of IV- and IP-inoculated mice at 180 dpi.
In 4/4 mice, PrP^{CWD} immunoreactivity (red) was seen in the raphe nuclei (C), the gigantocellular nucleus (D), 4th ventricle (E), LC (F), cerebellar cortex (G), parabrachial nucleus (H), central canal (I), PAGM (J), hypothalamus (K, L) amygdala (M), and medial habenular nucleus (N). Bar: C, D, F, H, J, M, N = 125 µm, E = 100 µm, G = 200 µm, I = 400 µm, K, L = 50 µm.

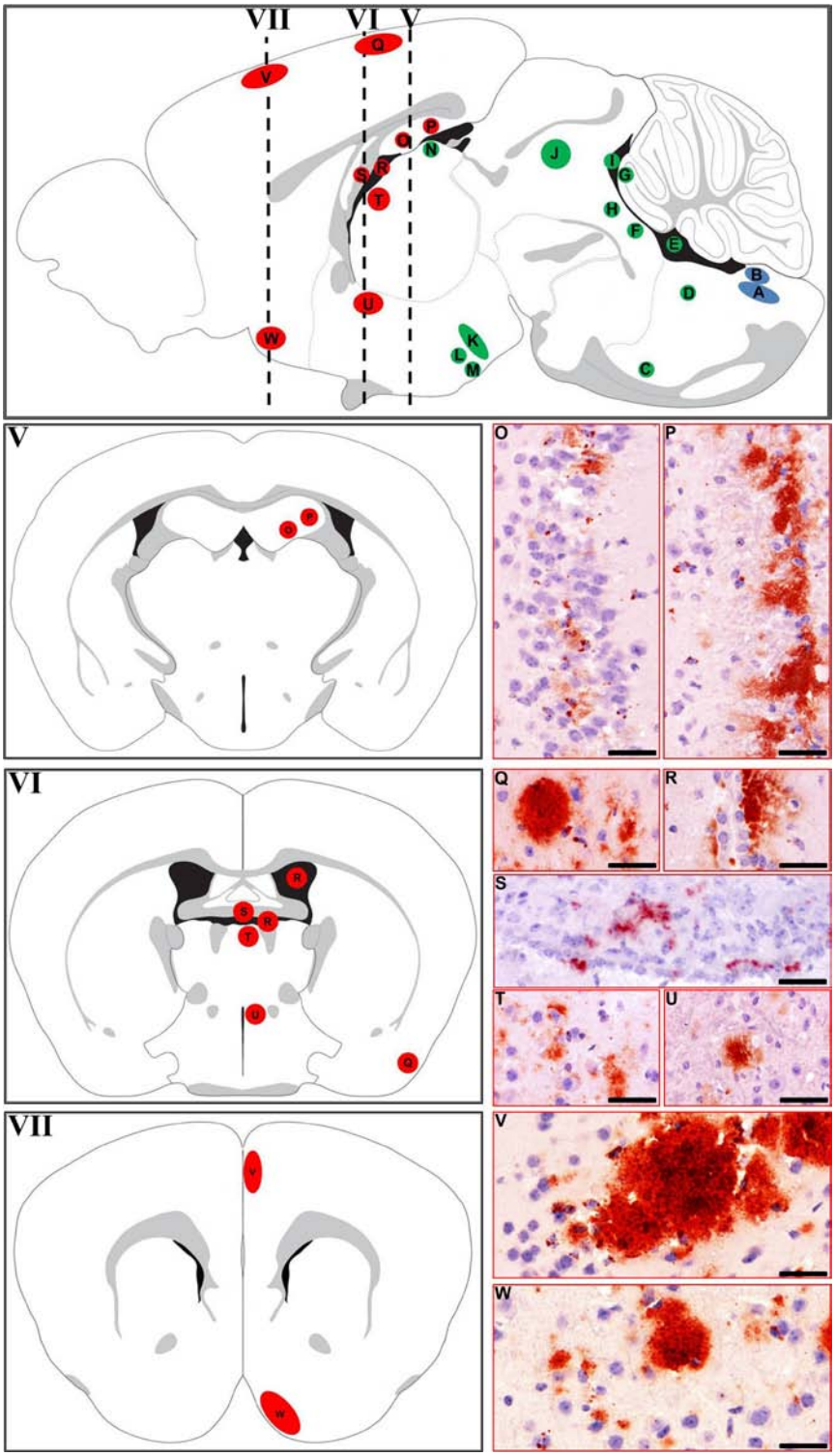

Figure 2.12 PrP^{CWD} in the CNS of IV- and IP-inoculated mice at terminal disease. In 4/4 mice, PrP^{CWD} immunoreactivity (red) was seen in the HPF (O, P), cerebral cortex (Q, V, W), lateral and 3rd ventricles (R), subfornical organ (S), thalamus (T), and hypothalamus (U). Bar: O-U = 100 µm, V-W = 75 µm.

PrP^{CWD} in the ENS of CWD-inoculated Tg[CerPrP-E] mice:

Morphologic pattern of PrP^{CWD} in the ENS of Tg[CerPrP-E] mice:

Accumulations of PrP^{CWD} were first identified in the myenteric and submucosal plexi of PO-inoculated mice at 60 dpi and in the IV-, IP-, and IC-inoculated mice at 180 dpi. In these animals, PrP^{CWD} immunoreactivity, which was most prominent in the caudal jejunum and ileum, was often unevenly distributed throughout the affected cells with a finely granular pattern dominating within the cytoplasm and a denser, clumped to aggregate pattern within the perinuclear area (Fig. 2.13 A). Additionally, PrP^{CWD} immunoreactivity was seen within the lamina propria of small intestinal villi (Fig. 2.13 B). The villus PrP^{CWD} was seen in 10-40% of evaluated villi within the caudal jejunum and ileum. Like the ENS immunoreactivity the villus PrP^{CWD} was finely granular to somewhat clumped in nature but, in contrast was somewhat linear in nature and appeared to extend along the long axis within affected villi. PrP^{CWD} immunoreactivity was not observed in any intestinal areas, including the ENS or villi, in any of the sham-inoculated mice.

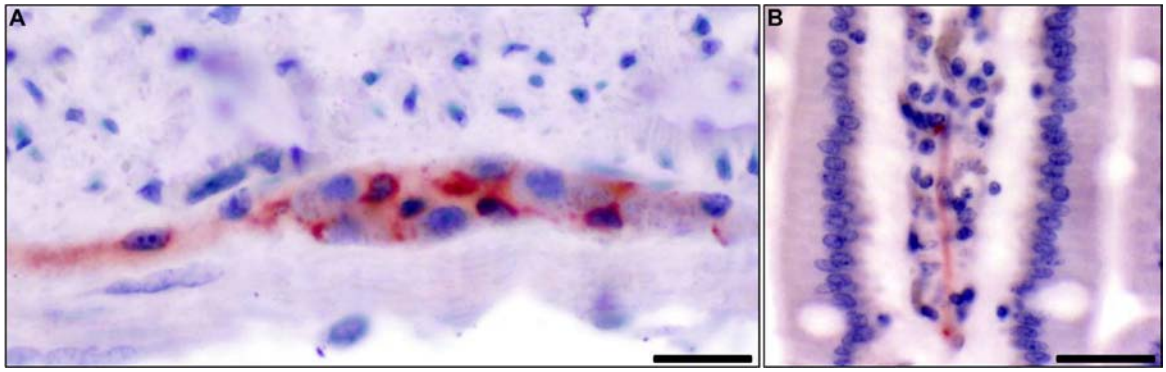

Figure 2.13 PrP^{CWD} in the ENS and intestinal villi of CWD-inoculated mice. PrP^{CWD} immunoreactivity (red) was detected in a finely granular to aggregate pattern in the myenteric (A) and submucosal plexi (not shown), and within the lamina propria of intestinal villi (B).

Co-localization of PrP^{CWD} with GFAP-positive processes in the intestinal villi of Tg[CerPrP-E] mice:

To evaluate for associations between cells of the ENS and the accumulation of CWD prions, intestinal sections were co-labeled for PrP^{CWD} and one of five cell-specific phenotype markers – 1) glial fibrillary acidic protein (GFAP), 2) Tyrosine hydroxylase (TH), 160 kD neurofilament (NF), and anti-Hu protein (Hu), and 3) LYVE-1. Previous work has confirmed the utility of these antibodies as markers of enteric glial cells (GFAP), enteric neurons (TH, NF, and Hu), and lymphatic endothelium (LYVE-1), respectively.(Odaka, Morisada et al. 2006; Albanese, Lawson et al. 2008; Qu, Thacker et al. 2008) Moreover, 4 of 5 antibodies demonstrated appropriate and expected immunoreactivity in PLP-fixed, paraffin-embedded sections from naive Tg[CerPrP-E] mice (Figure 2.14). Unfortunately, no anti-Hu immunoreactivity was observed in any positive control sections and was not utilized in further investigations.

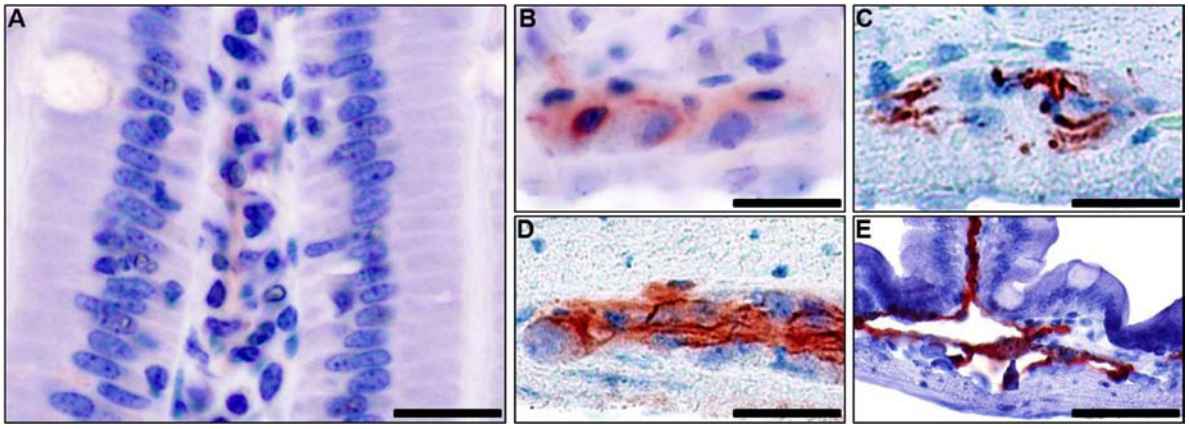

Figure 2.14 Utility of anti-cell phenotype antibodies within tissues of naive Tg[CerPrP-E] mice. GFAP immunoreactivity (red) was observed in the processes (A) and cell bodies (B) of EGCs. Tyrosine hydroxylase (C) and 160 kD neurofilament (D) immunoreactivity (red) were observed in neuronal cell bodies of the ENS. LYVE-1 immunoreactivity (red) was seen in intestinal lymphatic endothelium (E). Bar: A-D = 100 µm, E = 500 µm

In dual-label experiments, co-localization of PrP^{CWD} with GFAP was common and could be identified within the myenteric and submucosal plexi of all mice in which PrP^{CWD} had previously been seen (Fig. 2.15 A). In contrast, co-localization between PrP^{CWD} and either of the neuron-specific markers (TH or NF) was not identified (Fig. 2.15 B, C) nor was PrP^{CWD} seen within the lumena of lymphatics lined by LYVE-1-positive endothelial cells (Fig 2.15 D).

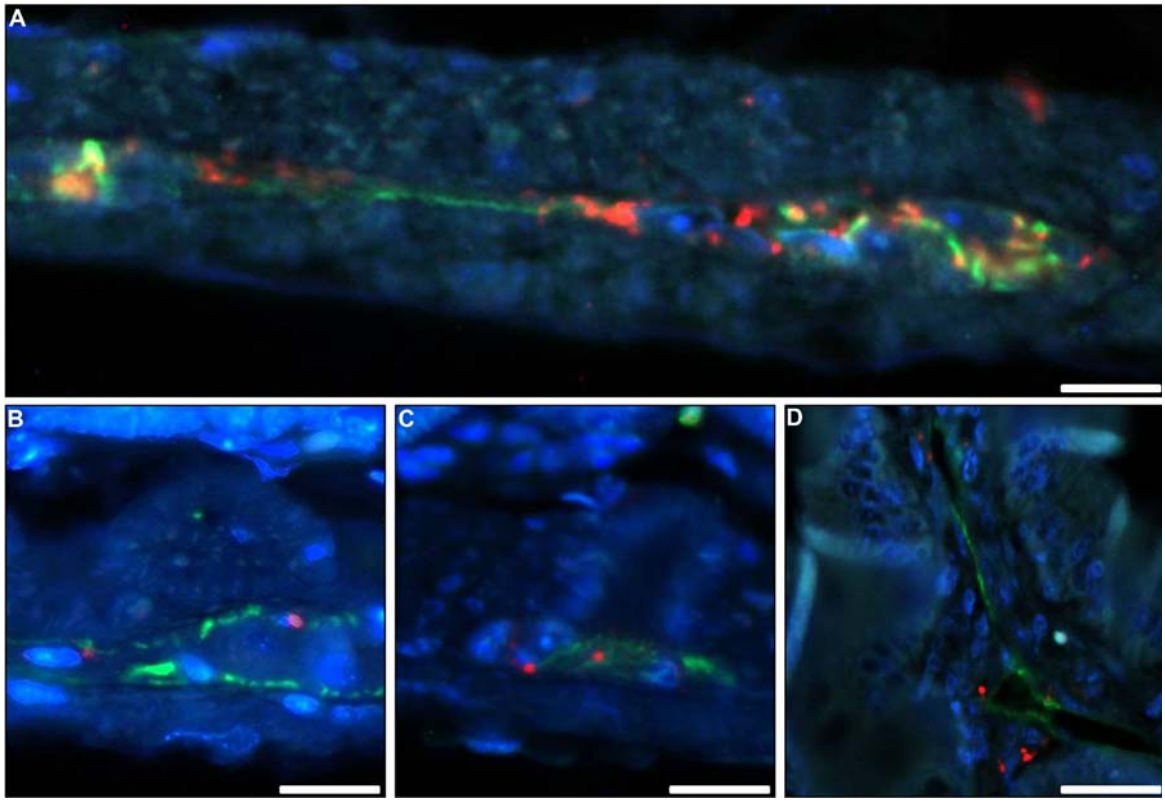

Figure 2.15 Co-localization of PrP^{CWD} with GFAP-positive EGCs within the ENS of CWD-inoculated Tg[CerPrP-E] mice.
PrP^{CWD} immunoreactivity (red) co-localized (yellow) with $GFAP^{+}$ (green) EGC cytoplasm and processes within myenteric plexi (A). In contrast, no such co-localization was detected between PrP^{CWD} in sections dual-stained with the anti-neuronal markers tyrosine hydroxylase (B) or 160 kD neurofilament (C). Additionally, PrP^{CWD} immunoreactivity (red) was identified to be distinct from LYVE-1-positive lined lymphatic lacteals (green, D). Blue = DAPI, nuclei. Bar: A-C = 50 µm, D = 200 µm.

Moreover, using confocal analysis, co-localization of GFAP with the linear aggregates of PrP^{CWD} could be readily identified in the intestinal villi (Fig. 2.16).

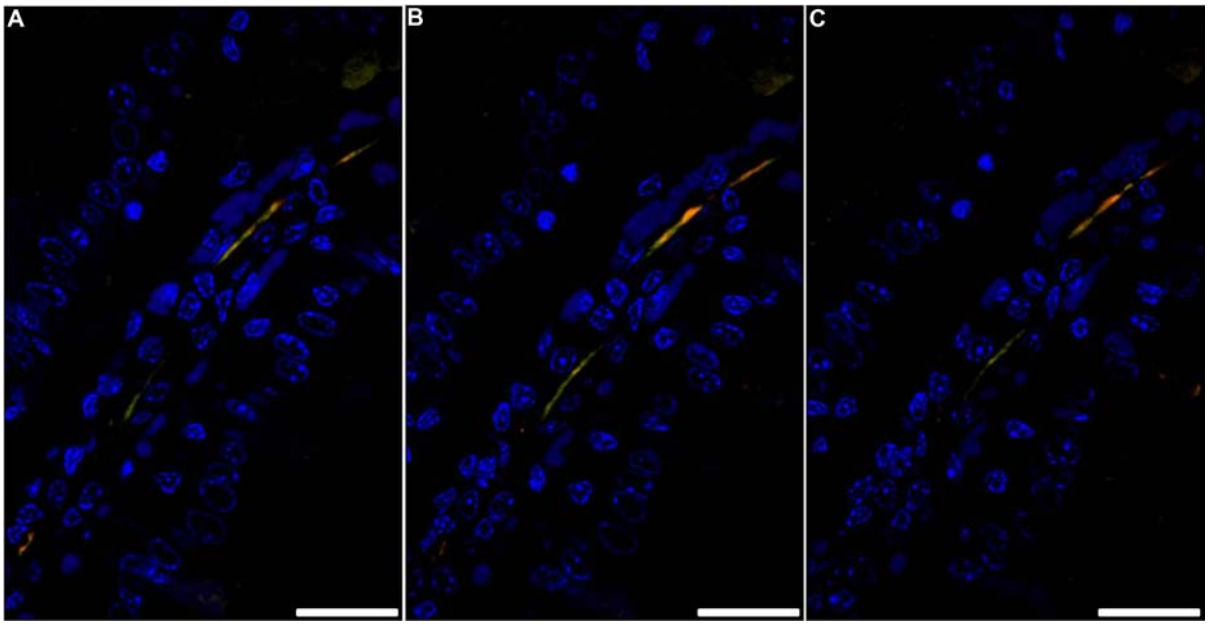

Figure 2.16 Co-localization of PrP^{CWD} with GFAP-positive processes of enteric glial cells within intestinal villi of CWD-inoculated Tg[CerPrP] mice.
Confocal analysis of Z-stack images demonstrates co-localization (yellow) of linear PrP^{CWD} immunoreactivity (red) with the GFAP-positive (green) processes of EGCs (A-C). Blue = DAPI, nuclei. Bar = 100 µm.

DISCUSSION

In the studies presented here, I report on the utility of elk prion protein-expressing (Tg[CerPrP-E]) mice in the study of CWD through studies documenting: (i) the expression of PrP^{C} in nervous and non-nervous tissues in naïve Tg[CerPrP-E] mice, (ii) the susceptibility of Tg[CerPrP-E] mice to CWD prions following IC, IP, and IV inoculation, (iii) the importance of the ANS in prion trafficking through the demonstration of progressive accumulations of PrP^{CWD} in tissues innervated by the peripheral branches of the ANS and in the nuclei and fiber tracts of the CAN, and (iv) the identification of PrP^{CWD} in intimate association with the processes and cell bodies of EGCs of the ENS.

In initial studies I sought to document the PrP^{C} expression profile in the Tg[CerPrP-E] mice because irrespective of the TSE, the expression of the normal host-encoded cellular membrane prion protein is considered vital for the development of prion disease. This essential role for PrP^{C} in prion disease pathogenesis is confirmed by work demonstrating that PrP^{C} non-expressing mice are resistant to prion infection and that there is an inverse relationship between normal cellular PrP^{C} expression levels with incubation period in transgenic mice.(Bueler, Aguzzi et al. 1993) Moreover, the importance of PrP^{C} expression is further demonstrated by work revealing that the efficacy of peripheral prion inoculation depends in part upon PrP^{C} expression in peripheral tissues.(Brandner, Isenmann et al. 1996; Blattler, Brandner et al. 1997; Glatzel and Aguzzi 2000)

In the IHC PrP mapping experiments performed here, including those detecting both PrP^{C} and PrP^{CWD}, I utilized a strategy of perfusion and immersion fixation with PLP. Such a protocol has proven to be sufficiently sensitive and specific for both isoforms of PrP.(Wiley, Burrola et al. 1987; McBride, Bruce et al. 1988; Seelig, Mason et al. 2010) The benefits provided by the choice of PLP as a fixative are uncertain, but PLP has been shown to react with sugars to stabilize proteins, which may be key in its ability to enhance the detection of the sialoglycoprotein PrP.(McLean and Nakane 1974) The superior immunolabeling of PrP using PLP-fixed tissues complements previous studies which have confirmed its enhanced efficacy as compared to either formalin- or glutaraldehyde-fixed tissue sections.(Bruce, McBride et al. 1989; Liu, Brown et al. 2003) The profile of PrP^{C} expression observed in the Tg[CerPrP-E] mice complements similar mapping experiments performed in a separate lineage of mule deer PrP-expressing mice and in a conventional strain of mouse.(Ford, Burton et al. 2002; Seelig, Mason et al. 2010) Moreover, the similar profile of PrP^{C} expression observed in the two strains of Tg[CerPrP] mice developed by Telling et. al; mimics their reported PrP^{C} expression data as determined by western blot, in which both strains are reported to have a 5-fold increase (vs. wild type mice) in brain PrP^{C} expression.(Angers, Seward et al. 2009)

When designing the most effective IHC protocols for the detection of PrP^{CWD}, I utilized two 88% formic acid (FA) immersion steps in conjunction with signal amplification using TSA. The utility of FA in IHC studies of prions is twofold – 1) it abolishes PrP^{C} immunoreactivity, thus allowing for specific detection of the PrP^{CWD} isoform and 2) it greatly enhances the immunoreactivity of PrP^{CWD} in paraffin-embedded

tissues sections.(Kitamoto, Ogomori et al. 1987; Bruce, McBride et al. 1989; Muramoto, Kitamoto et al. 1992; Liu, Brown et al. 2003) The incorporation of TSA into anti-PrP^{CWD} IHC protocols results in a dramatic increase in visually-detectable signal, similar to what has been reported in previous cervid and transgenic mice CWD studies.(Sigurdson, Barillas-Mury et al. 2002; Seelig, Mason et al. 2010) With these protocols I evaluated the sequential accumulation of PrP^{CWD} in tissues of multi-route inoculated Tg[CerPrP-E] mice, placing emphasis on tissues of the lymphoreticular, enteric nervous, and central nervous systems. Through these studies, I sought to evaluate tissues and cell populations which might accumulate PrP^{CWD} and thus provide insights into the pathways by which the infectious agent spreads.

While the strain of elk PrP-expressing mouse utilized in these studies has previously been shown susceptible to prions derived from elk and mule deer, this is the first study to demonstrate the susceptibility of these mice to prions derived from WTD.(Angers, Seward et al. 2009) The incubation periods for the mice inoculated with WTD prions in these studies are similar to what has been reported for a separate strain of mule deer PrP-expressing Tg[CerPrP] mice, although there was a slight prolongation of each of the three route-specific incubation periods.(Seelig, Mason et al. 2010) Although different inocula were used in each of these two studies, this lengthening of incubation period is likely, in part, a manifestation of the species barrier phenomenon. Specifically, in the studies here, there was a mismatch between the cervid species from which the CWD^{+} inocula was derived (WTD) and the cervid PrP coding sequence used to generate the Tg study mice (elk). Additionally, the failure of the PO-inoculated mice to

demonstrate susceptibility to a low dose CWD inoculum was not unexpected given the results of previous work in Tg[CerPrP] mice, which emphasized the importance of dosage.(Seelig, Mason et al. 2010)

Neuropathologic evaluation of the CWD-infected mice revealed: 1) two distinct patterns of spongiosis, 2) an apparently route-dependent pattern of plaque accumulation, and 3) two patterns of PrP^{CWD} immunoreactivity. With respect to spongiosis, given the temporal differences between the two patterns (such that the more discrete form was generally observed in animals sacrificed early in the course of disease whereas the raggedy form was most commonly seen in animals sacrificed later), it seems likely that the latter form represents a more severe manifestation of the former, with discrete vacuoles gradually coalescing into the raggedy form. Additionally, several different morphologic forms of PrP immunoreactivity were identified.

Such variations in PrP^{CWD} morphology depended according to inoculation route, degree of disease progression and neuroanatomic location. A granular, somewhat dispersed pattern of immunoreactivity: (i) was most commonly seen in mice inoculated either the IV or IP route, (ii) was observed largely in animals sacrificed early (60 dpi), (iii) was largely restricted to the gray matter neuropil in particular neuroanatomic areas - most notably within the medulla, pons, and stratum lucidum and radiatum of the HPF - and (iv) was the most common manifestation when cell-associated PrP^{CWD} was detected. In contrast, the plaque form: (i) was most common in IC-inoculated animals (irrespective of time-point), (ii) was frequently observed in animals late in disease progression (120 dpi +), (iii) was identified in areas with heavy PrP^{CWD} immunoreactivity, including the

stratum pyramidale of the HPF as well as the cerebral cortex, thalamus, and cerebellum, and (iv) was largely restricted to the extracellular neuropil. The reason for the variations in PrP^{CWD} immunoreactivity morphology is uncertain, but such patterns substantiate suggestions that intrinsic differences in cellular subpopulations within distinct microanatomic regions, including differential patterns of prion protein glycosylation, may be the cause.(DeArmond, Qiu et al. 1999) Moreover, these patterns of spongiosis and PrP^{CWD} immunoreactivity are quite consistent with findings in other reports of natural and experimental CWD.(Spraker, Miller et al. 1997; LaFauci, Carp et al. 2006; Sigurdson, Mathiason et al. 2008)

Despite inoculation route-dependent variations in the progressive temporal-spatial pattern of PrP^{CWD} accumulation, the overall kinetics of prion accumulation in all 3 groups were indicative of trafficking via the circuitry of the ANS. In the IV- and IP-inoculated groups, early and simultaneous accumulations of PrP^{CWD} in the spleen and MLN as well as subsequent accumulations in the DMNV, NTS and the thoracolumbar spinal cord segments, strongly implicate fibers of the PaNS and SNS, notably afferent and efferent fibers of the vagal and splanchnic tracts, respectively, as conduits of prion CNS invasion (Fig. 2.17 A-B). Such results support a pathogenesis model similar to that reported in both CWD-infected cervids and scrapie-infected sheep, namely that prion invasion of the CNS can occur by two routes: 1) via parasympathetic fibers directed to the DMNV and NTS, and 2) via sympathetic fibers to the thoracolumbar spinal cord segments.(van Keulen, Schreuder et al. 2000; Sigurdson, Spraker et al. 2001; Fox, Jewell et al. 2006) Subsequent to initial CNS invasion, PrP^{CWD} was found in the raphe nuclei,

gigantocellular reticular nucleus, LC, parabrachial nucleus, PAGM, dorsomedial and ventromedial nuclei of the hypothalamus, numerous thalamic nuclei, and the anterior cingulate and ventromedial cortices, all of which are components of, or connected to, the CAN.(Appenzeller 1999) Terminally, accumulations of PrP^{CWD} in the GI tract, including the ENS, PP, and intestinal villi, were likely the result of centrifugal prion trafficking, which could occur via either sympathetic or parasympathetic fiber systems (Fig 2.17 C).

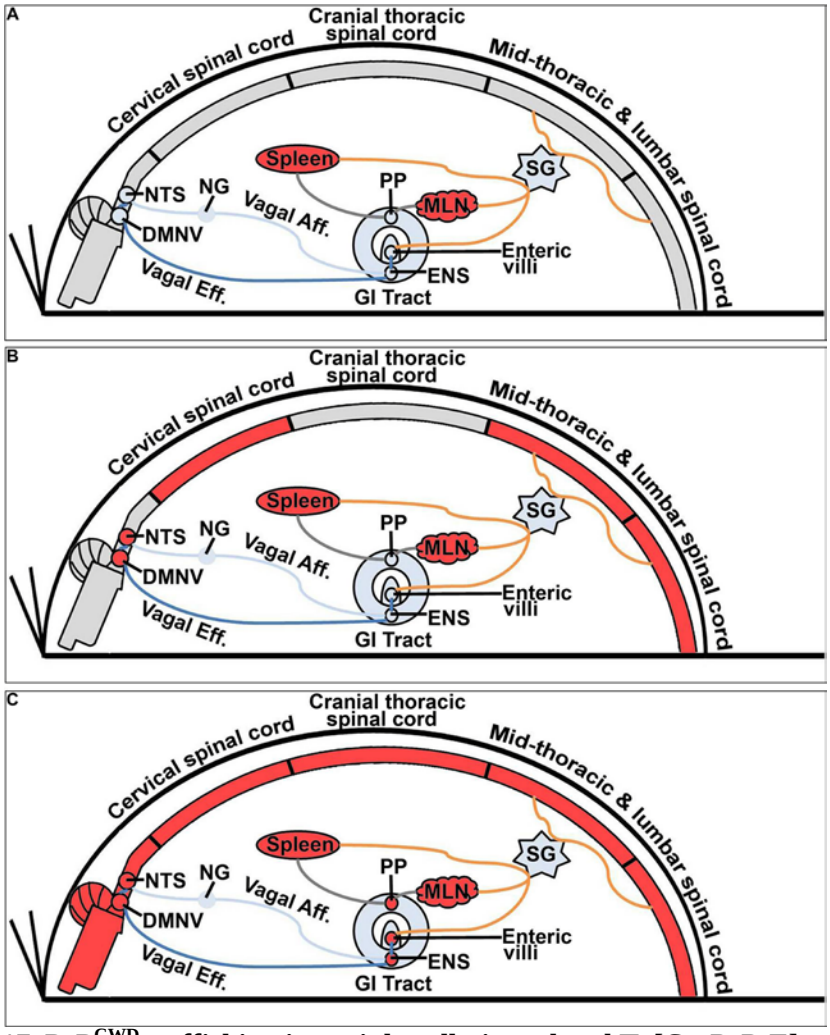

Figure 2.17 PrP^{CWD} trafficking in peripherally-inoculated Tg[CerPrP-E] mice.
In IV- or IP-infected mice, IHC mapping at 60 dpi (A), 120 dpi (B), and 180 dpi / terminal disease (C) revealed progressive spread of CWD prions (red) via the ANS. Blue lines represent parasympathetic fiber tracts and orange lines represent sympathetic fiber tracts. Abbreviations: PP = Peyer's patches, MLN = mesenteric lymph nodes, SG = sympathetic ganglia, ENS = enteric nervous system, NG = nodose ganglion, NTS = solitary tract nucleus, and DMNV = dorsal motor nucleus of the vagus.

In IC-inoculated animals PrP^{CWD} was first detectable in the HPF, most notably within the pyramidal cell layer of CA1-CA3 fields, which is similar to what has been reported in a separate strain of CWD-infected transgenic mice, as well as in scrapie and CJD-infected mice.(Muramoto, Kitamoto et al. 1992; Jeffrey, Martin et al. 2001; Seelig, Mason et al. 2010) The reason for this hippocampal-tropism is uncertain, but work in scrapie-infected mice has demonstrated increased hippocampal cellular stress, activated endoplasmic reticulum, and activated mitochondrial apoptotic pathways.(Brown, Rebus et al. 2005) In part, I speculate that such hippocampal-tropism may be a manifestation of high local levels of PrP^{C} expression. Such a hypothesis is supported by the initial PrP^{C} expression mapping work in that the most intense PrP^{C} immunoreactivity was localized to the hippocampus (Fig. 2.3). Interestingly, the apparent tropism of CWD and scrapie prions for the hippocampus differs from human prion disease, including CJD and GSS, in which hippocampal lesions are overwhelmingly mild, despite numerous prion deposits in other neuroanatomic locations.(Kaneko, Sugiyama et al. 2008)

Subsequent to its initial detection in the HPF, PrP^{CWD} in the CNS of the IC-infected mice became increasingly widespread, with trafficking occurring in both the rostral and caudal directions (Fig 2.18.B-C). While the determinants of prion spread in the IC-inoculated mice are less obvious than the peripherally-inoculated mice, the involvement of the DMNV, NTS, PAGM, and nuclei of the thalamus and hypothalamus suggest that CAN pathways are involved. Additional caudally-directed prion trafficking was demonstrated by progressive accumulations of PrP^{CWD} throughout the length of the spinal cord (Fig 2.18 B-C). Moreover, similar to the peripherally-inoculated animals,

progressive accumulations of PrP^{CWD} in spleen, mesenteric lymph node, PP, ENS, and intestinal villi implicate the peripheral autonomic fibers as conduits of prion transit, which substantiates findings reported in IC-inoculated, rodent models of CJD and scrapie.(Kimberlin, Field et al. 1983; Muramoto, Kitamoto et al. 1992)

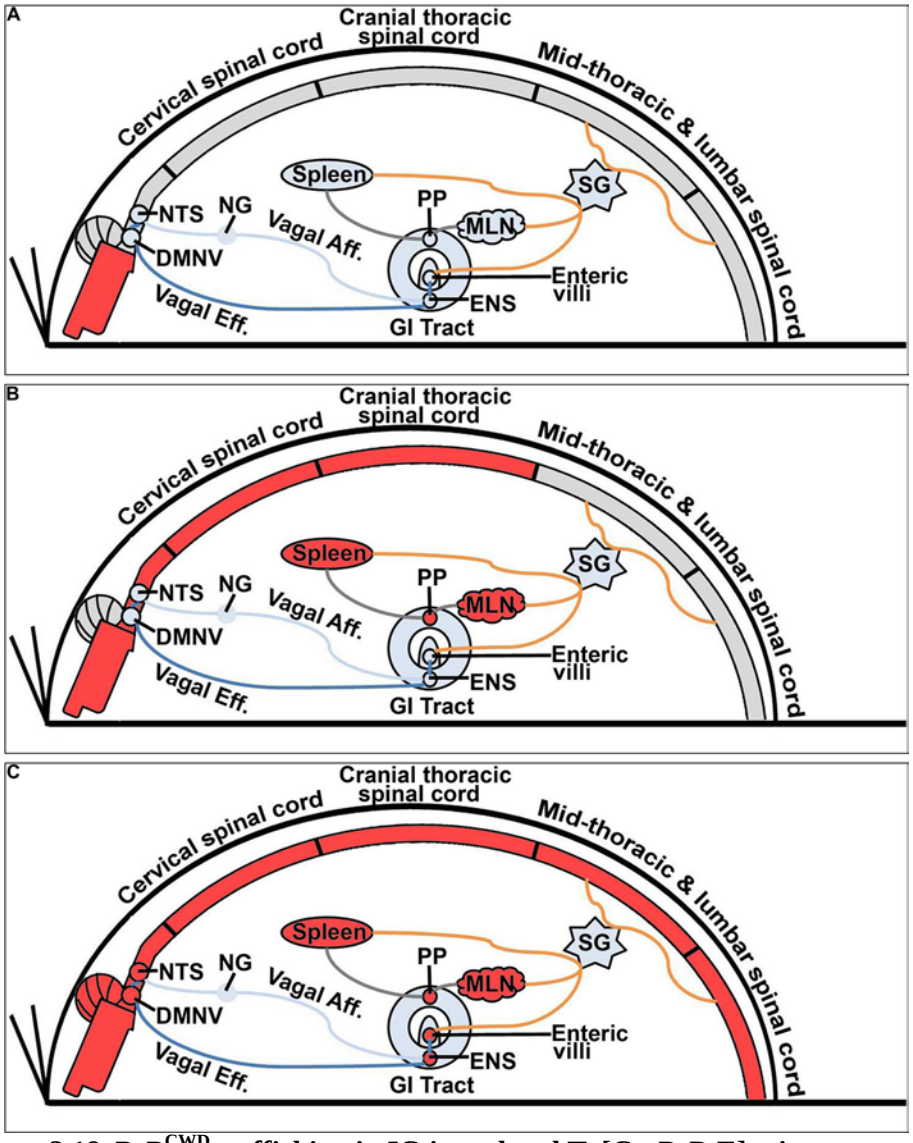

Figure 2.18 PrP^{CWD} trafficking in IC-inoculated Tg[CerPrP-E] mice.
In IC-infected mice, IHC mapping at 60 dpi (A), 120 dpi (B), and 180 dpi / terminal disease (C) revealed progressive spread of CWD prions (red) mediated in part, by the ANS. Blue lines represent parasympathetic fiber tracts and orange lines represent sympathetic fiber tracts. Abbreviations: PP = Peyer's patches, MLN = mesenteric lymph nodes, SG = sympathetic ganglia, ENS = enteric nervous system, NG = nodose ganglion, NTS = solitary tract nucleus, and DMNV = dorsal motor nucleus of the vagus.

In order to accurately identify regions of the GI tract in which prion accumulation could be detected, I used IHC to evaluate sections from the stomach, duodenum, small intestine, cecum, and large intestine. Through this work, I identified the distal jejunum and ileum as the sites most associated with PrP^{CWD} accumulation, which is consistent with previous work evaluating prion accumulation in intestinal sections from scrapie fed hamsters.(Kruger, Thomzig et al. 2009) In contrast, PrP^{CWD} was only rarely seen in the large intestine and I was unable to identify PrP^{CWD} in the esophagus, duodenum, or cecum. In the affected sites, irrespective of route of inoculation, patterns of PrP^{CWD} accumulation were similar, suggesting a common underlying pathogenesis. The preferential accumulation of CWD prions in the distal small intestine is similar to scrapie and has been suggested to be the result of delayed ileal transit time, although increased local expression of Peyer's patch-associated M-cells may also play a role.(Holgate and Read 1983)

Within PrP^{CWD}-positive intestinal sections, anti-prion immunoreactivity was found to be in part associated with the $GFAP^{+}$ EGC cell bodies and processes, which mimics what has been reported in sheep.(Marruchella, Ligios et al. 2007) However, there was a substantial amount of non-EGC associated PrP^{CWD} immunoreactivity (Fig. 2.15 A), suggesting that EGCs are not the only ENS constituent capable of prion accumulation. Unfortunately, further attempts to clarify the association between PrP^{CWD} and other ENS cell types were confounded by a failure to: 1) demonstrate co-labeling between PrP^{CWD} and either TH^{+} or NF^{+} enteric neurons and 2) an inability to effectively label enteric neurons with the anti-Hu antibody. The failure to demonstrate PrP^{CWD} in association with either TH^{+} or NF^{+} enteric neurons may truly reflect the inability of these two particular

subsets of enteric neurons to accumulate PrP^{CWD}, but just as likely, may be reflective of the relative insensitivity of these two antibodies as markers of enteric neurons. In the mouse, anti-TH and anti-NF antibodies have been described to label only 31% and 0.5% of enteric neurons, respectively.(Qu, Thacker et al. 2008) Unfortunately, the inability to effectively label enteric neurons with the anti-Hu antibody, which is reported to a very effective murine intestinal pan-neuronal marker, is the most likely culpable factor for the inability to identify non-EGC, PrP^{CWD}-positive ENS cells. Such a failure is likely the result of the use of PLP-fixed, paraffin-embedded tissues, as the most effective anti-Hu immunoreactivity has been described in formaldehyde-fixed, whole-mount tissues.(Qu, Thacker et al. 2008)

The GI tract is likely the natural tissue site by which prions begin their invasive journey, with the Peyer's patches, tonsils, M-cells, and ENS playing crucial roles in the early pathogenic events of entero- and neuro-invasion. However, the manner by which prions cross the GI mucosal barrier after they are ingested remains obscure. Currently, the bulk of the data implicates the M-cell, or microfold cell, as the most plausible mediator of the initial events in prion crossing of the GI tract. These cells, which are a highly specialized epithelial cell type present in the follicle-associated epithelium, function to transport substances and antigens from the gut lumen to cells of the lymphoid tissue.(Neutra, Frey et al. 1996) The role of the M-cell in prion disease has been best illustrated by an in vitro M-cell culture system in which a single layer of such cells was shown capable of transcytosing scrapie prions from the apical surface through to the basolateral side.(Heppner, Christ et al. 2001) However, the identification of PrP^{RES} and a possible prion receptor in and on the enterocytes of neonatal mice orally inoculated with

scrapie, suggests that suggests that alternative, non-M-cell-mediated, pathways of enteroinvasion remain possible.(Okamoto, Furuoka et al. 2003) One such M-cell independent pathway is transit via the neuronal and/or glial cell processes of the ENS.

In such an EGC-dependent pathway of prion transit, the ENS would act as the initial site of prion neuroinvasion and along with being a conduit for eventual entry into the CNS. Such a hypothesis is complemented by mapping studies confirming that the processes of these cells extend the length of the intestinal villi and by hamster studies demonstrating PrP^{RES}-EGC associations at early time-points following oral scrapie inoculation.(Furness, Jones et al. 2004; Marruchella, Ligios et al. 2007) Finally, these findings are: 1) consistent with reports of naturally and experimentally-infected mule deer with CWD and 2) suggestive of ENS plexi and EGC involvement in the shedding of infectious prions from the GI tract.(Sigurdson, Spraker et al. 2001; Fox, Jewell et al. 2006)

The conclusion that prion accumulation in the EGCs and ENS is a key determinants in either prion enteroinvasion or enteric shedding is not only supported by the microscopic co-localization data, but also by the temporal kinetics of the PrP^{CWD} mapping data. Through the simultaneous evaluation of all three relevant tissue compartments (the ENS, GALT, and CNS), it becomes possible to determine individual organ patterns of accumulations and ascertain possible trafficking pathways. The early colonization of the EGCs and ENS following PO inoculation, which was the only site in which PrP^{CWD} was identified, suggests prion accumulation was the result of prion transit from the gut lumen, rather than spread from another, PrP^{CWD}-containing organ. In contrast, accumulations of PrP^{CWD} in the ENS of the IV-, IP-, and IC-inoculated animals

were identified late in disease, only after the identification of PrP^{CWD} in the CNS, suggesting that prion invasion occurred as a result of centrifugal spread. This latter observation supports an additional hypothesis, one which implicates the ENS as a key mediator in the enteric shedding of infectious prions. The presence of infectious prions in the feces of CWD-infected animals has been demonstrated in both natural and experimental hosts, but the manner in which such infectivity is conferred is still uncertain.(Haley, Mathiason et al. 2009; Tamguney, Miller et al. 2009) It has been hypothesized that the alimentary excretion of prions is the result of the shedding of prion-infected cells or cell fragments, although this has yet to be clearly demonstrated.(Safar, Lessard et al. 2008) In one potential scenario, which is bolstered by this work, the shedding of prions from the GI tract is mediated entirely by the cells and processes of neurons and EGCs of the ENS. If this observed temporal-spatial pattern of PrP^{CWD} deposition in intestinal tissues is reflective of the spread of infection, these findings are suggestive of ENS involvement in: 1) the establishment of primary intestinal infection, 2) propagation of infection to the CNS, and 3) conferring prion infectivity to feces.

In other prion disease systems, the temporal sequence between the accumulations of PrP^{CWD} in the ENS versus the CNS is less clear. In orally-inoculated mule deer and cervidized mice, PrP^{CWD} was identified in the plexi of the ENS either following, or simultaneous with, its identification in the CNS.(Fox, Jewell et al. 2006; Trifilo, Ying et al. 2007) Similarly, in sheep and hamsters with scrapie, accumulations of prions were identifiable in the ENS simultaneous with its detection in the DMNV and thoracic spinal cord, but only following its identification in the GALT.(Andreoletti, Berthon et al. 2000; van Keulen, Vromans et al. 2008) More accurate statements regarding the sequence of

events in the process of CWD prion enteroinvasion, particularly providing temporal-spatial discriminatory information involving accumulation PrP^{CWD} within the EGCs, the ENS, and the GALT, will require PO-inoculation studies with earlier and more tightly staggered sacrifice time-points.

The failure of the PO-inoculated mice to either develop clinical disease or to progressively traffic PrP^{CWD}, despite accumulations within the ENS, was a surprising discovery. The mechanism underlying this cessation of PrP^{CWD} propagation and trafficking at the level of the ENS, is uncertain, but in one such scenario, inoculum dosage is the key determinant and, in the PO-inoculated mice in this study, the dosage may have been insufficient to reach a certain critical threshold. The nature of that threshold is uncertain, but number of infected cells or total infectivity in a particular cell or tissue remains plausible candidates. Additionally, it remains possible that there was successful infection of the PO-inoculated mice, but that the infection was subclinical and the IHC technique used was insufficiently sensitive to demonstrate PrP^{CWD} in affected tissues. Such a phenomenon has been recently described in a study with PO-inoculated WTD which required serial protein misfolding cyclic amplification (sPMCA), an exquisitely sensitive PrP^{CWD} detection technique, to identify prions in animals previously classified as CWD-negative.(Haley, Mathiason et al. 2009)

In summary, the findings reported here for CWD-infected Tg[CerPrP] mice provide strong circumstantial evidence for: (i) the trafficking of CWD prions via the parasympathetic and sympathetic branches of the autonomic nervous system during the process of CNS neuroinvasion, (ii) the trafficking of CWD prions in the CNS along fibers

and nuclei of the CAN, and (iii) the involvement of the EGCs and ENS in the process invasion and shedding of prions via the GI tract. These observations are consistent with previous reports in experimental and natural prion disease, yet offer new insights into the pathways of prion trafficking and prion shedding in CWD.

ACKNOWLEDGEMENTS

I would like to thank Jan Langeveld for his generous gift of anti-prion antibody R505.5. I thank Jeanette Hayes-Klug, Heather Bender, Kelly Anderson, Erin McNulty, and Kate Bruner for their excellent care and management of the Tg mice used in these studies. I thank Mark Zabel for his helpful comments on this work and for provision of the $PrP^{0/0}$ mice. This work was supported by contract NO1-AI-25491 from NIH, NIAID from T32-RR07072 from NIH, NCRR.

REFERENCES

(2010). "Chronic Wasting Disease Alliance." from http://www.cwd-info.org/index.php/fuseaction/news.main.

Albanese, V., V. A. Lawson, et al. (2008). "Evidence for prion protein expression in enteroglial cells of the myenteric plexus of mouse intestine." Auton Neurosci **140**(1-2): 17-23.

Andreoletti, O., P. Berthon, et al. (2000). "Early accumulation of PrP(Sc) in gut-associated lymphoid and nervous tissues of susceptible sheep from a Romanov flock with natural scrapie." J Gen Virol **81**(Pt 12): 3115-26.

Angers, R. C., S. R. Browning, et al. (2006). "Prions in skeletal muscles of deer with chronic wasting disease." Science **311**(5764): 1117.

Angers, R. C., T. S. Seward, et al. (2009). "Chronic wasting disease prions in elk antler velvet." Emerg Infect Dis **15**(5): 696-703.

Appenzeller, O. (1999). The autonomic nervous system. Amsterdam ; New York, Elsevier.

Beekes, M. and P. A. McBride (2000). "Early accumulation of pathological PrP in the enteric nervous system and gut-associated lymphoid tissue of hamsters orally infected with scrapie." Neurosci Lett **278**(3): 181-4.

Beekes, M., P. A. McBride, et al. (1998). "Cerebral targeting indicates vagal spread of infection in hamsters fed with scrapie." J Gen Virol **79 (Pt 3)**: 601-7.

Blattler, T., S. Brandner, et al. (1997). "PrP-expressing tissue required for transfer of scrapie infectivity from spleen to brain." Nature **389**(6646): 69-73.

Bolton, D. C., R. D. Rudelli, et al. (1991). "Copurification of Sp33-37 and scrapie agent from hamster brain prior to detectable histopathology and clinical disease." J Gen Virol **72 (Pt 12)**: 2905-13.

Brandner, S., S. Isenmann, et al. (1996). "Normal host prion protein necessary for scrapie-induced neurotoxicity." Nature **379**(6563): 339-43.

Brown, A. R., S. Rebus, et al. (2005). "Gene expression profiling of the preclinical scrapie-infected hippocampus." Biochem Biophys Res Commun **334**(1): 86-95.

Browning, S. R., G. L. Mason, et al. (2004). "Transmission of prions from mule deer and elk with chronic wasting disease to transgenic mice expressing cervid PrP." J Virol **78**(23): 13345-50.

Bruce, M. E., P. A. McBride, et al. (1989). "Precise targeting of the pathology of the sialoglycoprotein, PrP, and vacuolar degeneration in mouse scrapie." Neurosci Lett **102**(1): 1-6.

Bueler, H., A. Aguzzi, et al. (1993). "Mice devoid of PrP are resistant to scrapie." Cell **73**(7): 1339-47.

Carlson, G. A., D. T. Kingsbury, et al. (1986). "Linkage of prion protein and scrapie incubation time genes." Cell **46**(4): 503-11.

Castilla, J., A. Gutierrez-Adan, et al. (2004). "Subclinical bovine spongiform encephalopathy infection in transgenic mice expressing porcine prion protein." J Neurosci **24**(21): 5063-9.

DeArmond, S. J., Y. Qiu, et al. (1999). "PrPc glycoform heterogeneity as a function of brain region: implications for selective targeting of neurons by prion strains." J Neuropathol Exp Neurol **58**(9): 1000-9.
Ford, M. J., L. J. Burton, et al. (2002). "Selective expression of prion protein in peripheral tissues of the adult mouse." Neuroscience **113**(1): 177-92.
Fox, K. A., J. E. Jewell, et al. (2006). "Patterns of PrPCWD accumulation during the course of chronic wasting disease infection in orally inoculated mule deer (Odocoileus hemionus)." J Gen Virol **87**(Pt 11): 3451-61.
Furness, J. B., C. Jones, et al. (2004). "Intrinsic primary afferent neurons and nerve circuits within the intestine." Prog Neurobiol **72**(2): 143-64.
Glatzel, M. and A. Aguzzi (2000). "PrP(C) expression in the peripheral nervous system is a determinant of prion neuroinvasion." J Gen Virol **81**(Pt 11): 2813-21.
Haley, N. J. (2009). "Detection of CWD prions in urine and saliva of deer by transgenic mouse bioassay." PLoS ONE.
Haley, N. J., C. K. Mathiason, et al. (2009). "Detection of sub-clinical CWD infection in conventional test-negative deer long after oral exposure to urine and feces from CWD+ deer." PLoS One **4**(11): e7990.
Heinlich, H. and G. Bullock (2004). The laboratory mouse. London, Academic.
Heppner, F. L., A. D. Christ, et al. (2001). "Transepithelial prion transport by M cells." Nat Med **7**(9): 976-7.
Holgate, A. M. and N. W. Read (1983). "Relationship between small bowel transit time and absorption of a solid meal. Influence of metoclopramide, magnesium sulfate, and lactulose." Dig Dis Sci **28**(9): 812-9.
Jeffrey, M., S. Martin, et al. (2001). "Onset of accumulation of PrPres in murine ME7 scrapie in relation to pathological and PrP immunohistochemical changes." J Comp Pathol **124**(1): 20-8.
Kaneko, M., N. Sugiyama, et al. (2008). "Prion disease causes less severe lesions in human hippocampus than other parts of brain." Psychiatry Clin Neurosci **62**(3): 264-70.
Kimberlin, R. H., H. J. Field, et al. (1983). "Pathogenesis of mouse scrapie: evidence for spread of infection from central to peripheral nervous system." J Gen Virol **64 Pt 3**: 713-6.
Kitamoto, T., K. Ogomori, et al. (1987). "Formic acid pretreatment enhances immunostaining of cerebral and systemic amyloids." Lab Invest **57**(2): 230-6.
Kong, Q., S. Huang, et al. (2005). "Chronic wasting disease of elk: transmissibility to humans examined by transgenic mouse models." J Neurosci **25**(35): 7944-9.
Kruger, D., A. Thomzig, et al. (2009). "Faecal shedding, alimentary clearance and intestinal spread of prions in hamsters fed with scrapie." Vet Res **40**(1): 4.
LaFauci, G., R. I. Carp, et al. (2006). "Passage of chronic wasting disease prion into transgenic mice expressing Rocky Mountain elk (Cervus elaphus nelsoni) PrPC." J Gen Virol **87**(Pt 12): 3773-80.
Liu, W. G., D. A. Brown, et al. (2003). "Immunohistochemical comparison of anti-prion protein (PrP) antibodies in the CNS of mice infected with scrapie." J Histochem Cytochem **51**(8): 1065-71.

Maignien, T., C. I. Lasmezas, et al. (1999). "Pathogenesis of the oral route of infection of mice with scrapie and bovine spongiform encephalopathy agents." J Gen Virol **80 (Pt 11)**: 3035-42.
Marruchella, G., C. Ligios, et al. (2007). "Enteroglial and neuronal involvement without apparent neuron loss in ileal enteric nervous system plexuses from scrapie-affected sheep." J Gen Virol **88**(Pt 10): 2899-904.
Mathiason, C. K., J. G. Powers, et al. (2006). "Infectious prions in the saliva and blood of deer with chronic wasting disease." Science **314**(5796): 133-6.
McBride, P. A., M. E. Bruce, et al. (1988). "Immunostaining of scrapie cerebral amyloid plaques with antisera raised to scrapie-associated fibrils (SAF)." Neuropathol Appl Neurobiol **14**(4): 325-36.
McLean, I. W. and P. K. Nakane (1974). "Periodate-lysine-paraformaldehyde fixative. A new fixation for immunoelectron microscopy." J Histochem Cytochem **22**(12): 1077-83.
Muramoto, T., T. Kitamoto, et al. (1992). "The sequential development of abnormal prion protein accumulation in mice with Creutzfeldt-Jakob disease." Am J Pathol **140**(6): 1411-20.
Muramoto, T., T. Kitamoto, et al. (1993). "Accumulation of abnormal prion protein in mice infected with Creutzfeldt-Jakob disease via intraperitoneal route: a sequential study." Am J Pathol **143**(5): 1470-9.
Neutra, M. R., A. Frey, et al. (1996). "Epithelial M cells: gateways for mucosal infection and immunization." Cell **86**(3): 345-8.
Odaka, C., T. Morisada, et al. (2006). "Distribution of lymphatic vessels in mouse thymus: immunofluorescence analysis." Cell Tissue Res **325**(1): 13-22.
Okamoto, M., H. Furuoka, et al. (2003). "Experimental transmission of abnormal prion protein (PrPsc) in the small intestinal epithelial cells of neonatal mice." Vet Pathol **40**(6): 723-7.
Qu, Z. D., M. Thacker, et al. (2008). "Immunohistochemical analysis of neuron types in the mouse small intestine." Cell Tissue Res **334**(2): 147-61.
Race, R., A. Jenny, et al. (1998). "Scrapie infectivity and proteinase K-resistant prion protein in sheep placenta, brain, spleen, and lymph node: implications for transmission and antemortem diagnosis." J Infect Dis **178**(4): 949-53.
Ruhl, A. (2005). "Glial cells in the gut." Neurogastroenterol Motil **17**(6): 777-90.
Safar, J. G., P. Lessard, et al. (2008). "Transmission and detection of prions in feces." J Infect Dis **198**(1): 81-9.
Savidge, T. C., P. Newman, et al. (2007). "Enteric glia regulate intestinal barrier function and inflammation via release of S-nitrosoglutathione." Gastroenterology **132**(4): 1344-58.
Savidge, T. C., M. V. Sofroniew, et al. (2007). "Starring roles for astroglia in barrier pathologies of gut and brain." Lab Invest **87**(8): 731-6.
Seelig, D. M., G. L. Mason, et al. (2010). "Pathogenesis of Chronic Wasting Disease in Cervidized Transgenic Mice." Am J Pathol.
Shmakov, A. N. and S. Ghosh (2001). "Prion proteins and the gut: une liaison dangereuse?" Gut **48**(4): 443-7.

Sigurdson, C. J., C. Barillas-Mury, et al. (2002). "PrP(CWD) lymphoid cell targets in early and advanced chronic wasting disease of mule deer." J Gen Virol **83**(Pt 10): 2617-28.
Sigurdson, C. J., C. K. Mathiason, et al. (2008). "Experimental chronic wasting disease (CWD) in the ferret." J Comp Pathol **138**(4): 189-96.
Sigurdson, C. J., T. R. Spraker, et al. (2001). "PrP(CWD) in the myenteric plexus, vagosympathetic trunk and endocrine glands of deer with chronic wasting disease." J Gen Virol **82**(Pt 10): 2327-34.
Sigurdson, C. J., E. S. Williams, et al. (1999). "Oral transmission and early lymphoid tropism of chronic wasting disease PrPres in mule deer fawns (Odocoileus hemionus)." J Gen Virol **80 (Pt 10)**: 2757-64.
Spraker, T. R., M. W. Miller, et al. (1997). "Spongiform encephalopathy in free-ranging mule deer (Odocoileus hemionus), white-tailed deer (Odocoileus virginianus) and Rocky Mountain elk (Cervus elaphus nelsoni) in northcentral Colorado." J Wildl Dis **33**(1): 1-6.
Spraker, T. R., R. R. Zink, et al. (2002). "Distribution of protease-resistant prion protein and spongiform encephalopathy in free-ranging mule deer (Odocoileus hemionus) with chronic wasting disease." Vet Pathol **39**(5): 546-56.
Tamguney, G., K. Giles, et al. (2006). "Transmission of elk and deer prions to transgenic mice." J Virol **80**(18): 9104-14.
Tamguney, G., M. W. Miller, et al. (2009). "Asymptomatic deer excrete infectious prions in faeces." Nature **461**(7263): 529-32.
Trifilo, M. J., G. Ying, et al. (2007). "Chronic wasting disease of deer and elk in transgenic mice: oral transmission and pathobiology." Virology **365**(1): 136-43.
van Keulen, L. J., B. E. Schreuder, et al. (2000). "Pathogenesis of natural scrapie in sheep." Arch Virol Suppl(16): 57-71.
van Keulen, L. J., M. E. Vromans, et al. (2008). "Pathogenesis of bovine spongiform encephalopathy in sheep." Arch Virol **153**(3): 445-53.
Wiley, C. A., P. G. Burrola, et al. (1987). "Immuno-gold localization of prion filaments in scrapie-infected hamster brains." Lab Invest **57**(6): 646-56.
Williams, E. S. (2005). "Chronic wasting disease." Vet Pathol **42**(5): 530-49.
Williams, E. S. and S. Young (1980). "Chronic wasting disease of captive mule deer: a spongiform encephalopathy." J Wildl Dis **16**(1): 89-98.

CHAPTER 3:

Advanced Immunohistochemcal Evaluation of Prion Excretory Sites in CWD- Infected White-Tailed Deer

ABSTRACT

Chronic wasting disease (CWD) is an efficiently transmitted prion disease of cervids. Although bioassay and molecular experiments have confirmed the infectious nature, and the presence of pathogenic prions (PrP^{RES} or PrP^{CWD}) within numerous cervid-origin biologic materials – including urine, blood, saliva and feces – uncertainties remain regarding the mechanisms of CWD horizontal transmission. Notable among these is a lack of understanding by which prion infectivity is transferred to a particular body fluid. To address this uncertainty, I have sought to provide tissue-level insights into the process of prion shedding via the urinary, salivary, and hematopoietic systems. Here I show that enhanced immunohistochemical (IHC) techniques on formalin-fixed, paraffin-embedded (FFPE) tissues are capable of detecting PrP^{CWD} in excretory tissues of experimentally-infected white-tailed deer (WTD). Specifically, I demonstrate that powerful tyramide signal amplification (TSA)-based protocols greatly augment the ability to detect PrP^{CWD} in the kidney and bone marrow of CWD-infected white-tailed deer. These findings suggest that: (a) the renal tubules may be one route by which CWD prions are shed via the urinary tract, (b) the bone marrow is a target for PrP^{CWD} accumulation and (c) enhanced IHC techniques may offer insights into the kinetics by which pathogenic prions are readily transmitted via biologic excreta.

BACKGROUND

Chronic wasting disease (CWD) of deer, elk and moose is a prion disease first identified in the Rocky Mountain region and now recognized in 19 states, Canada, and one Asian country.(Williams and Young 1980; Williams 2005) Like other transmissible spongiform encephalopathies (TSEs) such as ovine scrapie, bovine spongiform encephalopathy (BSE) and human Creutzfeldt-Jakob Disease (CJD), CWD is caused by the conversion of normal, protease-sensitive PrP^{C} protein to a misfolded, protease-resistant conformation (PrP^{CWD}) which subsequently accumulates in the central nervous and lymphoid systems leading to wasting and spongiform encephalopathy.(Sigurdson, Williams et al. 1999; Sigurdson, Barillas-Mury et al. 2002; Spraker, Zink et al. 2002) CWD is unique as being the only TSE known to infect free-ranging wildlife species and in its efficient lateral transmission.(Williams and Young 1992; Miller, Wild et al. 1998; Miller and Wild 2004)

This facile spread of CWD is different from most TSEs and may reflect the transmission of infectious prions via the saliva, urine, feces, and blood of infected cervids. (Mathiason, Powers et al. 2006; Safar, Lessard et al. 2008; Haley 2009) However, the manner by which PrP^{CWD} infectivity accumulates in each of these biologic materials remains to be determined. A complete understanding of this process is vital for understanding the pathogenesis of CWD and for the development of interventional strategies which might preclude such shedding.

The detection of PrP^{RES} is long considered to be the most significant surrogate marker of prion disease and its presence has been shown to correlate strongly with

infectivity and disease.(Bolton, Rudelli et al. 1991; Race, Jenny et al. 1998) Moreover, the detection of PrP^{CWD} by IHC has long been considered a gold-standard for the diagnosis of CWD infection in cervids and was the assay of choice in many, seminal pathogenesis studies.(Guiroy, Williams et al. 1991; Sigurdson, Williams et al. 1999) Moreover, enhanced IHC utilizing tyramide signal amplification (TSA) has been successfully incorporated into CWD studies in both cervids and cervidized transgenic mice (Sigurdson, Williams et al. 1999; Seelig, Mason et al. 2010), but has yet to be applied in studies evaluating prion excretion.

In cervids, accumulations of PrP^{CWD} are heaviest in the CNS with terminal accumulations detectable in tissues of the endocrine, cardiovascular, respiratory, urinary, and musculoskeletal systems presumably the result of centrifugal dissemination of prions.(Fox, Jewell et al. 2006) To date PrP^{CWD} has yet to be detected in the salivary glands or bone marrow of CWD-infected cervids, which is seemingly at odds with results of bioassay experiments confirming the presence of infectious prions in their biologic material progeny.(Mathiason, Powers et al. 2006) Moreover, accumulations of PrP^{CWD} in the cervid kidney have only sporadically been described and then only in association with intra-renal lymphoid aggregates, but never with normal renal cellular constituents.(Fox, Jewell et al. 2006; Hamir, Kunkle et al. 2006)

To investigate accumulations of PrP^{CWD} in tissues associated with prion shedding, FFPE sections of parotid and submandibular salivary glands, kidney, urethra, ureter, urinary bladder, and bone marrow were immunostained using an enhanced IHC protocol. Through this work I report that the kidney and bone marrow of experimentally infected

white-tailed deer (WTD) contain PrP^{CWD}, thus implicating these tissues in the processes of prionuria and prionemia.

MATERIALS AND METHODS

Cervid tissue sources:

Tissues to be evaluated were collected at terminal disease from 8 experimentally infected WTD. Six deer in this cohort had been inoculated with CWD-positive materials including orally with brain (n = 2), intraperitoneally with whole blood (n = 1) or intravenously with either platelets (n=1) or whole blood (n = 2), while the remaining 2 animals served as negative controls and were inoculated orally or intracerebrally with CWD-negative brain (n=1 each).(Mathiason, Powers et al. 2006) All CWD-infected deer were in the terminal stages of CWD and demonstrated moderate to severe neurological signs, weight loss, polyuria and polydypsia and were confirmed to be CWD-positive by a combination of western blot and immunohistochemistry.(Mathiason, Powers et al. 2006)

Tissue collection and processing:

At necropsy, target tissues (kidney, ureter, urinary bladder, bone marrow, and parotid and submandibular salivary glands) were collected and immersion fixed in 10% neutral buffered formalin (NBF) for 1-3 days. Following standard trimming cassetted tissues were immersed in 88% formic acid for 1 hour followed by rinsing in running tap water for 1 hour prior to embedding in paraffin.

Histology and immunohistochemistry:

For all experiments, paraffin-embedded tissue sections (4-6 µm) were mounted onto positively charged glass slides, then deparaffinized in a heated oven followed by successive immersions in xylene, and rehydrated through graded ethanol. To enhance detection, tissues were subjected to Heat Induced Epitope Retrieval (HIER) using an automated antigen-retrieval system (Retriever™) and a proprietary buffer solution (DakoCytomation™ Target Retrieval Solution). For the enhanced detection of PrP^{CWD}, an IHC protocol was used that combined either a one- or two-step immunostaining procedure with tyramide signal amplification (TSA) (Fig. 3.1). Previous work in our laboratory has demonstrated this methodology to be more sensitive in the detection of PrP^{CWD} than traditional, two-step indirect IHC protocols.(Sigurdson, Barillas-Mury et al. 2002; Seelig, Mason et al. 2010)

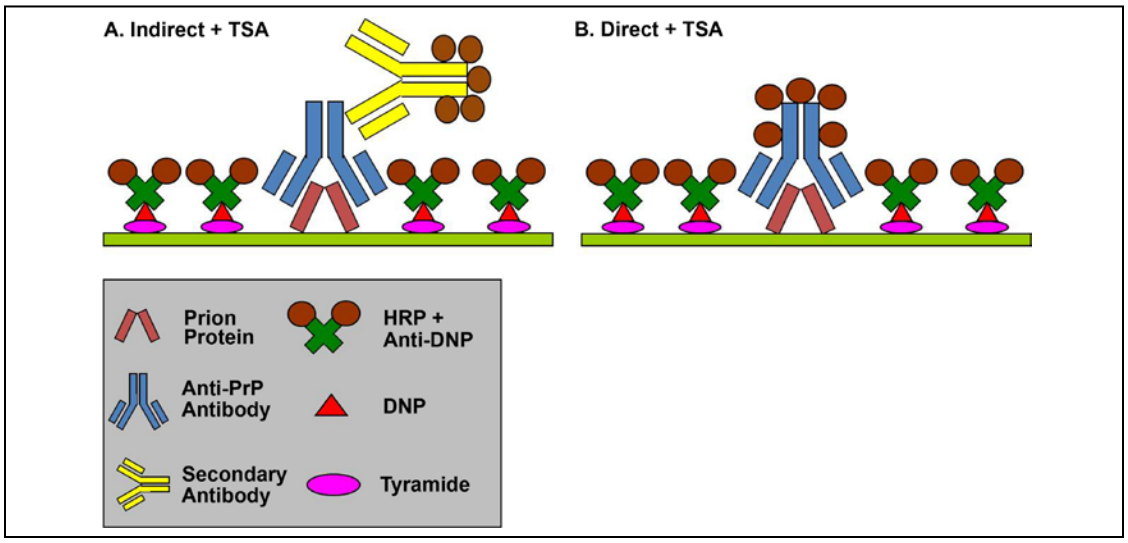

Figure 3.1 Techniques used in the detection of PrP^{CWD} in WTD.
For the detection of PrP^{CWD}, one of two protocols incorporating TSA was used - either indirect (A) or direct (B) in nature. In A, the anti-PrP antibody R505.5 was used, whereas in the latter, so as to eliminate the secondary antibody, the HRP-conjugated antibody BAR224 was used. For each of the protocols, labeled antigen was detected using either DAB or AEC. Abbreviations: TSA = Tyramide Signal Amplification, PrP = Prion protein, HRP = Horseradish peroxidase, DNP = Dinitrophenol, DAB = 3, 3'-Diaminobenzidine, AEC = 3-amino-9-ethyl-carbazole.

The TSA-PrP^{CWD} protocol used a proprietary TSA-detection kit (Perkin-Elmer™) and was conducted as follows. Following slide rehydration and HIER (as described above), tissue section endogenous peroxidase activity was quenched using 3% H_2O_2 for 60 minutes. Sections were further blocked using a proprietary protein block (TNB, Perkin-Elmer™) for 60 minutes. Slides were incubated with one of two anti-prion antibodies, either the rabbit polyclonal R505.5 antibody (courtesy of Jan Langeveld) or the mouse monoclonal HRP-conjugated antibody BAR224 (Cayman Chemicals), diluted 1:1000 and 1:500 in TNB, respectively.

In protocols incorporating the R505.5 antibody, slides were incubated with an HRP-conjugated anti-rabbit polymer (DakoCytomation™). Between all incubation steps, slides were washed three times (5 minutes each) in a TNT wash buffer (0.1M Tris-HCl, pH 7.5, 0.15M NaCl, and 0.05% Tween-20). Following the application of the antibodies, slides were sequentially incubated with two proprietary TSA reagents: 1) DNP Amplification Reagent (Perkin-Elmer™) for 4 minutes and 2) anti-DNP-HRP (Perkin-Elmer™) for 30 minutes. Antibody deposition was visualized using either 3,3'-diaminobenzidine (DAB) or 3-amino-9-ethylcarbazole (AEC) (Dako Cytomation™) and slides were counterstained with hematoxylin and incubated with a bluing reagent (0.1% sodium bicarbonate). Following immunostaining slides were, if needed, dehydrated through graded ethanol, cleared with xylene, and coverslipped. To ensure specificity of the IHC results, negative controls run concurrently consisted of: 1) omission of the primary antibody and 2) replacement of the primary antibody with serum from a non-immune-stimulated rabbit.

RESULTS

PrP^{CWD} in the kidneys of CWD-infected WTD:

Given previous work confirming the infectivity of urine from CWD-infected WTD (Haley 2009), I focused on the major anatomic sites responsible for the creation and flow of urine, namely the: (1) kidney, (2) ureter, and (3) urinary bladder. In the kidneys of 5/6 animals, granular to clumped, intracytoplasmic and interstitial PrP^{CWD} deposits were identified (Table 3.1). In all affected animals, PrP^{CWD} was seen within tubular epithelial cells, with apparent predilection for the proximal segment (Fig 3.2 A-B). In one animal, PrP^{CWD} was seen in the renal papilla – in both the interstitium and in association with capillary endothelium (Fig 3.2 C). PrP^{CWD} was not identified in the ureteral or urinary bladder sections of any CWD-infected animal (Fig. 3.2 D-E), nor was it detected in any sections from negative control animals (Fig. 3.2 F) or in tissue sections immunostained using a negative control anti-serum (Fig 3.2 G).

Tissue	**CWD-infected deer case number**						**CWD-negative deer number**	
	104[a]	**112[a]**	**108[b]**	**325[c]**	**372[d]**	**373[d]**	**103[e]**	**123[f]**
Kidney	+	–	+	+	+	+	–	–
Ureter	–	–	–	–	–	–	–	–
Urinary bladder	–	–	–	–	–	–	–	–
Parotid salivary gland	–	–	–	–	–	–	–	–
Submandibular salivary gland	–	–	–	–	–	–	–	–
Bone marrow	+	–	–	+	+	+	–	–

Table 3.1 PrP^{CWD} in selected tissues of CWD-infected white-tailed deer.
Enhanced IHC was used to evaluate FFPE tissues from CWD-positive and CWD-negative WTD. Abbreviations: FFPE = formalin-fixed, paraffin embedded. [a] = PO, CWD^+ brain, [b] = IP, CWD^+ blood, [c] = IV, CWD^+ platelets, [d] = IV, CWD^+ whole blood, [e] = IC, CWD^- brain, [f] = PO, CWD^- brain

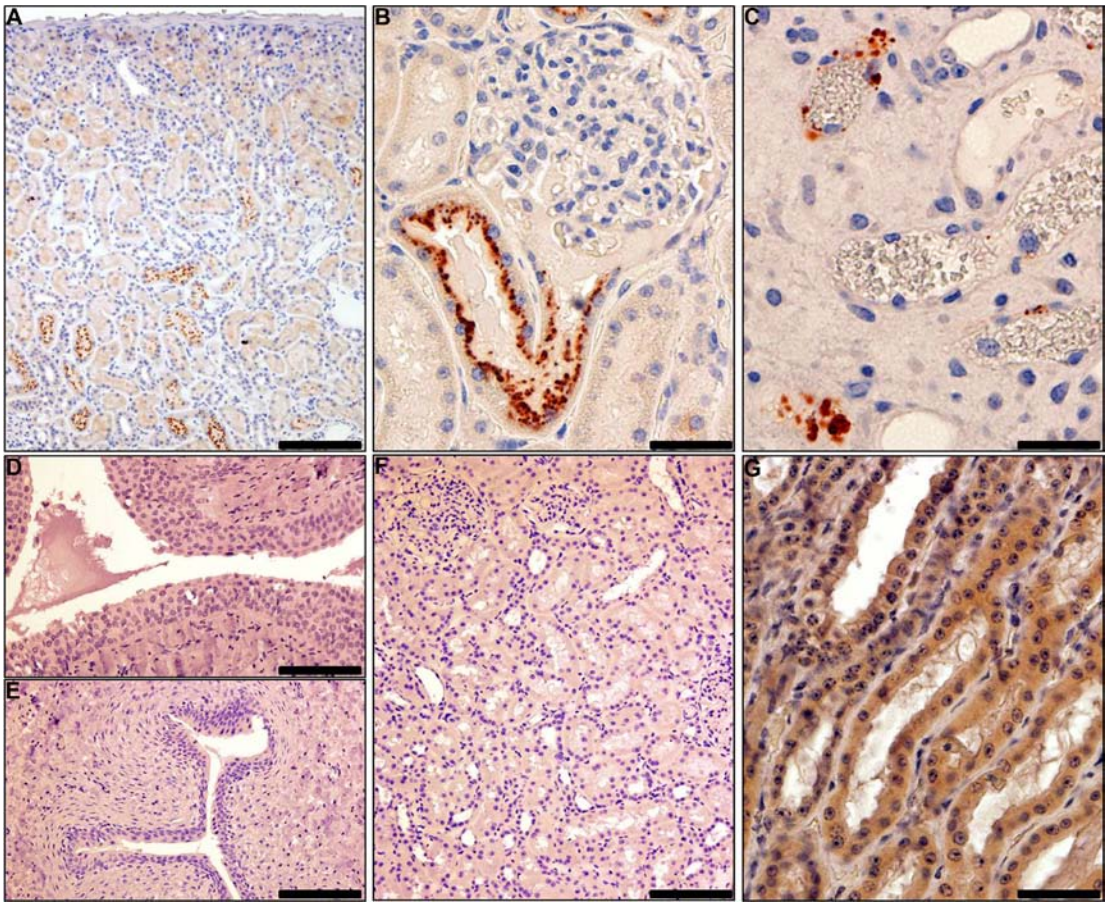

Figure 3.2 PrP^{CWD} in the kidneys of CWD-infected white-tailed deer.
PrP^{CWD} (red) was identified in kidneys of 5/6 CWD-infected WTD, (A) notably within proximal tubular epithelium (B) and rarely in the interstitium or in association with capillary endothelium (C). PrP^{CWD} immunoreactivity was not identified in any ureteral (D) or urinary bladder sections (E). Note the lack of immunoreactivity in the negative control deer (F) and in tissue sections stained with negative control antisera (G). Bars = 1000 µm (A, D-F), 200 µm (B, G), 150 µm (C).

PrP^{CWD} in the bone marrow of CWD-infected WTD:

The bone marrow sections of 4/6 deer (Table 3.1), each of which contained approximately 5,000 – 10,000 evaluable cells, contained granular to clumped PrP^{CWD} deposits confined to the cytoplasm of approximately 5-10% of cells. Affected cells were round with a modest amount of cytoplasm and a round to oval to somewhat lobulated

nucleus (Fig. 3.3 A-B). PrP^{CWD} was not seen in the marrow of CWD-negative deer (Fig. 3.3 C), nor was any immunoreactivity seen in sections stained with a negative control anti-serum (Fig. 3.3 D).

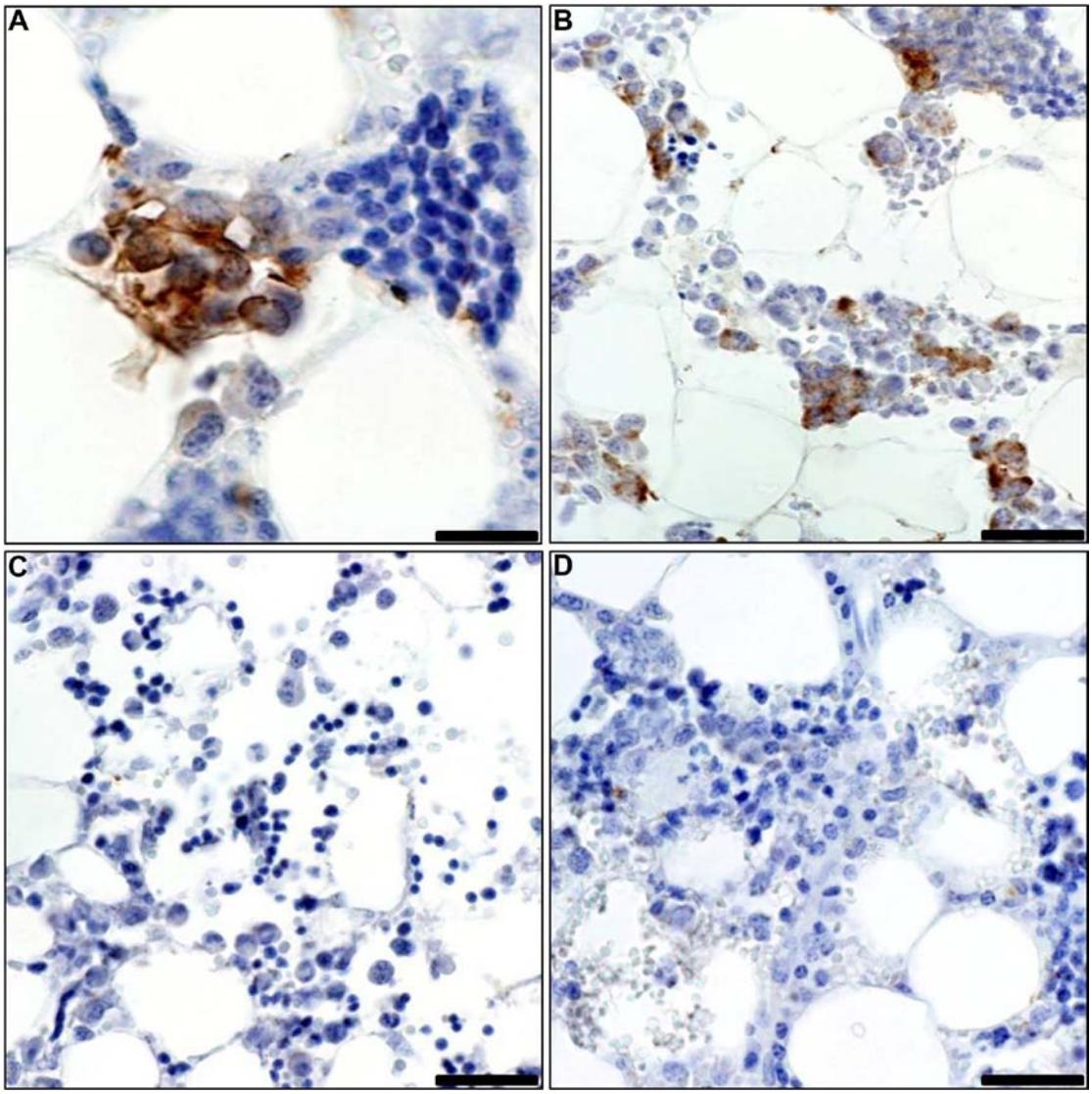

Figure 3.3 PrP^{CWD} in the bone marrow of CWD-infected white-tailed deer.
PrP^{CWD} (brown) was identified in the bone marrow of CWD-infected WTD (A, B) most notably within cells suggestive of myeloid progenitor cells. Note the lack of immunoreactivity in negative control deer (C) and in tissue sections immunostained with negative control antisera (D). Bars = 100 µm (A), 150 µm (B), 500 µm (C, D).

PrP^{CWD} is not observed in salivary glands of CWD-infected WTD:

In 8/8 animals, including all CWD-positive and CWD-negative animals, an identical pattern of immunoreactivity was observed in the parotid and submandibular salivary gland sections (Fig 3.4 A-D). Irrespective of antibody choice, including sections immunostained using negative control antisera, finely granular to somewhat clumped deposits of immunoreactivity were confined to the lumena of glandular ductules. Given that no distinction could be made between infected and negative deer, these findings were not interpreted to be CWD-specific and the tissues were classified as CWD-negative.

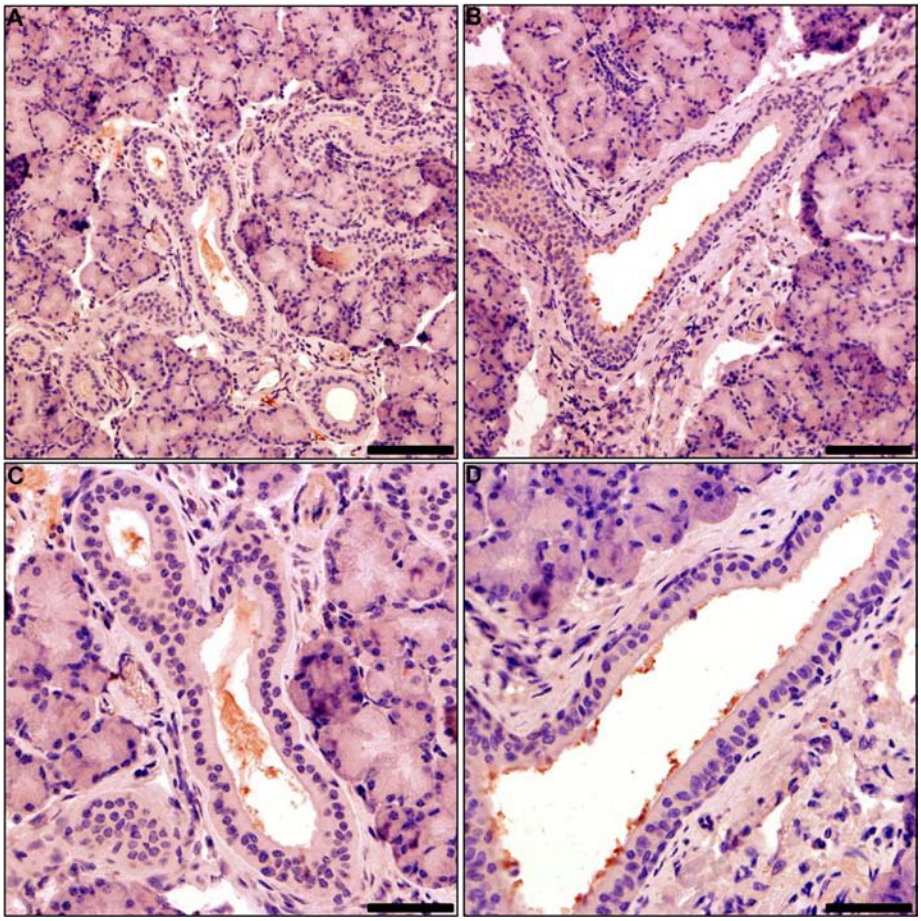

Figure 3.4 Failure to detect PrP^{CWD} in the salivary glands of CWD-infected white-tailed deer.
Identical immunoreactivity (red) was seen in the lumena of salivary gland ductules in both CWD-infected (A, C) and sham-inoculated WTD (B, D). Bars = 1000 µm (A, B), 500 µm (C, D).

DISCUSSION

One of the unique features of CWD is the apparent ease by which horizontal transmission occurs in its host cervid species. While recent work has demonstrated the infectious nature of numerous cervid biologic fluids, including blood, saliva, and bone marrow, the manner by which such infectivity is conferred through the demonstration of convincing tissue-level correlates to these findings remains unresolved. Through the use of enhanced IHC, I report on the novel detection of PrP^{CWD} within tissue sites and cellular populations that might mediate the shedding and trafficking of prions in CWD-infected WTD, including the epithelial cells of the renal nephron and nucleated cells of the bone marrow. This demonstration of CWD prions in the source tissues from which infectious biologic fluids are derived confirms the utility of enhanced IHC methods in cervid tissues and provides evidence for the manner by which certain cervid biologic fluids attain infectivity.

Previous reports of PrP^{RES} in kidney sections of TSE-infected mammals are limited to cats with feline spongiform encephalopathy, primates infected with variant CJD, and sheep infected with scrapie.(Lezmi, Bencsik et al. 2003; Herzog, Riviere et al. 2005; Siso, Gonzalez et al. 2006) Moreover, immunohistochemically demonstrated renal accumulations of PrP^{RES} have been described in scrapie-infected mice and in CWD-infected animals, but deposits were limited to accumulations within foci of lymphofollicular proliferation.(Heikenwalder, Zeller et al. 2005; Fox, Jewell et al. 2006; Hamir, Kunkle et al. 2006) In contrast, these studies are the first to demonstrate PrP^{RES} in association with tubular epithelial cells. The manner by which CWD prions

accumulate in renal tubular epithelial cells is uncertain, but possible pathways include: (i) delivery via the glomerular ultrafitrate, (ii) hematogenous delivery, or (iii) delivery via nerve fibers.

In one scenario, circulating PrP^{CWD} would be filtered through the glomerulus; delivered to the nephron, and subsequently reabsorbed into the tubular epithelial cells. Such reabsorption could be mediated by a non-specific receptor such as megalin – which is responsible for the uptake of many filtered proteins including albumin – or in a more specific manner such as by the putative prion protein receptor laminin, which has been shown to be expressed the sheep and human kidney.(Simon and McDonald 1990; Qiao, Su et al. 2009) The feasibility of prion glomerular filtration is further confirmed by ionizing radiation inactivation experiments that have suggested PrP^{CWD} aggregates could be as small as 55 kDa, which is a size sufficiently small to pass through the glomerular filtration barrier, which excludes proteins greater than approximately 66 kDa.(Bellinger-Kawahara, Kempner et al. 1988; Raila, Forterre et al. 2005) Moreover, the plausibility of hematogenous and/or neural delivery of prions to the kidneys is supported by work documenting the presence of PrP^{CWD} in the blood and in the sympathetic system of CWD-infected cervids, the latter of which constitutes the major pathway of innervation to the kidney.(Barajas, Liu et al. 1992; Fox, Jewell et al. 2006; Mathiason, Powers et al. 2006)

The identification of PrP^{CWD} in the bone marrow of CWD-infected WTD provides a tissue correlate for the recent demonstration of prion infectivity in the blood of CWD-positive cervids.(Mathiason, Powers et al. 2006) Without multi-label analysis, a

conclusion regarding the phenotypic nature of the CWD-positive cells is dependent upon cytomorphologic evaluation of the PrP^{CWD} positive cells. Based upon such morphology, these cells appear to be of the myeloid lineage (i.e., non-lymphoid, non-erythroid, and non-platelet), which is consistent with work documenting PrP^{C} expression on bone marrow cells, including hematopoietic stem cells, maturing granulocytes, and myeloid-derived dendritic cells.(Burthem, Urban et al. 2001; Liu, Li et al. 2001; Zhang, Steele et al. 2006) These findings mimic results in rodent models of CWD and scrapie in which bone marrow PrP^{RES} has been identified by IHC, bioassay, and immunoblotting.(Kimberlin and Walker 1989; Takakura, Yamaguchi et al. 2008; Seelig, Mason et al. 2010) Lacking temporal-spatial data terminal studies are inherently handicapped in positing pathogen trafficking pathways, however PrP^{CWD} accumulation in the bone marrow is likely the result of prion trafficking via either the hematogenous route or via trafficking by fibers of the sympathetic nervous system.(Field, A. et al. 1968; Felten, Felten et al. 1985; Hunter, Foster et al. 2002; Llewelyn, Hewitt et al. 2004; Peden, Head et al. 2004; Mathiason, Powers et al. 2006; Saa, Castilla et al. 2006)

This work fails to demonstrate PrP^{CWD} deposition in cervid salivary glands, which is surprising given the identification of CWD-infectivity in the saliva.(Mathiason, Powers et al. 2006; Haley 2009) This discrepancy could be the result of: (i) deficiencies inherent in the IHC protocol, including inappropriate antibody choice, (ii) low levels of PrP^{CWD}, or (iii) species of PrP^{CWD}, including possible protease-sensitive isoforms, whose immunoreactivity might be abrogated by one or more of the tissue or slide treatment steps, including formalin fixation or formic acid immersion. The tissues in these studies were immunostained with 2 antibodies, both which have proven successful in previous

CWD studies, (Haley 2009; Seelig, Mason et al. 2010) although others have shown antibody-dependent variations in salivary gland immunoreactivity, which may be the result of tissue-specific differences in PrP^{CWD} conformation and epitope exposure.(Vascellari, Nonno et al. 2007) The role of protease-sensitive PrP^{CWD} species in CWD is uncertain, but such isoforms have been isolated from humans with sporadic CJD and sheep with certain strains of scrapie.(Benestad, Sarradin et al. 2003; Safar, Geschwind et al. 2005)

In summary, the findings reported here provide evidence for: (a) the accumulation of PrP^{CWD} in the kidneys and their circumstantial implication as the source of prion shedding in conferring infectivity to cervid urine and (b) the presence of PrP^{CWD} in the bone marrow, which may mediate the documented prionemia in infected WTD. These results are consistent with the assembled findings in other experimental and natural TSEs and provide evidence demonstrating the beneficial applications of enhanced IHC in the detection of PrP^{CWD} in CWD-infected WTD.

ACKNOWLEDGEMENTS

I greatly appreciate the assistance of Sally Dahmes and David Osborne of the Warnell School of Forestry, University of Georgia, without whom the primary deer experiments could not have been performed. Moreover, I'd like to thank those who conceived and carried out these original cervid experiments: Candace Mathiason, Jeanette Hayes-Klug, Sheila Hays, and Amy Nalls. Additionally, I'd like to thank Nicholas Haley for valued assistance and Nate Denkers for assistance in troubleshooting the immunohistochemistry.

This work was supported by contract NO1-AI-25491 from NIH, NIAID from T32-RR07072 from NIH, NCRR.

REFERENCES

Barajas, L., L. Liu, et al. (1992). "Anatomy of the renal innervation: intrarenal aspects and ganglia of origin." Can J Physiol Pharmacol **70**(5): 735-49.

Bellinger-Kawahara, C. G., E. Kempner, et al. (1988). "Scrapie prion liposomes and rods exhibit target sizes of 55,000 Da." Virology **164**(2): 537-41.

Benestad, S. L., P. Sarradin, et al. (2003). "Cases of scrapie with unusual features in Norway and designation of a new type, Nor98." Vet Rec **153**(7): 202-8.

Bolton, D. C., R. D. Rudelli, et al. (1991). "Copurification of Sp33-37 and scrapie agent from hamster brain prior to detectable histopathology and clinical disease." J Gen Virol **72 (Pt 12)**: 2905-13.

Burthem, J., B. Urban, et al. (2001). "The normal cellular prion protein is strongly expressed by myeloid dendritic cells." Blood **98**(13): 3733-8.

Felten, D. L., S. Y. Felten, et al. (1985). "Noradrenergic and peptidergic innervation of lymphoid tissue." J Immunol **135**(2 Suppl): 755s-765s.

Field, E. J., C. E. A., et al. (1968). "Scrapie agent in blood." Vet Rec **83**: 109-10.

Fox, K. A., J. E. Jewell, et al. (2006). "Patterns of PrPCWD accumulation during the course of chronic wasting disease infection in orally inoculated mule deer (Odocoileus hemionus)." J Gen Virol **87**(Pt 11): 3451-61.

Guiroy, D. C., E. S. Williams, et al. (1991). "Topographic distribution of scrapie amyloid-immunoreactive plaques in chronic wasting disease in captive mule deer (Odocoileus hemionus hemionus)." Acta Neuropathol **81**(5): 475-8.

Haley, N. J. (2009). "Detection of CWD prions in urine and saliva of deer by transgenic mouse bioassay." PLoS ONE.

Hamir, A. N., R. A. Kunkle, et al. (2006). "Abnormal prion protein in ectopic lymphoid tissue in a kidney of an asymptomatic white-tailed deer experimentally inoculated with the agent of chronic wasting disease." Vet Pathol **43**(3): 367-9.

Heikenwalder, M., N. Zeller, et al. (2005). "Chronic lymphocytic inflammation specifies the organ tropism of prions." Science **307**(5712): 1107-10.

Herzog, C., J. Riviere, et al. (2005). "PrPTSE distribution in a primate model of variant, sporadic, and iatrogenic Creutzfeldt-Jakob disease." J Virol **79**(22): 14339-45.

Hunter, N., J. Foster, et al. (2002). "Transmission of prion diseases by blood transfusion." J Gen Virol **83**(Pt 11): 2897-905.

Kimberlin, R. H. and C. A. Walker (1989). "The role of the spleen in the neuroinvasion of scrapie in mice." Virus Res **12**(3): 201-11.

Lezmi, S., A. Bencsik, et al. (2003). "First case of feline spongiform encephalopathy in a captive cheetah born in France: PrP(sc) analysis in various tissues revealed unexpected targeting of kidney and adrenal gland." Histochem Cell Biol **119**(5): 415-22.

Liu, T., R. Li, et al. (2001). "Normal cellular prion protein is preferentially expressed on subpopulations of murine hemopoietic cells." J Immunol **166**(6): 3733-42.

Llewelyn, C. A., P. E. Hewitt, et al. (2004). "Possible transmission of variant Creutzfeldt-Jakob disease by blood transfusion." Lancet **363**(9407): 417-21.

Mathiason, C., J. G. Powers, et al. (2006). "Infectious Prions in the Saliva and Blood of Deer with Chronic Wasting Disease." Science **in press**.

Mathiason, C. K., J. G. Powers, et al. (2006). "Infectious prions in the saliva and blood of deer with chronic wasting disease." Science **314**(5796): 133-6.

Miller, M. W. and M. A. Wild (2004). "Epidemiology of chronic wasting disease in captive white-tailed and mule deer." J Wildl Dis **40**(2): 320-7.

Miller, M. W., M. A. Wild, et al. (1998). "Epidemiology of chronic wasting disease in captive Rocky Mountain elk." J Wildl Dis **34**(3): 532-8.

Peden, A. H., M. W. Head, et al. (2004). "Preclinical vCJD after blood transfusion in a PRNP codon 129 heterozygous patient." Lancet **364**(9433): 527-9.

Qiao, J. W., X. O. Su, et al. (2009). "Variable levels of 37-kDa/67-kDa laminin receptor (RPSA) mRNA in ovine tissues: potential contribution to the regulatory processes of PrPSc propagation?" Anim Biotechnol **20**(3): 151-5.

Race, R., A. Jenny, et al. (1998). "Scrapie infectivity and proteinase K-resistant prion protein in sheep placenta, brain, spleen, and lymph node: implications for transmission and antemortem diagnosis." J Infect Dis **178**(4): 949-53.

Raila, J., S. Forterre, et al. (2005). "[Physiologic and pathophysiologic fundamentals of proteinuria--a review]." Berl Munch Tierarztl Wochenschr **118**(5-6): 229-39.

Saa, P., J. Castilla, et al. (2006). "Presymptomatic detection of prions in blood." Science **313**(5783): 92-4.

Safar, J. G., M. D. Geschwind, et al. (2005). "Diagnosis of human prion disease." Proc Natl Acad Sci U S A **102**(9): 3501-6.

Safar, J. G., P. Lessard, et al. (2008). "Transmission and detection of prions in feces." J Infect Dis **198**(1): 81-9.

Seelig, D. M., G. L. Mason, et al. (2010). "Pathogenesis of Chronic Wasting Disease in Cervidized Transgenic Mice." Am J Pathol.

Sigurdson, C. J., C. Barillas-Mury, et al. (2002). "PrP(CWD) lymphoid cell targets in early and advanced chronic wasting disease of mule deer." J Gen Virol **83**(Pt 10): 2617-28.

Sigurdson, C. J., E. S. Williams, et al. (1999). "Oral transmission and early lymphoid tropism of chronic wasting disease PrPres in mule deer fawns (Odocoileus hemionus)." J Gen Virol **80 (Pt 10)**: 2757-64.

Simon, E. E. and J. A. McDonald (1990). "Extracellular matrix receptors in the kidney cortex." Am J Physiol **259**(5 Pt 2): F783-92.

Siso, S., L. Gonzalez, et al. (2006). "Prion protein in kidneys of scrapie-infected sheep." Vet Rec **159**(10): 327-8.

Spraker, T. R., R. R. Zink, et al. (2002). "Distribution of protease-resistant prion protein and spongiform encephalopathy in free-ranging mule deer (Odocoileus hemionus) with chronic wasting disease." Vet Pathol **39**(5): 546-56.

Takakura, Y., N. Yamaguchi, et al. (2008). "Bone marrow stroma cells are susceptible to prion infection." Biochem Biophys Res Commun **377**(3): 957-61.

Vascellari, M., R. Nonno, et al. (2007). "PrPSc in salivary glands of scrapie-affected sheep." J Virol **81**(9): 4872-6.

Williams, E. S. (2005). "Chronic wasting disease." Vet Pathol **42**(5): 530-49.

Williams, E. S. and S. Young (1980). "Chronic wasting disease of captive mule deer: a spongiform encephalopathy." J Wildl Dis **16**(1): 89-98.

Williams, E. S. and S. Young (1992). "Spongiform encephalopathies in Cervidae." Rev Sci Tech **11**(2): 551-67.

Zhang, C. C., A. D. Steele, et al. (2006). "Prion protein is expressed on long-term repopulating hematopoietic stem cells and is important for their self-renewal." Proc Natl Acad Sci U S A **103**(7): 2184-9.

CONCLUSIONS AND FURTHER DIRECTIONS

Through the investigation of patterns of PrP^{CWD} tissue tropism in CWD-infected Tg[CerPrP] mice and WTD, I have shown that: (1) Tg[CerPrP] mice are effective surrogates for the study of CWD through their recapitulation of the clinical, neuropathologic, transmission, and PrP^{CWD} tropism features as reported in native cervids, (2) Tg[CerPrP] mice are capable of providing novel insights into the uptake, trafficking, and shedding of CWD prions and (3) PrP^{CWD} in WTD accumulates in the kidney and bone marrow, providing a tissue level correlate to the documented infectivity of urine and blood in CWD-infected deer.

Through the course of evaluating the temporal-spatial patterns of prion accumulation in the CNS of Tg[CerPrP] mice, it was identified that PrP^{CWD} has an apparent tropism for specific regions of the CNS, including the thalamus, hypothalamus and olfactory tract of the cerebral cortex. These findings, in conjunction with the identification of an apparently paradoxical syndrome of wasting and hyperphagia in both deer and Tg[CerPrP] mice, form the basis for questions regarding the mechanisms of wasting in CWD including: (1) Are the metabolic derangements in CWD-infected Tg[CerPrP] mice and cervids the result of dysfunction of the centers of appetite regulation?, (2) Is appetite dysregulation mediated by a combination of increased pro-inflammatory mediators (i.e., TNF-α) in concert with altered levels of appetite-regulating neuropeptides (i.e., neuropeptide Y, NPY)?, and (3) Does apparent ablation of the olfactory tract through massive PrP^{CWD} accumulation result in loss of smell (anosmia), which is in part responsible for the wasting in CWD-infected animals? Specific studies

which might answer these questions include: (1) The quantification of the role of the central mediators of appetite regulation through the measurement of TNF-α and NPY in plasma, cerebrospinal fluid, and brain homogenates from experimentally-infected white-tailed deer and Tg[CerPrP] mice, (2) multi-label, immunofluorescent analysis of hypothalamic and thalamic sections to co-localize such mediators in proximity to areas of PrP^{CWD} deposition and apoptotic neurons and (3) clinical assays in CWD-infected animals to determine if anosmia develops during the course of disease and how such a phenomenon relates to PrP^{CWD} accumulation and metabolic status.

In Tg[CerPrP] mice, the identification of PrP^{CWD} in the ENS indicates its cellular constituents, including the EGCs, could mediate intestinal prion trafficking, which may facilitate prion enteroinvasion and/or prion shedding via the GI tract. However questions remain regarding the significance of this finding in animals inoculated via the natural route of infection (i.e., PO-inoculated animals). One might continue this work by orally inoculating Tg[CerPrP] mice with either unlabelled or fluorescently-labeled CWD prions and mapping PrP^{CWD} accumulations in the ENS at earlier stages (i.e., within minutes to hours post-inoculation). Additionally, an understanding of the sufficiency of the EGCs in the process of prion enteroinvasion could be acquired through the creation and PO inoculation of a lineage of transgenic mice with glial cell-restricted prion protein expression (e.g., PrP expression under the control of the GFAP promoter).

In addition to evaluating the role of the ENS in prion trafficking, this work provides a foundation for future studies evaluating for possible GI dysfunction resultant from the accumulation of PrP^{CWD} in the ENS including alterations in GI motility, altered

mucosal barrier function, and dysphagia. Such studies would involve the evaluation of GI function in CWD-infected Tg[CerPrP] mice via measurements of: stool weight, GI transit time, and colonic motility simultaneous with quantification of PrP^{CWD} within the ENS.

The identification of PrP^{CWD} in the bone marrow of CWD-infected Tg[CerPrP] mice and cervids suggests that myeloid-origin cells, either myeloid-origin dendritic cells or myeloid-origin microglial precursors, once infected with prions, may facilitate the process of neuroinvasion along a hematogenous route. Questions derived from these bone marrow findings include: (1) What marrow cells are the targets of PrP^{CWD} infection? and (2) How might such cells participate in the pathogenesis of CWD, including the process of neuroinvasion? Studies which would serve to address these questions include: (1) Using single and dual label immunocytochemistry and flow cytometry to document the expression of PrP^{C} on bone marrow cells of Tg[CerPrP] mice, (2) The evaluation of sequential bone marrow samples from CWD-inoculated Tg[CerPrP] mice for the presence of PrP^{CWD} using IHC, western blot (WB), mouse bioassay, and/or serial protein misfolding cyclic amplification (sPMCA) and (3) The utilization of reciprocal adoptive bone marrow transfer to create 2 lineages of bone marrow chimeric mice, which will have PrP^{C} expression restricted to either hematopoietic or non-hematopoietic compartments. By restricting PrP^{C} expression to the bone marrow, other routes of neuroinvasion, most notably one utilizing the peripheral nervous system, would be excluded and the hematogenous pathway could be exclusively evaluated. Following their creation, mice could be PO and IV inoculated and PrP^{CWD} accumulation analyzed in the bone marrow and CNS through IHC, WB, mouse bioassay, and sPMCA.

The identification of PrP^{CWD} in the kidneys of the CWD-infected WTD implicates tubular epithelial cells in the uptake and shedding of prions via the urinary tract. Questions derived from this work are many and include: (1) How do prions arrive at the kidney (i.e., a neural vs. hematogenous route of prion invasion)?, (2) Are renal tubular epithelial cells are capable of amplifying PrP^{CWD}?, (3) How might CWD prions be shed from these cells?, and (4) What, if any, functional impairments are associated with renal prion accumulation?. Further directions of this work might involve: (1) Co-localization studies to determine which particular renal cell populations accumulate PrP^{CWD}, (2) Ultrastructural analysis to aid in elucidating if the glomerular filtration apparatus is responsible for the delivery of PrP^{CWD} to the kidneys, (3) The development of a cervid, tubular epithelial cell culture system to evaluate, in vitro, the effects of PrP^{CWD} exposure, (4) The creation and inoculation of a line of cervidized transgenic mice with PrP expression limited to the peripheral nervous system to evaluate if renal prion trafficking is nerve fiber-mediated, and (5) Functional analysis studies (i.e., electrolyte and glucose excretion studies, microalbuminuria quantification, renal urine concentration analysis, etc.) to determine what, if any, physiologic impairments result from renal PrP^{CWD} accumulation.

The studies comprising this thesis have contributed to furthering the understanding of the pathogenesis and trafficking of prions in CWD. Moreover, these studies lay an important foundation for future CWD studies, which will answer questions key to enhancing the knowledge of this, and other protein-misfolding, neurodegenerative diseases.